

Development of High Temperature Fixed Points for Application in Radiometry and Thermometry

by

Natasha Nel-Sakharova

Submitted in partial fulfilment of the requirements for the degree

Magister Scientiae

In the Faculty of Natural & Agricultural Sciences

University of Pretoria

Pretoria

1 August 2015



I, Natasha Nel-Sakharova, declare that the dissertation, which I hereby submit for the degree Magister Scientiae at the University of Pretoria, is my own work and has not previously been submitted by me for a degree at this or any other tertiary institution.

Signature:

Date: 13 August 2015

Condensed Abstract

Many National Metrology Institutes (NMIs) realise the spectral irradiance scale by obtaining traceability from a cryogenic radiometer through the use of calibrated filter radiometers. The filter radiometers are used to determine the temperature of a high temperature black body which is then used as a reference source, which spectral radiance can be determined from Planck's equation. The uncertainty of the temperature measurement makes the most significant contribution to the uncertainty of realising the spectral irradiance scale. High temperature fixed points (HTFPs), above the copper point, can be used to improve these uncertainties. After more than ten years of research, results obtained on metal-carbon eutectic fixed points by several NMIs, showed that these novel high temperature fixed points could lead to significant improvements in high temperature metrology and could be considered as potential fixed points in a future international temperature scale. This paper describes the development and characterisation of Re-C and $\delta(\text{MoC})\text{-C}$ fixed points at NMISA. It is demonstrated that these fixed points can be utilised as reproducible, stable reference standards for temperatures above the copper point.

Abstract

Metrology is the science of measurement. It involves the formulation of the theoretical principles related to the definition of the International System of Units (Système International d'Unités, SI) and the development of the technology for realising these units in practise. Reliable measurement is important all areas of human activity. Decisions are based on measurement results. Incorrect measurement results can lead to incorrect decisions, which may have significant health, economic or environmental consequences.

Applications of sources of optical radiation are wide-ranging, including: medical treatment, diagnosis and sterilisation; quality control in production processes; stimulation of plant growth in agriculture; lighting and signalling for transport; interior and exterior lighting for buildings; solar power generation; and earth observation. The spectral power distribution of a source must often be known in order to ensure that the selected radiation source (and detector) is suitable for the intended purpose and to optimise process efficiency. Sometimes spectral measurements are required to demonstrate compliance with regulatory requirements (such as Occupational Health and Safety, Aviation Authority regulations, Emergency Lighting and Road Lighting regulations). Spectral measurements in the ultraviolet region are especially important due to its associated biological hazard.

The accuracy of a measurement result can only be known if it is traceable to a national measurement standard. The National Metrology Institute of South Africa (NMISA) realises and maintains the national measurement standards for South Africa. Sources of optical radiation can be calibrated in terms of spectral irradiance over the wavelength range 250 nm to 1 300 nm. The NMISA currently imports traceability for spectral irradiance by sending primary standard lamps to another National Metrology Institute (NMI) for calibration. The uncertainties of calibration are 4 % to 8 % ($k = 2$) over the wavelength range of 400 nm to 1 500 nm. A primary spectral irradiance facility is being developed, which will allow the NMISA to realise the scale independently, eliminating the need to import traceability. Through developing this facility, the NMISA aims to achieve an

uncertainty of $< 1 \%$ over the visible wavelengths.

Many NMIs realise the spectral irradiance scale by obtaining traceability from a primary standard cryogenic radiometer through calibrated filter radiometers. The filter radiometers are used to determine the temperature of a high temperature black body functioning as a reference source, which spectral radiance can be determined from Planck's equation. The uncertainty of the temperature measurement makes the most significant contribution to the uncertainty of realising the spectral irradiance scale. High temperature fixed points, above the copper point, can be used to improve these uncertainties. After more than ten years of research, results obtained on metal-carbon eutectic fixed points by several NMIs, showed that these novel high temperature fixed points could lead to significant improvements in high temperature metrology and could be considered as potential fixed points in a future International Temperature Scale.

This dissertation describes the development and characterisation of high temperature metal-carbon fixed points at NMISA. It is demonstrated that these fixed points can be utilised as reproducible, stable reference standards for temperatures above the copper point. The melt temperature of Re-C cells was repeatable within 60 mK, which is equal to a relative spectral radiance value of 0,02 % at 650 nm. The melt temperature of the $\delta(\text{MoC})\text{-C}$ cell was repeatable within 100 mK, which is equal to a relative spectral radiance value of 0,03 % at 650 nm. Without implementing eutectics, NMIs typically achieve a best measurement capability of 3 K ($k = 2$) at 2 800 K, which contributes approximately 1 % to the overall spectral radiance measurement uncertainty. By using eutectics the reproducibility of spectroradiometric scales can be improved by a factor of 10.

The NMISA result for Re-C (2 747,51 K \pm 2,43 K, ($k = 2$)) is consistent with international values and agrees with the preliminary consensus value (2 747,35 K \pm 1 K, ($k = 2$)) within the stated uncertainties. Only one published result for $\delta(\text{MoC})\text{-C}$ eutectics could be found, which was by NMIJ (Japanese NMI). The NMISA result for $\delta(\text{MoC})\text{-C}$ (2 856,76 K \pm 2,89 K, ($k = 2$)) corresponds with that published by NMIJ (2 856 K \pm 4 K, ($k = 2$)) and compares well with the result of measurements performed at VNIIOFI (Russian NMI) (2 856,40 K \pm 2,0 K, ($k = 2$)) on this particular cell. As far as can be ascertained, the most comprehensive study of $\delta(\text{MoC})\text{-C}$ was done by the NMISA.

Once internationally agreed to melt temperatures for a selected set of high temperature eutectics are approved and incorporated into an updated *mise en pratique* for the definition of the kelvin, the NMISA could assign the international consensus value to its Re-C cells and re-realise its high temperature scale from 961,78 °C (the silver freeze point) up to 2 474 °C (or higher) and immediately, in retrospect, realise the substantially reduced uncertainty of 1 % ($k = 2$).

Dedication

I dedicate this dissertation to my grandmother, Ms. Dorothy Frances Kilian, who instilled in me at an early age the importance of knowledge and education.

“I often say that when you can measure what you are speaking about, and express it in numbers, you know something about it; but when you cannot express it in numbers, your knowledge is of a meagre and unsatisfactory kind; it may be the beginning of knowledge, but you have scarcely, in your thoughts, advanced to the stage of science, whatever the matter may be.”

- Lord Kelvin (Lecture on "Electrical Units of Measurement", 3 May 1883, Popular Lectures Vol. I, p. 73)

Acknowledgements

I would like to sincerely thank the following persons for their contribution towards the completion of this study:

- Mr. Ndwakhulu Mukhufhi, in his capacity as the Chief Executive Officer of the National Metrology Institute of South Africa, for affording me the opportunity to undertake this study;
- Professor Johan B. Malherbe, my study leader, for his guidance and advice;
- Mr. Hans G. Liedberg for helpful discussions concerning the practical implementation of ITS-90;
- Mr. Roko Popich for his assistance with the mechanical setup of the black body;
- My parents, Mr. Pieter W. Nel and Ms. Frances E. van der Merwe, for providing me with the initial opportunity to further my education; and finally
- a very special word of gratitude to my husband, Mr. Mikhail Sakharov, for his encouragement, support, advice and patience during this study.

Contents

1	Introduction	1
1.1	Definition of Metrology	1
1.2	History of Metrology	2
1.2.1	International Developments	2
1.2.2	Units of Measurement in South Africa	4
1.3	International Organisation of Metrology	5
1.4	Problem Statement	7
1.5	Literature Review	9
1.5.1	Introduction	9
1.5.2	Eutectic Fixed Points	10
1.5.3	Fixed Point Crucibles	12
1.5.4	Phase Transition Temperatures	13
1.5.5	Measurement of Transition Temperatures	16
1.5.5.1	Theoretical background	16
1.5.5.2	Experimental Application of Planck's Law	18
1.6	International Results	21
1.7	Objectives	22
1.8	Significance and Relevance of Research	23
1.9	Scope of Study	24
1.10	Structure of Dissertation	25
2	Experimental Procedure	27
2.1	Selection of Eutectics	27
2.2	Eutectic Cell Preparation	28

2.3	Experiment and Method	33
2.3.1	Fixed Point Measurement Configuration	33
2.3.1.1	Measurement of the phase transition plateaux	33
2.3.1.2	Measurement process	34
3	Results and Data Analysis	36
3.1	Phase Transition Curves Obtained	36
3.1.1	Re-C Eutectic Cells	36
3.1.2	$\delta(\text{MoC})$ -C Eutectic Cells	42
3.2	Measurement Uncertainties in Temperature Determination	51
3.2.1	Typical Sources of Uncertainty	52
3.2.1.1	Calibration of the standard pyrometer	52
3.2.1.2	Size of source effect	52
3.2.1.3	Drift	52
3.2.1.4	Non-linearity	52
3.2.1.5	Positioning and alignment	52
3.2.1.6	Emissivity of the crucible cavity	53
3.2.1.7	Temperature drop at the cavity bottom	53
3.2.1.8	Determination of the point of inflection	53
3.2.1.9	Impurities	54
3.2.1.10	Repeatability	54
3.2.2	Uncertainty Budgets for the Eutectic Cells	54
3.3	Summary of Results	56
4	Discussion of Results	58
5	Conclusion	61
A	NMISA Spectral Irradiance Scale	64
B	Certificate of Calibration for Pyrometer	66
C	Research Output	68
	Bibliography	76

List of Figures

1.1	Schematic diagram showing the international organisation of metrology	7
1.2	Assigned temperatures for ITS-90 HTFPs and approximate transition temperatures for metal-carbon and metal carbide-carbon eutectics	9
1.3	Phase diagram for a binary eutectic	11
1.4	A typical design of a eutectic crucible	12
1.5	Black body radiation spectra for different temperatures	18
2.1	Crucible dimensions	29
2.2	The left image depicts the crucible (with the plug on the left-hand side). The right image depicts a carbon ring attached to the right-hand side of the crucible to enable fitment inside the black body.	29
2.3	Filling and weighing of crucibles in an argon environment	30
2.4	Schematic layout of the high temperature BB3200pg black body	30
2.5	NMISA's high temperature black body (BB3200pg)	31
2.6	Main cavity of the black body, consisting of graphite rings	31
2.7	Black body operated in a vertical position while filling the crucible with the eutectic alloy	32
2.8	A schematic illustration of the eutectic filling procedure. The crucible is filled with a mixture of the carbon and metal powders at the eutectic composition (A); heated to approximately 20 K above the eutectic melting point (B); cooled to room-temperature (C), re-filled with the powder mixture and re-heated to approximately 20 K above the melting point (D). This process (B to D) is repeated until the space surrounding the cavity is completely filled with the eutectic alloy (E).	32
2.9	A picture of the NMISA's LP4 radiation thermometer supplied by IKE (Stuttgart, Germany)	33

2.10	A schematic presentation of the optical configuration of the LP4 radiation thermometer	34
2.11	The position of the eutectic cell inside the black body furnace during measurement of the phase transition plateaus	34
2.12	Observation of melt and freeze phase transitions	35
3.1	Typical phase transition plateaux observed for a Re-C eutectic cell	37
3.2	A typical melting plateau observed for Re-C eutectic cells	37
3.3	Determination of the point of inflection of the melting plateau for a Re-C eutectic cell	38
3.4	A typical freezing plateau observed for Re-C eutectic cells	38
3.5	Melt temperatures of the Re-C (2) cell measured over four different days	39
3.6	Freeze temperatures of the Re-C (2) cell measured over four different days	40
3.7	Melt temperatures of the Re-C (1) cell measured over three different days	40
3.8	Freeze temperatures of the Re-C (1) cell measured over three different days	41
3.9	Typical phase transition plateaux observed for the RU $\delta(\text{MoC})$ -C eutectic cell	43
3.10	Typical melting plateaux observed for the RU $\delta(\text{MoC})$ -C eutectic cell	44
3.11	Determination of the point of inflection of the melting plateau for the RU $\delta(\text{MoC})$ -C eutectic cell	44
3.12	Typical freezing plateaux observed for the RU $\delta(\text{MoC})$ -C eutectic cell	45
3.13	Melt temperature measurement results for the RU $\delta(\text{MoC})$ -C eutectic cell	45
3.14	Freeze temperature measurement results for the RU $\delta(\text{MoC})$ -C eutectic cell	46
3.15	The SA $\delta(\text{MoC})$ -C eutectic cell showing the leakage of the eutectic within the hairline crack and the resulting small dent inside the cylindrical cell holder	47
3.16	Typical phase transition plateaux observed for the SA $\delta(\text{MoC})$ -C eutectic cell	48
3.17	Typical melting plateaux observed for the SA $\delta(\text{MoC})$ -C eutectic cell	48
3.18	Determination of the point of inflection of the melting plateau for the SA $\delta(\text{MoC})$ -C eutectic cell	49
3.19	Typical freezing plateaux observed for the SA $\delta(\text{MoC})$ -C eutectic cell	49
3.20	Melt temperature measurement results for the SA $\delta(\text{MoC})$ -C eutectic cell	50
3.21	Freeze temperature measurement results for the SA $\delta(\text{MoC})$ -C eutectic cell	50
A.1	Schematic diagram of the primary spectral irradiance facility being established at the NMISA	64

List of Abbreviations

BIPM	International Bureau of Weights and Measures (Bureau International des Poids et Mesures)
CIE	Commission Internationale de l'Éclairage (International Commission on Illumination)
CGPM	General Conference on Weights and Measures (Conférence Générale des Poids et Mesures)
CIPM	International Committee for Weights and Measures (Comité International des Poids et Mesures)
CCPR	Consultative Committee for Photometry and Radiometry
CCT	Consultative Committee for Temperature
CSIR	Council for Scientific and Industrial Research
CMC	calibration and measurement capability
HTFP	high temperature fixed point
ITS-90	International Temperature Scale of 1990
LED	light emitting diode
LNE-INM	Laboratoire National de Métrologie et d'Essais - Institut National de Métrologie
MRA	Mutual Recognition Arrangement
NIST	National Institute of Standards and Technology
NMI	national metrology institute
NMIJ	National Metrology Institute of Japan
NMISA	National Metrology Institute of South Africa
NMS	national measurement standard
NPL	National Physical Laboratory
NRC	National Research Council

POI	point of inflection
PTB	Physikalisch-Technische Bundesanstalt
SI	International System of Units (Système International d'Unités)
SSE	size-of-source effect
TBT	technical barrier to trade
VNIIOFI	All-Russian Research Institute for Optical and Physical Measurements (<i>English translation</i>)

List of Terms and Definitions

Term	Definition	Reference
measurement accuracy	closeness of agreement between a measured quantity value and a true quantity value of a measurand	2.13
measurement precision	closeness of agreement between indications or measured quantity values obtained by replicate measurements on the same or similar objects under specified conditions	2.15
repeatability condition	condition of measurement, out of a set of conditions that includes the same measurement procedure, same operators, same measuring system, same operating conditions and same location, and replicative measurements on the same or similar objects over a short period of time	2.20
measurement repeatability	measurement precision under a set of repeatability conditions of measurement	2.21
reproducibility condition	condition of measurement, out of a set of conditions that includes different locations, operators, measuring systems, and replicate measurements on the same or similar objects	2.24
measurement reproducibility	measurement precision under reproducibility conditions of measurement	2.25
measurement uncertainty	non-negative parameter characterising the dispersion of the quantity values being attributed to a measurand, based on the information used	2.26
uncertainty budget	statement of a measurement uncertainty, of the components of that measurement uncertainty, and of their calculation and combination	2.33

Term	Definition	Reference
metrological traceability	property of a measurement result whereby the result can be related to a reference through a documented unbroken chain of calibrations, each contributing to the measurement uncertainty	2.41
metrological traceability to a measurement unit	metrological traceability where the reference is the definition of a measurement unit through its practical realisation	2.43
national measurement standard	measurement standard recognised by national authority to serve in a state or economy as the basis for assigning quantity values to other measurement standards for the kind of quality concerned	5.3
primary standard	measurement standard established using a primary reference measurement procedure, or created as an artefact, chosen by convention	5.4
secondary standard	measurement standard established through calibration with respect to a primary measurement standard for a quantity of the same kind	5.5
reference measurement standard	measurement standard designated for the calibration of other measurement standards for quantities of a given kind in a given organisation or at a given location	5.6
working standard	measurement standard that is used routinely to calibrate or verify measuring instruments or measuring systems	5.7
transfer standard	device used as an intermediary to compare measurement standards	5.9
intrinsic standard	measurement standard based on an inherent and reproducible property of a phenomenon or substance	5.10
type-A evaluation of uncertainty	evaluation of a component of measurement uncertainty by a statistical analysis of measured quantity values obtained under defined measurement conditions (see also GUM:2008, 2.3.2)	2.28
type-B evaluation of uncertainty	method of evaluation of uncertainty by means other than the statistical analysis of series of observations (see also GUM:2008, 2.3.3)	2.29
standard measurement uncertainty	measurement uncertainty expressed as a standard deviation (see also GUM:2008, 2.3.1)	2.30

Term	Definition	Reference
combined standard measurement uncertainty	standard measurement uncertainty that is obtained using the individual standard measurement uncertainties associated with the input quantities in a measurement model (see also GUM:2008, 2.3.4)	2.31
coverage factor (k)	number larger than one by which a combined standard measurement uncertainty is multiplied to obtain an expanded measurement uncertainty (see also GUM:2008, 2.3.6).	2.38
expanded measurement uncertainty	product of a combined standard measurement uncertainty and a factor larger than the number one (see also GUM:2008, 2.3.5) NOTE 1: The factor depends upon the type of probability distribution of the output quantity in a measurement model and on the selected coverage probability. NOTE 2: The term “factor” in this definition refers to a coverage factor.	2.35
uncertainty budget	statement of a measurement uncertainty, of the components of that measurement uncertainty, and of their calculation and combination	2.33

The terms and definitions listed above are given in the International Vocabulary of Metrology (VIM (abbreviation for the French term)) - Basic and General Concepts and Associated Terms (BIPM, 2012) and the VIM reference number for each term is indicated. The definitions related to uncertainty of measurement are also explained in the Evaluation of measurement data - Guide to the expression of uncertainty in measurement (GUM) (BIPM-JCGM, 2008).

Chapter 1

Introduction

1.1 Definition of Metrology

Metrology is the science of measurement. It involves the formulation of the theoretical principles related to the definition of the International System of Units (Système International d'Unités, SI) and the development of the technology for realising these units in practise. Seven base units, which by convention are regarded as dimensionally independent (the metre, the kilogram, the second, the ampere, the kelvin, the mole, and the candela), and derived units (those formed by combining base units algebraically according to the fundamental physical relations linking the corresponding quantities), are defined. New measurement techniques, standards, instruments and procedures need to be continuously researched and developed to meet a continuously growing demand for improved accuracy, reliability and rapidity of measurement.

Reliable measurement is important all areas of human activity. Measurement of ionising radiation controls the dose of radiation received by patients treated for cancer, chemical analysis determines if food and drink meet regulations for food safety, water and electricity consumption is metered, food and petroleum are sold by weight or volume, the result of a breathalyser test determines if a law was broken or not, pilots are guided by their instrument panels, manufacturers expect product components to meet stringent tolerances, measurements during production processes controls the quality of the end-product and reduce waste, navigation systems rely on accurate time signals, the reliability of telecommunication systems is ensured by testing the performance of components in fibre optic networks, scientific research relies on measurements to quantify and compare results, and so forth. Decisions are based on measurement results. Incorrect

measurement results can lead to incorrect decisions, which may have significant health, economic or environmental consequences.

1.2 History of Metrology

1.2.1 International Developments

Measurement standards, although in primitive form, have been used by mankind since the earliest organised societies. These rudimentary standards were used to construct ancient dwellings, temples and monuments, to estimate quantities during the exchange of household goods and to administer the prescribed doses of traditional remedies. Length was first measured with the forearm, hand and finger; time was measured by the periods of the sun, moon and other extraterrestrial bodies; the volume of containers were estimated by counting the number of plant seeds used to fill them; and the weight of objects were estimated by comparison to stones or seeds. One of the earliest known units of length is the cubit, which is believed to have originated in Egypt around 3 000 BC. According to the Britannica Encyclopaedia, it is usually considered equal to 457 mm, based on the length of the arm from the elbow to the tip of the middle finger. An ancient unit, which is still in use today, is the carat. It is a unit of mass used to measure the weight of precious gemstones such as diamonds. Originally the carob seed was used as a reference weight due to its uniform size and weight. In 1907 one carat was internationally defined to be equivalent to 200 mg.

Countries, and sometimes even cities, defined measurement units and standards to be used throughout the realm in order to achieve local uniformity in the expression of measurement results to facilitate trade. Some units, such as a unit for length, the foot, was used in different countries, but the sizes of it varied. In pre-revolutionary France, the number of measurement units was exceptionally high in comparison to other industrialised countries. Furthermore, the quantities associated with many of these units varied significantly. This lack of standardisation created opportunities for fraud and was exploited by traders, hindering trade and industrial development. In August 1789, during the French Revolution, the nobility surrendered their privileges, including control over weights and measures. The French revolutionary Assemblée Constituante decided to replace the existing French units of measurement with a completely new system. It was a metric system, which was a practical realisation of the work of three scientists: the Flemish mathematician, Simon Stevin, who employed decimal fractions for the extraction of square roots in 1586; a British clergyman and philosopher, John Wilkins, the first secretary of the Royal Society of London in 1668,

who proposed the idea of a “universal measure” based on natural phenomena and a metric system of units in which length, mass, volume and area would be related to each other; and a French abbot and scientist, Gabriel Mouton, who proposed a decimal system of measurement based on the circumference of the Earth in 1670, which demonstrated the advantages of a system based on nature. The French Revolutionary government adopted a system of 5 measurement units (metre for length, are for area of land, stère for volumes of liquid, gram for mass) on 10 December 1799. Two platinum artefact reference standards for the metre (known as the "mètre des Archives") and the kilogram (known as the "kilogramme des Archives"), respectively, were placed in the French National Archives in the same year (Zupko, 1990).

Since then many countries followed suit and adopted the metric system as their system of measure, including the Netherlands, Germany, Italy, Spain and the Latin American countries. They purchased standard metre bars from France, which were intended to be equal in length to the mètre des Archives. Over time, these artefacts proved to be prone to wear with use and different standard bars would wear at different rates. Furthermore, the standard bars flexed slightly when in use. These concerns about the reproducibility of the standards, which could have led to rival standards being set up, prompted Napoleon III to invite scientists from all other countries to attend a conference in Paris in 1870. The purpose of this conference was to discuss the creation of a new international prototype metre and to arrange a system for comparing national standards to it. On 19 July 1870, two weeks before the conference was due to take place, war broke out between France and Prussia, with the result that only sixteen of the twenty-six countries which accepted the invitation, were able to attend. France was defeated in the war, the prototype copies of the metre and kilogram became under the control of the Third French Republic. In 1872 the new government issued invitations to a diplomatic conference on measurement units addressed to a committee called “Commission Internationale du Metre”. This conference resulted in an international treaty, known as the Convention of the Metre (Convention du Mètre), providing for world-wide uniformity of measurement among its member governments. As this required the support of governments at the highest level, the Convention of the Metre was only signed three years later at another meeting in Paris, France, on 20 May 1875 by seventeen nations. It created the International Bureau of Weights and Measures (BIPM), an intergovernmental organisation under the authority of the General Conference on Weights and Measures (CGPM) and the supervision of the International Committee for Weights and Measures (CIPM) (Hänsch et al., 2007).

Thereafter, the CIPM coordinated the construction of prototype length and mass standards. At the first meeting of the CGPM in 1889, the new international prototypes for the metre and the

kilogram was sanctioned and, together with the astronomical second as unit of time, created the first international system of units. This was known as the MKS system. In 1901, an Italian physicist, Giovanni Giorgi, published a proposal for a measurement system combining the MKS system with a fourth unit to be selected from the electrical units. This proposal was recommended by the CIPM in 1946 and approved by the CIPM in 1948, with the fourth fundamental unit being that of electrical current, the ampere. In 1954, the units for thermodynamic temperature (the kelvin) and luminous intensity (the candela) were added as base units. At the eleventh meeting of the CGPM in 1960, the unit system was named the International System of Units (SI, the abbreviation for “Système International d’Unités”). The present day SI system was defined in 1971 when the base unit for amount of substance (the mole) was added. This brought the total number of base units to seven and these combined with a hierarchy of derived units and quantities provide a coherent system serving society’s measurement needs (Leschiutta & Quinn, 2001).

1.2.2 Units of Measurement in South Africa

The Royal Observatory, which was built in Cape Town in 1820, was the first permanent scientific institute established in South Africa. Later on it shared joint responsibility for the national time standards with the Union Observatory in Johannesburg, which were primarily responsible for providing the national time service since 1910. As a British colony, the system and units of measurement were avoirdupois (i.e. based on a pound of 16 ounces). In 1961, British colonial rule came to an end with the establishment of the Republic of South Africa. British influence on measurement units in South Africa diminished as the metric system was accepted in the mid sixties and rapidly implemented thereafter.

South Africa’s involvement in World War II brought about tremendous growth of its manufacturing industry and with it an appreciation for organised research in support of technological development. General J.C. Smuts, the Prime Minister of the Republic of South Africa from 5 September 1939 to 4 June 1948, recognised the need for scientific leadership and appointed an internationally recognised physicist, Dr Basil Schonland, as the Scientific Advisor to the Prime Minister on 1 January 1945. Dr Schonland’s proposal for a national research organisation, which was to be called the Council for Scientific and Industrial Research (CSIR), was tabled in Parliament in May 1945. The inaugural meeting of this Council was held on 8 October 1945 and Dr Schonland accepted the position of its first President. The National Physical Laboratory (NPL) was one of the first laboratories to be established and Professor Stefan Meiring Naude of the University of Stel-

lenbosch became its Director in January 1946. The NPL was responsible for “the determination of fundamental standards of physical quantities or units as well as research in this context” (Kingwill, 1990). Dr Naude appointed outstanding graduates from South African universities and sent them to selected overseas institutes for training while the instrumentation was being procured. The first calibration certificates were issued in 1947 and this year is taken as the inception of the entity which is presently called the National Metrology Institute of South Africa (NMISA) (McDowell, 1997, p. 16).

In July 1950, Dr Naude wrote to the BIPM to enquire about membership and subsequently recommended to the CSIR President, Dr Schonland, that the South African Government be requested to sign the Convention of the Metre. The request was conveyed to the Department of External Affairs, but the reply obtained was that an investigation should be made as to which government department should assume responsibility. In 1951, the Department of Commerce and Industry was approached to take the necessary steps for accession. The Minister replied that a decision be deferred to February 1952 due to other financial priorities. The immediate need of the NPL for a reference standard for mass was satisfied through purchase of a prototype kilogram (No. 56) in the United Kingdom and subsequent standardisation by the BIPM. The CSIR raised the question of BIPM membership again in 1959 with the Department of External Affairs and offered to pay the membership and initial registration fees. The Minister expressed agreement in principle, but since the government would be joining, the funds had to be made available from government sources. Indications were that Cabinet would consider the matter towards mid 1960, but at this time South Africa’s withdrawal from the Commonwealth was high on the agenda. Membership of the BIPM was only raised again in 1963 in terms of the CSIR’s responsibilities related to the national measurement standards according to the new Act 32 of 1962. Cabinet resolved that South Africa should become a signatory of the Convention of the Metre in 1963 and formal adherence followed in 1964 (McDowell, 1997, p. 24).

1.3 International Organisation of Metrology

The BIPM, established under the Convention of the Metre, is a permanent scientific organisation situated at the Pavillon de Breteuil in the Parc de Saint-Cloud in Paris, France. The status of the BIPM in relation to the French government was formalised in an agreement between the two entities on 25 April 1969. Since then the site has been considered international territory and the BIPM has been afforded the rights of an intergovernmental organisation (Quinn, 1991). Its mandate is to

provide the basis for a single, coherent system of measurements throughout the world, traceable to the SI. This task includes direct dissemination of units (as in the case of the quantities mass and time), coordination of international comparisons of national measurement standards (as in length, electricity and ionising radiation) and performance of measurement science research directed at updating the SI as dictated by the needs of society. The BIPM maintains laboratories in the areas of: mass, time, frequency and gravimetry, electricity, ionising radiation and chemistry. It is financed by the member states and associates, and operates under the exclusive supervision of the CIPM.

The CIPM is appointed by the CGPM and is responsible for planning and executing the decisions of the CGPM. The eighteen members of the CIPM are eminent scientists, each from a different member state under the Convention of the Metre. This committee meets annually and prepares recommendations and financial and administrative reports for submission to the CGPM. Ten consultative committees have been established by the CIPM specifically to advise it on scientific matters related to the various areas of metrology. These committees consist of scientists, mostly from national metrology institutes (NMIs), who study the advances in physics and chemistry that influences metrology. One of the main tasks of the consultative committees is to define, plan and coordinate international comparisons of the national measurements standards of member states in order to assess the degree of equivalence of these standards and to quantify the practical realisation of the units.

The CGPM is the supreme policy and decision making body under the treaty. It consists of delegates from the governments of the member states. Associate states of the CGPM can attend its meetings as observers. Meetings are held every four years to discuss the propagation and improvement of the SI, to endorse the results of scientific resolutions of international scope and to decide all major issues concerning the organisation of the BIPM (including its budget for the next four-year period). A schematic representation of the international organisation of metrology is given in Figure 1.1

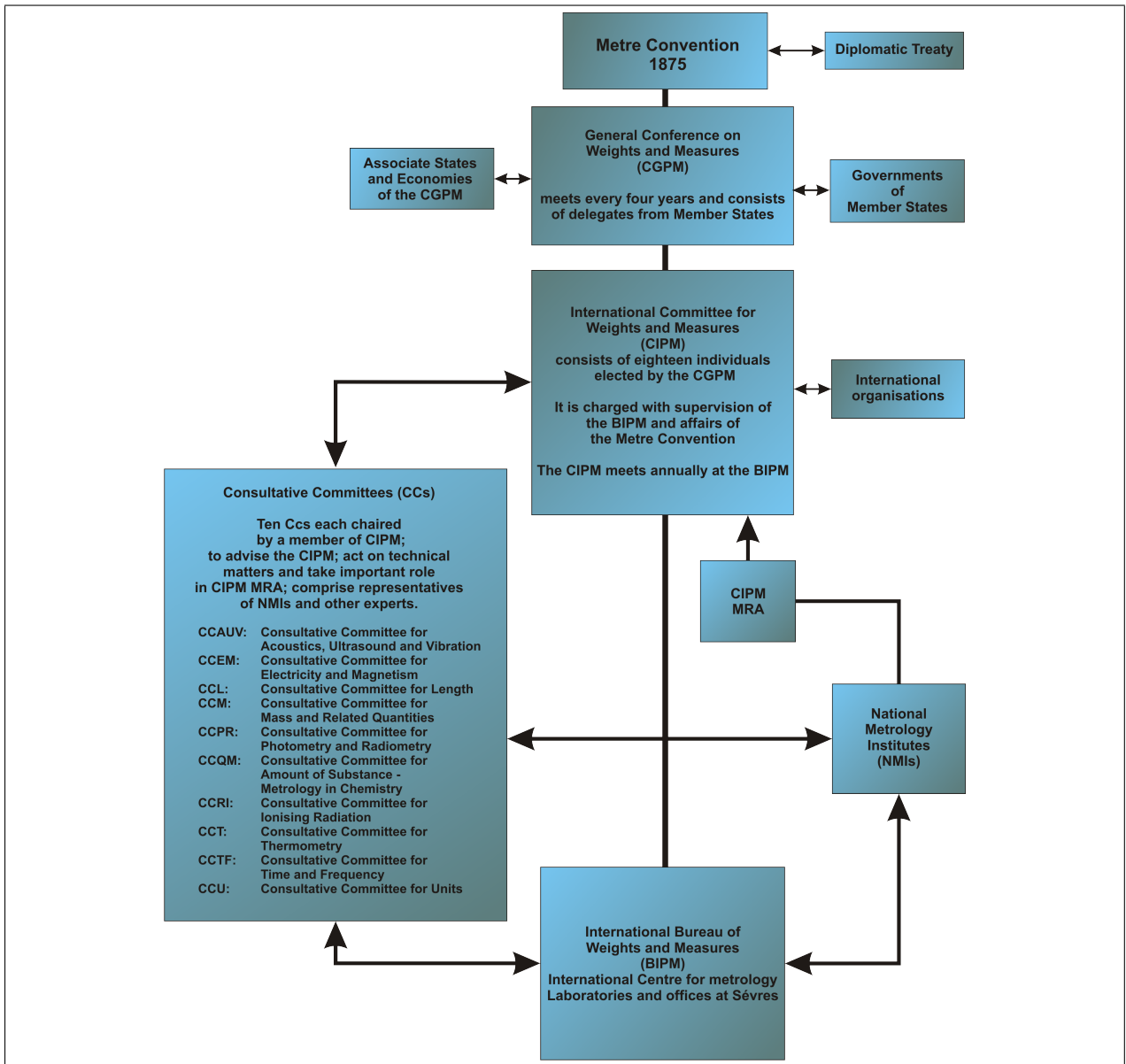


Figure 1.1: Schematic diagram showing the international organisation of metrology

1.4 Problem Statement

Accurate measurements are those which provide a close representation of nature. Also referred to as “absolute” measurements, these are made in terms of units linked to fundamental physics to ensure long-term reproducibility and consistency with measurements made in other areas of

science and technology. The accuracy and precision of a measurement must correspond: if the precision is not sufficient, the measurement result will not be meaningful even if the accuracy is high; conversely, a precise measurement is not correct if the accuracy does not match the precision.

Measurement units defined in terms of material artefacts are not ideal as the long term stability is unknown. The SI unit for mass, the kilogram, is presently the only unit still realised through an international prototype. A major disadvantage of this definition is that the amount of material constituting this prototype changes with time. Over hundred years of observation of the relative mass drift between the international prototype and its copies indicate that the long-term variation in the kilogram could be as much as 5 parts in 10^9 per year. The drift in the unit for mass also influences the stability of the electrical units, which are linked to mass through the definition of the ampere. Although the variation in these units are still not large enough to affect most practical applications, research are under way to define the kilogram in terms of fundamental constants in anticipation of future scientific and technological requirements. The definition of the kilogram is expected to be redefined as soon as the experiments linking the unit for mass to fundamental constants reach a relative uncertainty of $\leq 10^{-8}$ (Hänsch et al., 2007, p. 501).

The definition of the kelvin was given in substance by the tenth CGPM in 1954 and the unit was redefined between 1967 and 1968 to read as follows:

“The kelvin, unit of thermodynamic temperature, is the fraction $1/273,16$ of the thermodynamic temperature of the triple point of water.”

In essence it is defined by assigning the value $273,16$ K to the triple point of water. The triple point can be realised in practice very precisely and reproducibly, using clean glass cells filled with water of specified purity under vacuum (i.e. at its vapour pressure). It would be impractical to measure temperature from first principles over a wide section of the scale, therefore the International Temperature Scale of 1990 (ITS-90), incorporating fixed points and interpolation methods, was constructed to service as the basis for everyday measurement standards (Hänsch et al., 2007, p. 393-448). However, only two fixed points are available above $1\ 000$ °C; namely gold ($1\ 064,18$ °C) and copper ($1\ 084,62$ °C). The temperature range above the silver point ($961,78$ °C) is therefore realised by extrapolation, resulting in large uncertainties (approximately four orders of magnitude greater than that at the triple point of water) (Yamada, 2005). International research effort is focussed on identifying, constructing and characterising fixed points that are sufficiently stable and reproducible to be introduced in a future International Temperature Scale. High temperature fixed

points (HTFPs) using metal-carbon and metal-carbide-carbon eutectic alloys can potentially be suitable for this purpose. Several international studies have shown that some HTFPs (such as Co-C, Pd-C, Pt-C and Re-C) have proved sufficiently reproducible through comparisons and long-term studies to be considered sufficiently well characterised and known. Other fixed points, such as the metal carbide-carbon (MC-C) fixed points, still require further study before temperatures can be assigned to it with acceptable uncertainties. The eutectic fixed points being studied internationally are given in Figure 1.2.

Improved accuracy of realisation of the high temperature scale would also reduce the uncertainty of realisation of spectroradiometric scales (spectral radiance and irradiance), since these scales are linked through Planck's law. A description of the primary spectral irradiance facility being established at the NMISA is given in Appendix A.

The main aim of this study is to demonstrate that reproducible, stable reference standards can be developed for temperatures above the copper point.

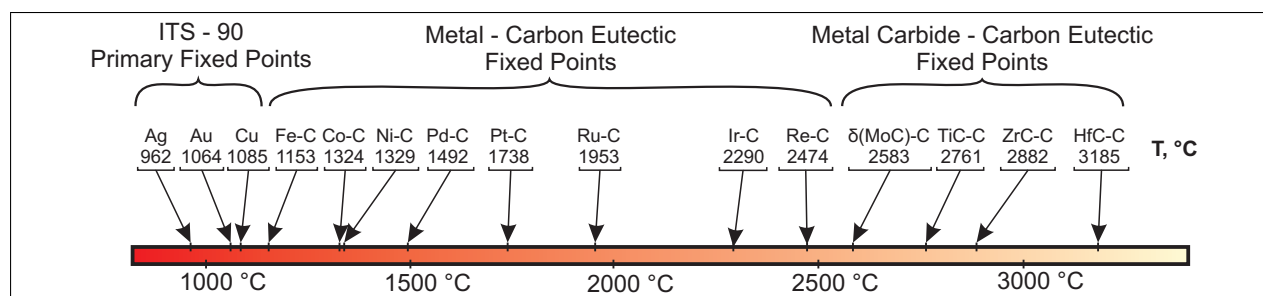


Figure 1.2: Assigned temperatures for ITS-90 HTFPs and approximate transition temperatures for metal-carbon and metal carbide-carbon eutectics

1.5 Literature Review

1.5.1 Introduction

Many NMIs realise the spectral irradiance scale by linking it to a cryogenic radiometer through the use of calibrated filter radiometers. The filter radiometers are used to determine the temperature of a high temperature black body which is then used as a reference source, which spectral radiance can be determined from Planck's equation.

The uncertainty of the temperature measurement makes the most significant contribution to the uncertainty of realising the spectral irradiance scale. HTFPs, above the copper point, can be used to improve these uncertainties. After more than ten years of research, results obtained on metal-carbon eutectic fixed points by several NMIs, showed that these novel high temperature fixed points could lead to significant improvements in high temperature metrology and could be considered as potential fixed points in a future international temperature scale.

In 1996, the joint working group of the Comité Consultatif de Photométrie et Radiométrie (CCPR) and the Comité Consultatif de Thermométrie (CCT) encouraged NMIs to develop high temperature fixed points above 2 300 K with a reproducibility better than 100 mK (BIPM, 1998). Three years later, in 1999, Yamada et al. published the first results of melt and freeze of metal-carbon eutectic points (Yamada et al., 1999). Since then, many NMIs have initiated cooperative projects and comparisons to characterise these points with the aim to reach a consensus on the transition temperatures and implementation procedures.

In order to be accepted as a secondary reference point (SRP), an eutectic point must be highly reproducible. It needs to be demonstrated that different cells, of different designs, filled with metals from different suppliers of different purities are sufficiently reproducible (in the short and long term) to reliably decrease uncertainties of the temperature scale.

Some metal-carbon eutectic points (such as Co-C, Pd-C, Pt-C and Re-C) have reached such a level of confidence and proved sufficiently reproducible, through comparisons and long-term studies, that they should be considered sufficiently well characterised and known. Other fixed points, such as the metal carbide-carbon $\delta(\text{MoC})\text{-C}$ fixed point for radiometry applications, still require further study before temperatures can be assigned to it with acceptable uncertainties.

1.5.2 Eutectic Fixed Points

The word “eutectic” originates from the Greek word “eutektos”, which means “most fusible” or “easily melted”. A binary eutectic phase diagram is observed when two materials are not completely soluble. Figure 1.3 shows a simplified phase diagram for a mixture of substances A and B with an eutectic point at E. The possible phases are: pure crystals of A, pure crystals of B, and liquid with compositions ranging from pure A to pure B. Composition can be expressed as a percentage or as a mole fraction of either one of the two substances, and is depicted on the horizontal axis. Temperature is plotted on the vertical axis (pressure is considered to be constant). The liquidus is the line separating the field of all liquid from that of liquid plus crystals. The solidus is

the line separating the field of all solid from that of liquid plus crystals.

Consider the crystallisation of a liquid with composition X. Since this composition is to the left-hand-side of the eutectic composition, it is referred to as a hypo-eutectic composition. Above temperature T_1 it will be all liquid. As the temperature is lowered to T_1 , crystals of A begin to form. The further the temperature is lowered, the more crystals of A are formed. As a result, the composition becomes more enriched in B. Therefore, as the temperature is lowered from T_1 to T_2 to T_3 down to T_E , the composition will change from point 1 to point 2 to point 3 down to point E, which is the eutectic temperature. This is the point where the maximum number of allowable phases (i.e. liquid, crystals of A and crystals of B) are in equilibrium and this temperature remains constant until one of the phases disappears. It is an invariant point as it occurs under equilibrium conditions at a specific temperature and specific composition which cannot be varied (Woolliams et al., 2006). A similar process follows from a hyper-eutectic composition (to the right-hand-side of the eutectic composition). The eutectic composition solidifies at a lower temperature than all other compositions.

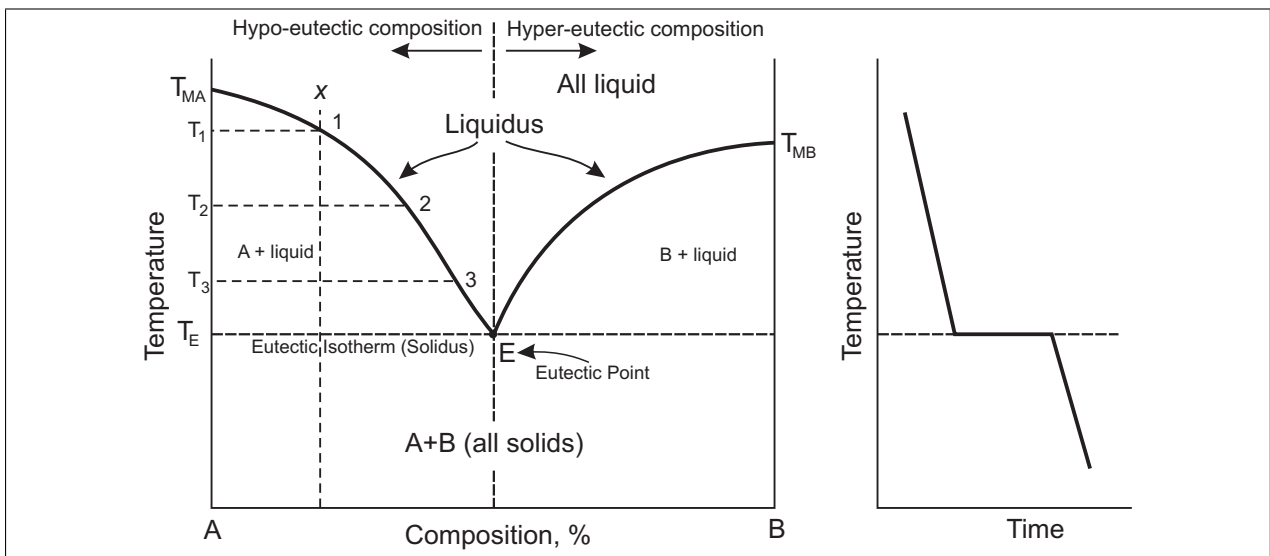


Figure 1.3: Phase diagram for a binary eutectic

The property which makes eutectic alloys feasible as fixed points in a temperature scale is that the lowest point in the liquid phase occurs at a specific composition for eutectic alloys. It means that the freezing temperature cannot be further decreased by carbon contamination (as would happen with a pure metal melted in a graphite crucible). For hypo-eutectic metal alloys the crucible will supply more carbon and the composition reaches that of the eutectic. For hyper-eutectic metal

allows the excess graphite will precipitate during cooling so that the composition again automatically reaches that of the eutectic. Repeatable melting and freezing plateaus should thus be observed. This makes it possible to construct metal-carbon fixed points using graphite crucibles (Yamada, 2005).

Phase transitions for metal carbide-carbon systems are more complex but the process related to the eutectic transition is functionally the same as described above. The eutectic reaction takes place between a metal carbide compound and pure carbon.

1.5.3 Fixed Point Crucibles

Graphite crucibles are constructed such that the eutectic alloy surrounds a black body cavity. A typical design is shown in Figure 1.4. It is made from high purity (0,999 995 or better) graphite and is annealed in an inert atmosphere prior to filling. This is necessary because the graphite wall partially dissolves in the ingot and any impurities within the graphite crucible will contaminate the fixed point. The crucible is filled with a high purity metal powder mixed with high purity graphite powder at approximately the eutectic composition. The filling is done in an argon environment to prevent contamination. The cell is then heated to just above the melting temperature of the eutectic, cooled, refilled and reheated. This cycle is repeated until the crucible is filled and may take between 5 and 25 fills to ensure complete filling.

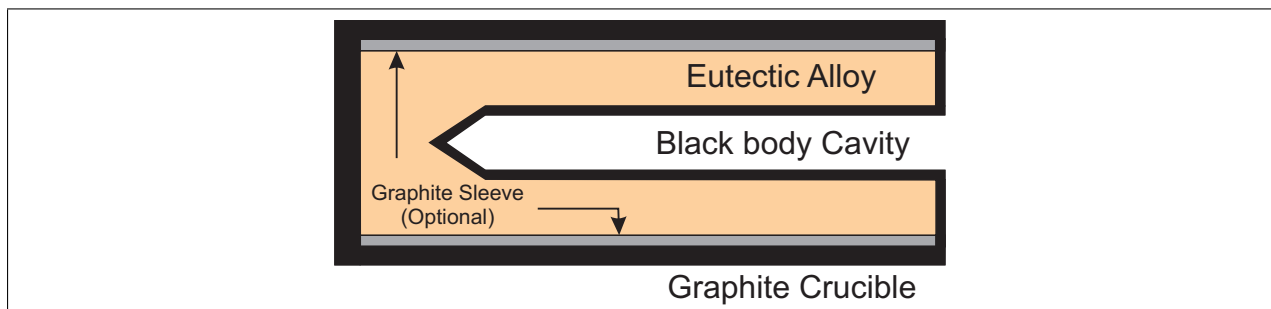


Figure 1.4: A typical design of a eutectic crucible

Some eutectic cells are prone to breaking during the filling process (hairline cracks are formed in the crucible wall). For these cells the coefficient of thermal expansion was found to differ substantially between different grades of graphite. This effect was especially problematic for eutectics with lower coefficients of thermal expansion, such as $\delta(\text{MoC})\text{-C}$, Ir-C and Re-C . A possible solu-

tion implemented by some laboratories was to insert a thin layer of graphite felt inside the cavity wall.

The filled crucible is placed inside a furnace and the furnace temperature is slowly increased up to a few tens of degrees below the melting temperature of the eutectic. Thereafter the temperature is increased to a temperature above the melting temperature and the melt transition plateau is observed. After a few minutes the temperature is reduced to below the freezing point and the cell undergoes super-cooling before the freeze transition plateau is observed.

1.5.4 Phase Transition Temperatures

For metal-carbon eutectics, the melt curve is used as the reference as it was found to be more repeatable than the freeze curve. In practice the melt is not a completely flat plateau. According to theory, the liquidus point (i.e. the temperature at which the last solid melts) should define the unique transition temperature point, but this point is not clearly identifiable due to the influence of furnace effects. Studies showed that the melting range of all eutectics studied thus far exceeds 100 mK (Lowe & Machin (2012)). It raised the question as to which feature of the melt curve should be assigned a temperature. Yamada et al. (1999) defined the point of inflection (POI) of the melting curve as the melting temperature and the most commonly used method to determine it is by calculating the minimum of the first differential of the melting with respect to time. However, different approaches are being used and international consensus needs to be reached on a recommended method before metal-carbon eutectic fixed points can be incorporated into a future temperature scale. Ideally this method should be linked to a feature of the melt curve which can be identified in a reliable and reproducible manner.

A recent study (Lowe & Machin, 2012) investigated the different approaches being used by the various international laboratories and applied these to the melting curves of a cobalt-carbon cell frozen at a wide range of solidification rates under very uniform furnace conditions. Five different approaches have been identified and studied. These included: the determination of the POI of the melting curve; extrapolation to the liquidus temperature just at the end of melting; and three methods based on the analytical Scheil model of solidification, which attempts to identify the liquidus temperature and give an impurity correction. The Scheil model describes the distribution of impurities in a solidified ingot under conditions where solidification is sufficiently slow. The freezing rate typical of many contact thermometry fixed-point realisations is considered to be well described by the Scheil model and it has been shown that a better value for the liquidus temperature

can be obtained than for any point on the freezing curve, even if only partial knowledge of the impurities present is available (Malik et al., 2011). The study found a 70 mK variation in the specification of the melting temperature between the different approaches (not taking the preceding freeze effect into account). This factor will make a significant contribution to the uncertainty of temperature assignment of reference cells and needs consideration. It was recommended that the POI continue to be used as a pragmatic measure of temperature due to its high repeatability (less than 20 mK of the same cell, even at the highest temperatures (Woolliams et al., 2006)) and reproducibility (better than 100 mK between different cells (Lowe & Yamada, 2006)), but that the specified limits approach developed by Bloembergen et al. (2007) be used to define and determine the melting temperature. This approach sets upper and lower limits for the liquidus point (which are determined from the POI) with a rectangular type-B uncertainty.

Temperature gradients within the furnace can affect the length and quality of the plateau shape as well as the measured melting temperature of the eutectic alloy. Furnace temperature uniformity is a critical factor for repeatable and reproducible phase transition plateaus and is therefore of the highest priority in the design of furnaces for eutectic research applications. A comparison of Re-C and TiC-C eutectic fixed point cells between two NMIs (VNIIOFI (Russia) and NMIJ (Japan)) and the BIPM showed that the furnace uniformity (also termed “furnace effect”) can be as high as several hundredths of a degree (Sasajima et al., 2004).

Some NMIs developed furnaces specifically to meet the requirements of eutectics. NMIJ, in collaboration with a Japanese company, Nagano, built high-temperature furnaces for realising HTFPs. These include three-zone furnaces and as well as a compact single-zone furnace, which is transportable. Carbon-fibre-reinforced-carbon-composite heater elements are used to allow it to operate at low currents and high voltages. All components are made of graphite, can operate without a window at the view port and have maximum operating temperatures of 2 500 °C and 2 800 °C, respectively. A three-zone furnace was used to investigate the effect of temperature uniformity on the plateau shape of fixed points. A Cu-point cell with the same dimensions as the eutectic cell was placed inside the furnace and the temperature was varied from -1 °C to +1 °C relative to the melting point. The non-uniformity introduced a break-off point in the middle of the plateau where the temperature started to rise. The same effect was observed when the experiment was repeated with a Ni-C eutectic cell of the same size, although it was not so pronounced as in the case of the very flat plateau of the Cu point. It was concluded that the absence of such a break-off point in the curve can be interpreted as an indication that sufficient temperature uniformity of the furnace has been achieved Yamada et al. (2002).

VNIIOFI is a recognised world leader in the development of variable high temperature black bodies (operating above 2 000 °C) for thermometry and radiometry applications and has supplied black bodies to many NMIs for this purpose. The BB3200pg and BB3500 black bodies have easily been adapted to serve as furnaces for high temperature eutectics. Since these were designed as black bodies, their temperature uniformity is sufficient. VNIIOFI has since developed new furnaces specifically for high temperature eutectics (Ogarev et al., 2004).

Furnaces designed for routine radiation thermometry applications (and therefore made to respond quickly to changes in temperature settings) are not sufficiently uniform for eutectic characterisation. The uniformity of these furnaces can be improved by increasing the amount of insulation by introducing additional radiation shields made of carbon-carbon composite or graphite.

In contrast to binary metal eutectics, metal-carbon eutectics show excellent melting temperature repeatability without taking special precaution to ensure very slow ingot freezing in order to remove sensitivity to the rate of the previous freeze. The plateau shape (and therefore the melt transition temperature) has also not been found to be affected by the rate of heating, although it is inversely proportional to the duration of the plateau. However, the freeze temperature is sensitive to the step change that initiates the freeze transition, but this effect is more pronounced for the lower temperature eutectics such as Fe-C, Co-C and Ni-C.

An exception to the above is the Re-C eutectic, in which case the melt temperature can be affected by the alloy's thermal history. If Re-C is heated to 50 K above the melting point, the subsequent freeze has a super-cool of more than 200 K and the freeze transition takes less than a second. Subsequent melt and freeze cycles have poor phase transition plateaux. It has been solved by overheating by about 30 K, where-after repeatable plateaus have been regained (Woolliams et al., 2006).

The results of direct comparison of metal-carbon eutectics originating from different sources seem to indicate that the melt curve shape may be significantly affected by the impurities in the ingot. A study analysed the purity of two cobalt powders by glow discharge mass spectrometry and found that both samples were less pure than the nominal values given by the manufacturers. The results of the analysis were 0,9988 and 0,999 93 while the manufacturer quoted 0,9999 and 0,999 98, respectively. Eutectic cells were constructed from each of the cobalt samples and the melting temperatures were determined. The measurement repeatability was 40 mK, while the melting temperature of the less pure cell was 130 mK lower (Woolliams et al., 2006).

The magnitude of any impurity effect depends on the type of impurity present as well as on the eutectic material. Elements with similar atomic radii and crystal structures are expected to have

relatively flat melting plateaux, even if the metal is relatively impure. Bloembergen et al (2002) provided a practical description of the effect of impurities on the melting curve of Fe-C. The same author subsequently lead several studies related to the modelling of uncertainties due to impurity effects, leading up to the most recent paper (Bloembergen et al., 2011), which calculated impurity parameters for the impurities detected in the eutectics Co-C and Pt-C and used these to estimate the uncertainty of the eutectic temperatures due to impurities. These eutectics were chosen to make it possible to utilise the software and associated databases (with extensive thermodynamic data) developed by the steel manufacturing industry. It was shown that the impurities dominated the overall uncertainty in determining the melting temperature of Co-C, with the standard uncertainty of the impurity correction amounting to 43 mK. The purity required to attain a standard uncertainty of 10 mK would be 0,999 99 while the actual value was 0,999 89 (Bloembergen et al., 2007). These studies have quantified the effect of impurities to some extent and have provided guidelines as to how to model and estimate the related uncertainties. However, more experimental and practical work is required before a clear conclusion on the effect of impurities on the different eutectics can be reached.

The BIPM (through a joint working group between the CCT and CCPR) set an objective for NMIs to produce stable and robust HTFPs with reproducibility within 100 mK. It means that cells of different designs, constructed in different laboratories with materials from different suppliers, should be in agreement within acceptable uncertainties. Further research is required to gain sufficient knowledge of the sensitivities to impurities, filling procedure and furnace uniformity. A better understanding of these effects is expected to enable improved agreement in comparisons between NMIs.

1.5.5 Measurement of Transition Temperatures

1.5.5.1 Theoretical background

A black body is a hypothetical body which absorbs all incident electromagnetic radiation, regardless of the frequency or angle of incidence, and emits this radiation after reaching thermal equilibrium. In 1900 Max Planck, a German physicist, defined the spectral-energy distribution of radiation emitted by a black body, which became known as Planck's radiation law. He assumed that: the sources of radiation are atoms in a state of oscillation; the vibrational energy of each oscillator is discreet and values in between cannot be assumed; and when an oscillator changes from one energy state (E_1) to another state with lower energy (E_2), a discreet amount of energy (or

quantum of radiation) is emitted, which is equal to $h\nu$:

$$h\nu = E_1 - E_2 \quad (1.1)$$

where ν is the frequency of the radiation and h is Planck's constant ($6,626\ 069\ 57(29) \times 10^{-34}$ J·s). The spectral radiance, $L_{BB,\lambda}$, of a black body, that is the power emitted per unit area per solid angle per unit wavelength interval, is given by Planck's law:

$$L_{BB,\lambda}(\lambda, T) d\lambda = \varepsilon(\lambda, T) \cdot \left(\frac{2hc^2}{n^2\lambda^5} \right) \cdot \frac{d\lambda}{\exp(hc/n\lambda kT) - 1} \quad (1.2)$$

where c is the speed of light in vacuum ($299\ 792\ 458$ m·s⁻¹), k is the Boltzman constant ($1,380\ 6488 \times 10^{-23}$ J·K⁻¹), T is the absolute temperature in kelvin, n is the refractive index of the gas in the optical path, λ is the wavelength in that gas and $\varepsilon(\lambda, T)$ is the spectral emissivity of the black body.¹ This is illustrated in Figure 1.5. Wien's law gives an approximation of Planck's law in the limit $h\nu \gg kT$:

$$L_{BB,\lambda}(\lambda, T) d\lambda = \varepsilon(\lambda, T) \cdot \left(\frac{2hc^2}{n^2\lambda^5} \right) \cdot \exp\left(-\frac{hc}{n\lambda kT}\right) d\lambda \quad (1.3)$$

from which Wien's displacement law can be derived by applying $dL_{BB,\lambda}/d\lambda = 0$:

$$\lambda_{max} = \frac{2897 [\mu m \cdot K]}{T} \quad (1.4)$$

It follows that an inverse relationship exists between the wavelength of peak emission (λ_{max}) of a black body and its temperature (for $h\nu \gg kT$). Equation 1.4 requires the temperature in kelvin and provides the wavelength in micrometer. The Stefan Boltzmann law states that the total black body radiance is directly proportional to the fourth power of the black body's thermodynamic temperature:

¹Emissivity is defined as the ratio of the energy generated from a real body to that radiated from a black body at the same temperature, wavelength and viewing conditions. It is a dimensionless number between 0 (for a perfect reflector) and 1 (for a perfect emitter) (Fukuyama & Waseda (2009)).

$$L(T) = \frac{\epsilon n^2 \sigma T^4}{\pi} \quad (1.5)$$

where σ is the Stefan-Boltzmann constant, equal to $5,670\,373(21) \times 10^{-8} \text{ W}\cdot\text{m}\cdot\text{K}^{-4}$, and given by:

$$\sigma = \frac{2\pi^5 k^4}{15h^3 c^2} \quad (1.6)$$

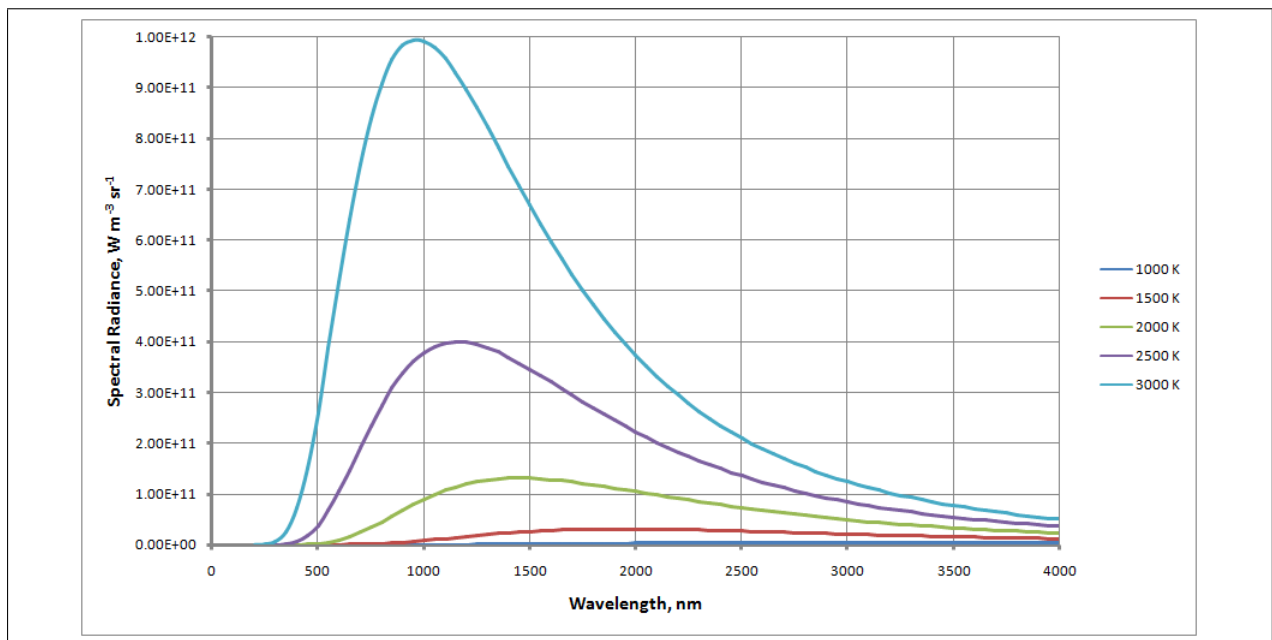


Figure 1.5: Black body radiation spectra for different temperatures

1.5.5.2 Experimental Application of Planck's Law

Linked to ITS-90

For temperatures above the freezing temperature of silver ($961,78 \text{ }^\circ\text{C}$), the ITS-90 is defined in terms of spectral radiance ratio's to one of the silver, gold ($1\,064,18 \text{ }^\circ\text{C}$) or copper ($1\,084,62 \text{ }^\circ\text{C}$) black bodies utilising Planck's law. The unknown temperature of the black body under test can be measured with a pyrometer (an instrument which measures optical radiation and determines the surface temperature of objects at high temperatures (usually $> 600 \text{ }^\circ\text{C}$)) and calculated from the

following radiance ratio:

$$\frac{i_{BB}}{i_u} = \frac{\int r(\lambda) \epsilon_{BB} L_{BB}(\lambda, T) d\lambda}{\int r(\lambda) \epsilon_u L_u(\lambda, T) d\lambda} \quad (1.7)$$

where i denotes the photo-current from the black body with known (BB) or unknown (u) temperatures, $r(\lambda)$ is the spectral responsivity of the pyrometer, ϵ is the emissivity and $L(\lambda, T)$ is the spectral radiance of the respective black bodies. The temperature of the reference fixed points can be extremely well reproduced and determined using the ITS-90 temperature assignments, making this the standard procedure for calibrating radiation sources.

Information regarding the contribution from the surroundings to the measured signal from the target area is required when sources with different size apertures are compared. The detector signal is increased by emission from outside the nominal target size due to aberrations of the optics, light scattering inside or outside the instrument, multiple reflections on surrounding surfaces and diffraction at the system apertures. The dependence of the pyrometer signal on the area surrounding the target area is described as the size-of-source effect (SSE). It is one of the most important systematic errors in the calibration of a pyrometer and needs to be corrected or taken into account in the calculation of the measurement uncertainties. Typical relative standard uncertainty values for SSE for research type pyrometers built and used at NMIs is approximately $7,0 \times 10^{-4}$, which corresponds to an absolute standard uncertainty component of 64 mK at 1 357 K (Cu fixed point), 141 mK at 2 011 K (Pt-C fixed point) and 262 mK at 2 747 K (Re-C fixed point).² In comparison, the combined uncertainty of measurement ($k = 1$) for these fixed points were 190 mK, 418 mK and 77 mK (Lowe, 2013).³ It has been shown that SSE can be reduced to $< 5 \times 10^{-5}$ with commercial achromatic lenses, but even further reductions may be possible with custom lens designs (Yoon et al., 2005). Where possible, large uncertainty of measurement due to SSE can be avoided by calibrating the pyrometer against a black body with the same size aperture as that of the unknown sources to be calibrated.

The black bodies used for radiation thermometry provides a nearly isothermal cavity constructed from material with high intrinsic emissivity, especially when operated above 2 000 K. The emissivity of these blackbodies is typically $> 0,99$ (normally estimated by calculation), but less

²It is calculated from the ratio of the change in pyrometer signal when the size of the source increase or decrease, while the temperature of the black body and the pyrometer focus area remain unchanged.

³The definitions for standard measurement uncertainty, coverage factor (k) and combined standard measurement uncertainty are given in the List of Terms and Definitions.

than 1 due to construction limitations. It is however sufficiently close to ideal as make no practical difference in realising the temperature scale with a standard pyrometer and the ITS-90 fixed points.

Detector linearity is another important consideration in ensuring accurate measurement. The dynamic range of the pyrometer must be such that it accommodates both the reference signal and the signal from the unit under test. This can be tested by using radiance sources with different power output comparing the pyrometer signal to that of a Si diode with known linearity, or by testing the pyrometer's current-to-voltage amplifier using a precision resistor with a current source.

Higher accuracies can be achieved by linking the standard pyrometer to detector scales in stead of to ITS-90. In this case, the radiance responsivity of the pyrometer needs to be known or, alternatively, the temperature of the fixed points can be measured with filter radiometers.

Linked to Primary Standards for Radiance Responsivity

The thermodynamic temperature of the black body cavity can be measured with a filter radiometer, which is directly traceable to a primary standard detector, a cryogenic radiometer. The filter radiometer consists of detector (usually a photo-diode), an interference filter with a bandwidth of 10 nm to 20 nm, and a precision aperture. Measurements can be made either in "irradiance mode", by placing another precision aperture in front of the black body opening, or in "radiance mode" by using a lens and aperture combination to focus radiation from the black body onto the filter radiometer aperture. The photo-current (i) of the filter radiometer with known spectral responsivity, $r(\lambda)$, induced by the spectral radiance at temperature T given by Planck's law, $L(\lambda, T)$, from a source filtered by means of an interference filter having spectral transmittance $\tau(\lambda)$ is given by:

$$i = \pi C \int L(\lambda, T) r(\lambda) \tau(\lambda) d\lambda \quad (1.8)$$

where C is a constant including a geometrical factor, amplifier gain, size-of-source effect and diffraction at the apertures.

For radiometric measurements, even small deviations from an ideal Planckian radiator have to be considered. This is particularly true for deviations of the emissivity from the ideal value of 1. Tests done on the BB3200pg black body found that its emissivity is $> 0,9997$ for all temperatures above 2 500 K (Galal Yousef et al., 2000).

1.6 International Results

After more than 10 years of research by various NMIs, nominal melting temperatures can be assigned to metal-carbon high temperature fixed points (see Table 1.1).

Table 1.1: Nominal Melting Temperatures for Metal-Carbon and Metal-Carbide-Carbon Eutectics

Eutectic	Approximate Melting Temperature (K)	Approximate Melting Temperature (°C)
Metal-carbon eutectics		
Fe-C	1426	1153
Co-C	1597	1324
Ni-C	1602	1329
Pd-C	1765	1492
Rh-C	1930	1657
Pt-C	2011	1738
Ru-C	2227	1954
Ir-C	2565	2292
Re-C	2747	2474
Metal-carbide-carbon eutectics		
B ₄ C-C	2659	2386
δ(MoC)-C	2856	2583
TiC-C	3032	2759
ZrC-C	3155	2882
HfC-C	3458	3185

Sadli et al. (2004) defined the following criteria for a HTFP to be accepted as a SRP:

- the SRP must be highly reproducible;
- there should be more than one experimental measurement of the value of the temperature;
- an estimate of the uncertainty of the assigned temperature should be given;
- the purity of the material corresponding to the assigned temperature should be stated; and
- references to the original experiments should be given.

An additional requirement that the impurity amount in the metal should not be lower than 4N, was added because this can affect the quality of the plateau and the melting temperature. According

to these criteria, only four eutectics are recommended as SRPs (see Table 1.2). The temperature is simply the mean of reported readings and the uncertainty is only a statistical estimate with the standard deviation of the reported temperatures (excluding outliers attributed to poor-purity cells). The temperature assignments and associated uncertainties given are considered to be a provisional list and further research by NMIs is required to refine the data.

Table 1.2: Provisional recommended temperatures for a selected set of HTFPs

HTFP	Thermodynamic Temperature (°C)	Uncertainty ($k = 2$)°C
Co-C	1 324,0	0,6
Pd-C	1 491,7	0,7
Pt-C	1 737,9	0,6
Re-C	2 474,2	1,0

The CCT has established a working group (CCT WG 5) to investigate and make recommendations regarding the realisation and dissemination of thermodynamic temperature above the silver point (1 234,93 K). It expected that the subset of HTFPs given in Table 1.2 will have final thermodynamic temperatures, with their associated uncertainties, assigned within the next five years under the research plan of CCT WG 5. This will be followed by all HTFPs from Table 1.1 which proof to be of utility. It is envisaged that primary methods of realising thermodynamic temperature above the silver point by interpolation between two or more fixed points, will be implemented.

1.7 Objectives

The objectives set for this project are to:

- develop the capability to construct metal-carbon eutectic fixed points, which could be used as high temperature reference standards, at the NMISA;
- characterise the phase transition characteristics of the constructed eutectic cells to determine its suitability as reference standards in terms of reproducibility and stability;
- assign temperature values to the melt and freeze points of the eutectics and compare these values with published values from other NMIs, in order to validate results;

- demonstrate that these high temperature reference standards can reduce the uncertainty of realisation of spectroradiometric scales (spectral radiance and irradiance) and make recommendations for implementation; and
- contribute to the international effort to gain sufficient data from research results by NMIs in order to implement appropriate high temperature fixed points into a future international temperature scale, by publishing the results.

1.8 Significance and Relevance of Research

Sources of optical radiation can be calibrated in terms of spectral irradiance (250 nm to 1 300 nm) by the NMISA. Specific parameters can be derived from the spectral data, namely colour temperature, colour coordinates and effective erythemal irradiance (ultra-violet sources). Spectral irradiance measurements are required by the aerospace, defence, agriculture and medical industries for spectroradiometric analysis of solid state lighting, lamps, flat panel displays and other radiant sources, as well as solar radiation.

Currently, the NMISA imports traceability for spectral irradiance by sending the primary standard lamps to another NMI for calibration. The uncertainties of calibration are 4 % to 8 % ($k = 2$) over the wavelength range of 400 nm to 1 500 nm. A primary spectral irradiance facility is being developed, which will allow the NMISA to realise the scale independently, eliminating the need to import traceability from overseas NMIs. Through developing this facility, the NMISA aims to achieve an uncertainty of < 1 % over the visible wavelengths. The preliminary design of the facility has been completed and will be refined over the next three years as the facility is built, tested and implemented.

Realising a scale from fundamental physical principles allows a NMI to take part in the international CIPM key comparisons for that parameter. Participation is open to those laboratories having the highest technical competence and experience in that field, as this type of comparison leads to a key comparison reference value, which is considered to be a close approximation of the corresponding SI value. The results of CIPM key comparisons are published in an international journal (Metrologia Technical Supplement) and support the calibration and measurement capability (CMC) claims by NMIs (published in the BIPM Appendix C database, which is also publicly available). Results which successfully demonstrate international equivalence of the NMISA's national measurement standards, endorse user confidence in the institute's measurement capability.

ies. Through a calibration service offered to commercial calibration laboratories, traceability to the NMS is disseminated to industry, enabling a sound measurement infrastructure within South Africa. It brings about readily acceptance of the country's measurement results, both locally and internationally. It fosters a perception of quality of locally produced goods and in turn enhances the competitiveness of South African companies, benefiting the economy.

It is important to note the contribution of a sound metrology infrastructure to the removal of technical barriers to trade (TBTs). Since measurement plays an integral part in production processes and in trade, the need for measurements can be applied as a TBT. For example, national regulations can require traceability to a specific NMI, or very small measurement uncertainties requiring sophisticated measuring instruments and expertise. This is resolved by ensuring that measurements made in different parts of the world, traceable to different NMIs, can be demonstrated to be equivalent in a clear, transparent and reliable manner (this is the purpose of the CIPM Mutual Recognition Arrangement (MRA)).

A robust technical infrastructure (including standardisation, accreditation, quality assurance and metrology) also play an integral role in protecting citizens (and the environment) from unsafe and low-quality imports. Unless appropriate standards, regulation and testing capabilities are implemented, the country can become a dumping ground for inferior products and hazardous waste. A relevant example is solid state lighting (such as light emitting diodes (LEDs)) products. A LED is currently the most energy efficient light source. Government initiatives and incentives to drive energy saving measures cannot be successful unless the performance of such (imported and locally assembled) products can be verified. It ensures that compliant manufacturers remains economically competitive and that the quality of lighting required by humans to perform daily activities efficiently is not compromised. The measurement expertise and traceability to NMS (spectral irradiance) necessary to achieve this, is provided by the NMISA and is supported by this study.

1.9 Scope of Study

The aim of this study is to investigate the phase transition temperature characteristics of selected eutectics constructed from materials with given specifications. The intrinsic material properties (including interactions between the graphite crucible and eutectic material, and the influence of impurities) was not investigated. The main objective of this work is to examine the reproducibility of the melt and freeze temperatures of eutectics constructed from readily available materials with specifications similar to those used by other NMIs for the same purpose. These results can then

contribute to the international metrology community's collective knowledge of the melt and freeze temperature characteristics of the specific eutectics, which will inform the selection of secondary reference points for a future international temperature scale. Once such reference points have been formally approved, further reduction of its uncertainty of measurement of the melt temperatures could be attempted by studying the intrinsic material properties in order to quantify their effect on the phase transition temperatures.

1.10 Structure of Dissertation

An introduction to the research work presented in this dissertation, is given in Chapter 1 (above). It provides a definition of metrology and explains the importance of reliability of measurement results in all spheres of human activity. These concepts are further developed by a summary of the international history of metrology and concurrent development of units of measurement in South Africa from the early twentieth century onwards. It demonstrates how measurement units and standards were continuously developed in response to growing economic, social and scientific requirements. The chapter also includes an explanation of the international organisation and co-ordination of metrological activities, which facilitate accomplishment of international equivalence of national measurement standards.

This outline sets the background for defining the research problem statement: the requirement for and development of reproducible and stable high temperature fixed points in order to improve the accuracy of realisation of the high temperature scale and subsequent reduction of the uncertainty of realisation of the spectroradiometric scales.

A literature review presents this study in the wider research context. It gives a scientific introduction to high temperature metal-carbon fixed points (eutectics) and explains its potential solution to the problem statement. Recent international research findings, on-going investigations and open questions for further study are discussed. Whilst some metal-carbon eutectic points are showing promising results in terms of being sufficiently reproducible to be considered adequately characterised and known, others still require further study before temperature values can be assigned to it with acceptable uncertainties. Provisionally proposed melt temperatures with associated uncertainties for selected eutectics, resulting from international research efforts, are given.

The objectives set for this study are stated and all key concepts and terms are defined and explained. This chapter concludes with a structure of the dissertation.

The experimental procedure is outlined in Chapter 2. The rationale behind selecting Re-C and

$\delta(\text{MoC})\text{-C}$ eutectics for investigation is explained. Materials used to construct the selected eutectic cells are specified and the procedure for preparing these cells are described. The equipment, experimental configuration and method used to measure the phase transition temperatures of the eutectic cells are given in detail. References are made to traceability to national measurement standards to give confidence in the reliability of results.

The results of measurement of melt and freeze temperatures for the eutectics are presented and analysed in Chapter 3. The uncertainty of measurement is investigated and estimated in order to quantify the accuracy of results and to allow for comparison with results published by other NMIs.

The evaluation and interpretation of results in relation to internationally published findings follow in Chapter 4.

Finally, Chapter 5 summarises and concludes the dissertation addressing the objectives stated in Chapter 1. It also highlights possible industrial applications and makes suggestions for future work.

Chapter 2

Experimental Procedure

2.1 Selection of Eutectics

Incandescent lamps are used in many indoor lighting applications and are therefore of important interest in the field of photometry. The International Commission on Illumination (CIE - French abbreviation) defined a standard light source (CIE Standard Illuminant A) to be used in all applications of colorimetry involving incandescent lighting (CIE (2007)). NMIs use standard luminous intensity lamps at a colour temperature of 2 856 K for photometric measurements as the best approximation of incandescent lamps. The expected melt temperature for the $\delta(\text{MoC})\text{-C}$ eutectic is 2 586 K and is therefore of special interest for photometry. For this reason, $\delta(\text{MoC})\text{-C}$ eutectics were selected for investigation.

Since only one published melt temperature value for $\delta(\text{MoC})\text{-C}$ eutectics was available at the start of this study, it was necessary to construct a eutectic more extensively studied internationally in order to compare and verify the new NMISA capability. According to literature, Re-C eutectics were the most promising option at the time and was therefore also selected. Should the more uncertain $\delta(\text{MoC})\text{-C}$ eutectic prove not to be a suitable reference point, the Re-C eutectic could be an alternative for NMISA as its expected melt temperature is only 109 K lower. Re-C is the metal-carbon HTFP with the highest melt temperature, allowing interpolation from the copper point over the full temperature range required for NMISA applications.

2.2 Eutectic Cell Preparation

Graphite crucibles supplied by VNIIOFI and designed to fit into the high-temperature black body BB3200pg (used as a furnace), were used. The cells were made from fine-grained pure (> 99,9995 %) graphite. The construction was similar to the eutectic-containing crucibles commonly used by NMIs and was cylindrical, with a length of 54 mm and a diameter of 24 mm. The black body cavity in the centre of the cylindrical crucible had a depth of 35 mm, a diameter of 4 mm and was conical at the bottom. The emissivity of the cavity was taken as 0,9995 based on estimations done by Hanssen et al. (2005) using the Monte Carlo method and assuming an isothermal cavity surrounded by graphite walls with a 0,15 % diffuse reflection. The design specifications for the crucible are given in Table 2.1.

Table 2.1: Crucible specifications

Parameter	Value
Cell diameter	24 mm
Cell length	54 mm
Cavity diameter	4 mm
Cavity depth	35 mm
Bottom type, angle	Conical, 120°
Emissivity	0,9995

The crucible was fitted with a plug at the opposite end of the cavity opening to enable filling with eutectic. An internal graphite sleeve, as was proposed by the National Physical Laboratory (the NMI for the United Kingdom), was added to the crucible used for the $\delta(\text{MoC})\text{-C}$ eutectic alloy to prevent the crucible from cracking (Lowe & Machin (2002)). A diagram showing the crucible dimensions is given in Figure 2.1 and images of the crucibles used are shown in Figure 2.2.

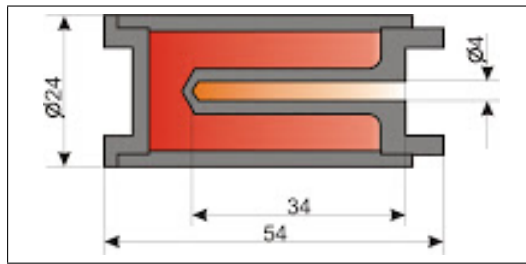


Figure 2.1: Crucible dimensions

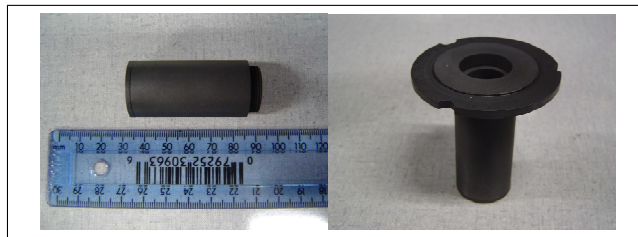


Figure 2.2: The left image depicts the crucible (with the plug on the left-hand side). The right image depicts a carbon ring attached to the right-hand side of the crucible to enable fitment inside the black body.

Pure carbon (99,9999 %) and metal powders (99,999 %) were used to prepare the eutectic mixture. Table 2.2 shows the material purities and mixture proportions for each type of eutectic. The metal and graphite powders were supplied by the company “Alfa Aesar”. The purity specifications shown in the table were provided by the supplier. The powders were mixed in an air-tight “glove-box” in an argon atmosphere as shown in Figure 2.3.

Table 2.2: Material specifications and powder mixing proportions

Material	Purity	Proportion of Graphite in Mixture (per weight)
Rhenium (Re)	99,999 % (5N)	1,0 - 1,5 %
Molybdenum (Mo)	99,999 % (5N)	~ 10 %
Graphite powder	99,9999 % (6N)	n/a
Solid graphite (crucible material)	99,9995 % (5N5)	n/a

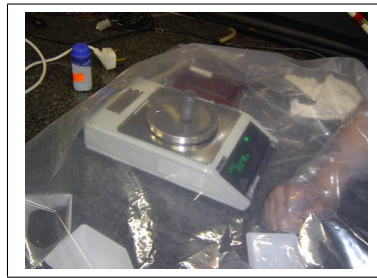


Figure 2.3: Filling and weighing of crucibles in an argon environment

The NMISA's BB3200pg black body (purchased from VNIIOFI) was used as a furnace for these investigations. This black body was developed to achieve better accuracy of spectral radiance measurements in the ultra-violet wavelength region. The schematic layout of the BB3200pg black body is shown in Figure 2.4. The radiating cavity is assembled from pyrolytic graphite rings with inner and outer diameters of 40 mm and 54 mm, respectively, arranged to give a total cavity length of 200 mm. Pyrolytic graphite is an an-isotropic refractory material, having high electrical resistance along the layers and high thermal conductivity across the layers, therefore keeping temperature variations within the cavity small. This material provides a longer service life at high temperatures. The maximum operating temperature of the BB3200pg is 3 200 K and the expected service life at this temperature is 100 hours. The design allows the replacement of individual rings after prolonged operation and not the whole cavity. The nominal effective emissivity is 0,999 at 500 nm.

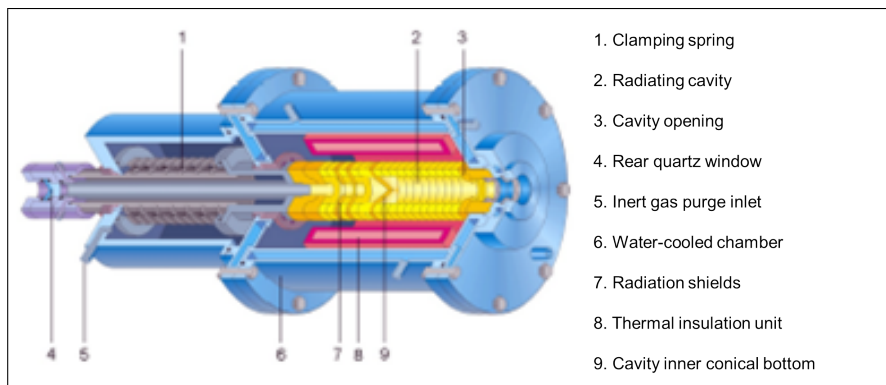


Figure 2.4: Schematic layout of the high temperature BB3200pg black body

A picture of the NMISA's BB3200pg black body is shown in Figure 2.5. As described above, its main cavity consists of a cylinder made from pyrolytic graphite rings (shown in Figure 2.6),

which are heated directly by electrical current. The eutectic cell is mounted inside this cavity and is heated radiatively.

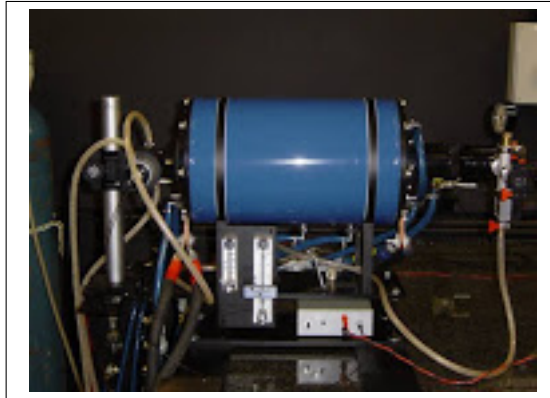


Figure 2.5: NMISA's high temperature black body (BB3200pg)



Figure 2.6: Main cavity of the black body, consisting of graphite rings

The empty crucible and black body were purified by annealing above the eutectic material melting temperature (at approximately 2 800 K) for 1 hour. It was then filled with a metal-carbon powder mixture in an argon atmosphere and placed inside the black body (in the centre of the main cavity with the plug facing the opening) operated in a vertical position as shown in Figure 2.7. The black body cavity was purged with argon to prevent electrical arcing while heated to melt the powder mixture to form the eutectic alloy. The filling process involved heating the crucible with the power mixture to approximately 20 K above the eutectic melting point, cooling to room-temperature, re-filling with the powder mixture and re-heating to approximately 20 K above the

melting point. This process was repeated until the space surrounding the cavity was completely filled with the eutectic alloy, as illustrated in Figure 2.8. Between 8 (typical for $\delta(\text{MoC})\text{-C}$) and 20 (typical for Re-C) mixture-adding and melting cycles were necessary to fill each crucible completely (taking up to one month per eutectic).



Figure 2.7: Black body operated in a vertical position while filling the crucible with the eutectic alloy

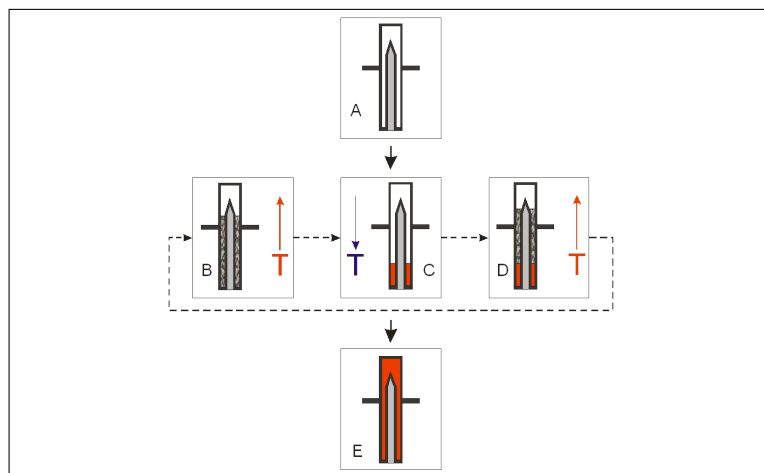


Figure 2.8: A schematic illustration of the eutectic filling procedure. The crucible is filled with a mixture of the carbon and metal powders at the eutectic composition (A); heated to approximately 20 K above the eutectic melting point (B); cooled to room-temperature (C), re-filled with the powder mixture and re-heated to approximately 20 K above the melting point (D). This process (B to D) is repeated until the space surrounding the cavity is completely filled with the eutectic alloy (E).

Two Re-C eutectic cells, denoted Re-C (1) and Re-C (2), respectively, and two $\delta(\text{MoC})\text{-C}$ eutectic cells, denoted $\delta(\text{MoC})\text{-C}$ (1) and $\delta(\text{MoC})\text{-C}$ (2), respectively, were constructed.

2.3 Experiment and Method

2.3.1 Fixed Point Measurement Configuration

2.3.1.1 Measurement of the phase transition plateaux

A linear pyrometer (LP4), calibrated by the Physikalisch-Technische Bundesanstalt (PTB) in Germany, was used to measure the phase transition temperatures of the eutectic cells. It was operated with an internal interference filter with an effective wavelength of approximately 650 nm and a bandwidth of approximately 20 nm. The LP4 was focussed on the eutectic cell aperture plane at a target distance of 750 mm. An image of a LP4 radiation thermometer is shown in Figure 2.9 and a schematic presentation of the optical configuration is given in Figure 2.10.



Figure 2.9: A picture of the NMISA's LP4 radiation thermometer supplied by IKE (Stuttgart, Germany)

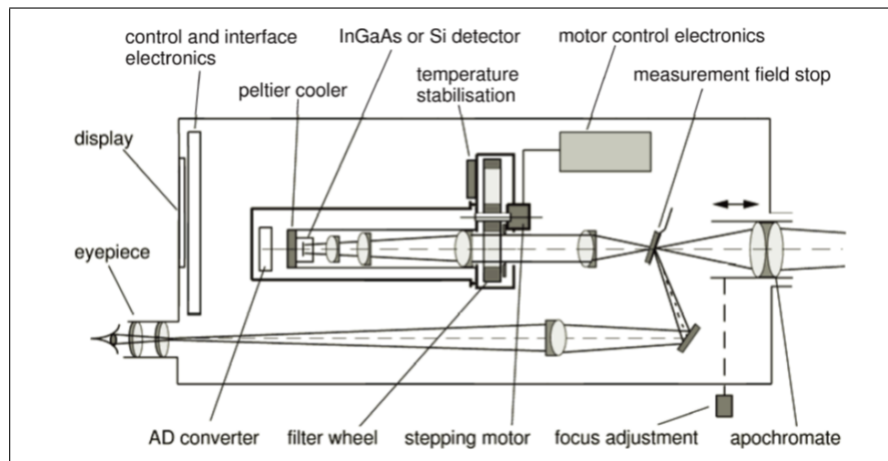


Figure 2.10: A schematic presentation of the optical configuration of the LP4 radiation thermometer

2.3.1.2 Measurement process

In order to measure the phase transition characteristics of the eutectic cells, the black body was operated in a horizontal position. The crucible was placed inside the black body cavity, at the centre, with the crucible cavity facing the detector (LP4). This configuration is shown in Figure 2.11.

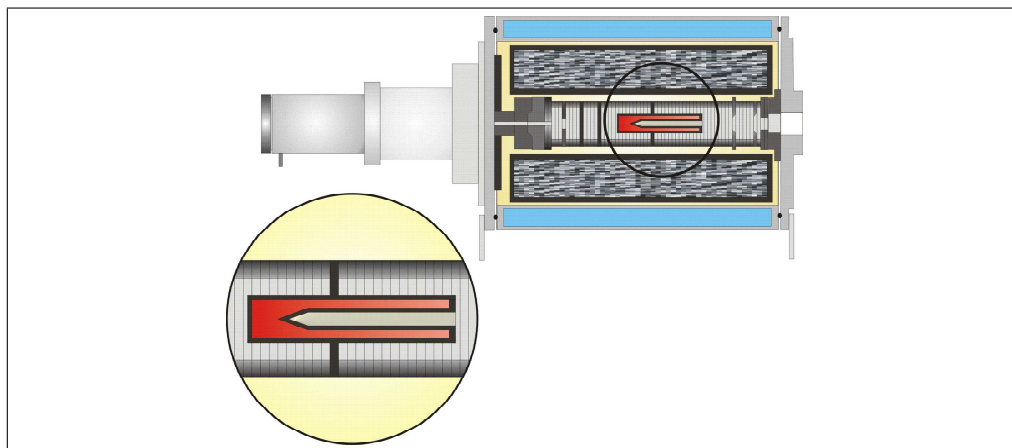


Figure 2.11: The position of the eutectic cell inside the black body furnace during measurement of the phase transition plateaus

The black body was heated to approximately 20 K below the expected melt temperature of the eutectic material. Once the system had stabilised at this temperature, the current supply to the

black body was increased and the eutectic melt was observed as a plateau on the eutectic cavity's temperature versus time diagram. The melt finishes with a break-off point followed by a sharp temperature rise from the plateau to the set temperature of the black body. The system was again stabilised at approximately 20 K above the melt temperature. Thereafter, the current supply to the black body was decreased to reach a temperature below the freezing point of the eutectic material. The freeze plateau was observed, usually after undergoing super cool. The temperature of the system was stabilised at approximately 20 K below the freeze temperature before the next cycle was started. This process is shown in Figure 2.12.

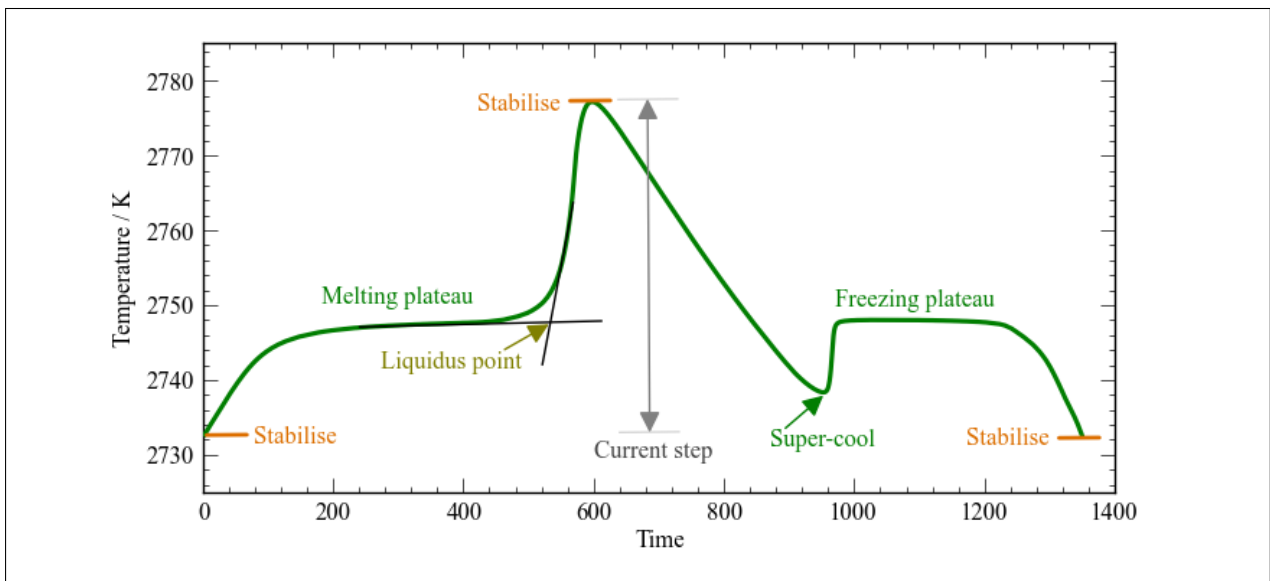


Figure 2.12: Observation of melt and freeze phase transitions

The unique temperature at which the eutectic material melts is the liquidus point. It is defined as the maximum temperature at which crystals can be present in the melt at thermal equilibrium (i.e. it is the temperature at which the last solid melts) (Callister (2007)). In practice, the presence of impurities in the eutectic material obscures the liquidus point. The point of inflection (POI) of the melting curve has been found to be a reproducible indicator of the melting temperature (Lowe & Machin (2012)) and has been used in most studies.

Chapter 3

Results and Data Analysis

3.1 Phase Transition Curves Obtained

If a mixture of a pure metal and pure carbon at the eutectic composition is heated under near-equilibrium conditions from the solid state and its temperature is plotted as a function of time, the resulting heating curve will show a plateau at a constant temperature (the liquidus temperature), the ends of which correspond to the start and end of liquidisation. Similarly, if a eutectic alloy in the liquid phase is cooled below its freezing temperature, the temperature versus time curve also shows a plateau. As was observed in this study, the liquid may cool to a temperature below its freezing point before solidification occurs (a feature referred to as “super-cool”). Once solidification begins, the temperature rises to the freezing point and remains constant until solidification is complete. The presence of impurities results in distortion of the plateau shape. The melting and freezing curves for the Re-C and $\delta(\text{MoC})\text{-C}$ eutectics obtained in this study are discussed below.

3.1.1 Re-C Eutectic Cells

The phase transition temperatures of the Re-C (1) and Re-C (2) eutectic cells were measured over 3 (13 melt-and-freeze cycles) and 4 (14 melt-and-freeze cycles) days, respectively. A typical melt-and-freeze cycle for Re-C eutectic cells is shown in Figure 3.1. A temperature plateau indicates a phase transition.

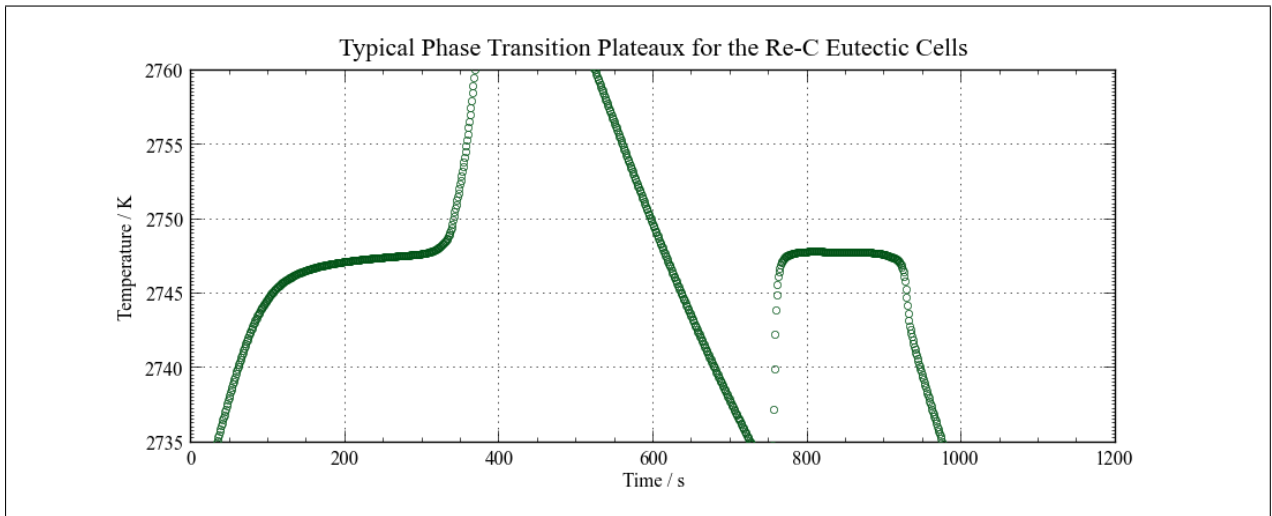


Figure 3.1: Typical phase transition plateaux observed for a Re-C eutectic cell

A melting plateau observed for the Re-C (1) cell is shown in Figure 3.2. The first derivative of melting temperature with respect to time is shown in Figure 3.3. The melt temperature is by definition the minimum value of this curve (i.e. the POI) and has been estimated after applying a moving average curve smoothing technique.¹ It was found that visual estimation of the POI corresponds very well (within the stated uncertainty of measurement) with the mathematical results and therefore curve smoothing was applied mostly for verification purposes.

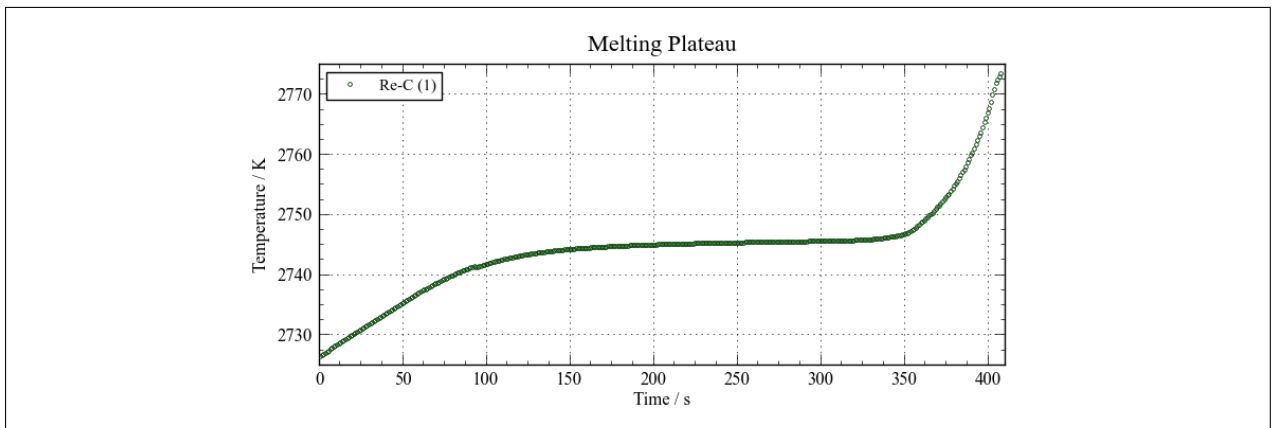


Figure 3.2: A typical melting plateau observed for Re-C eutectic cells

¹CurveExpert Professional v2.2.0 was used to calculate moving averages with a rectangular, centred averaging window.

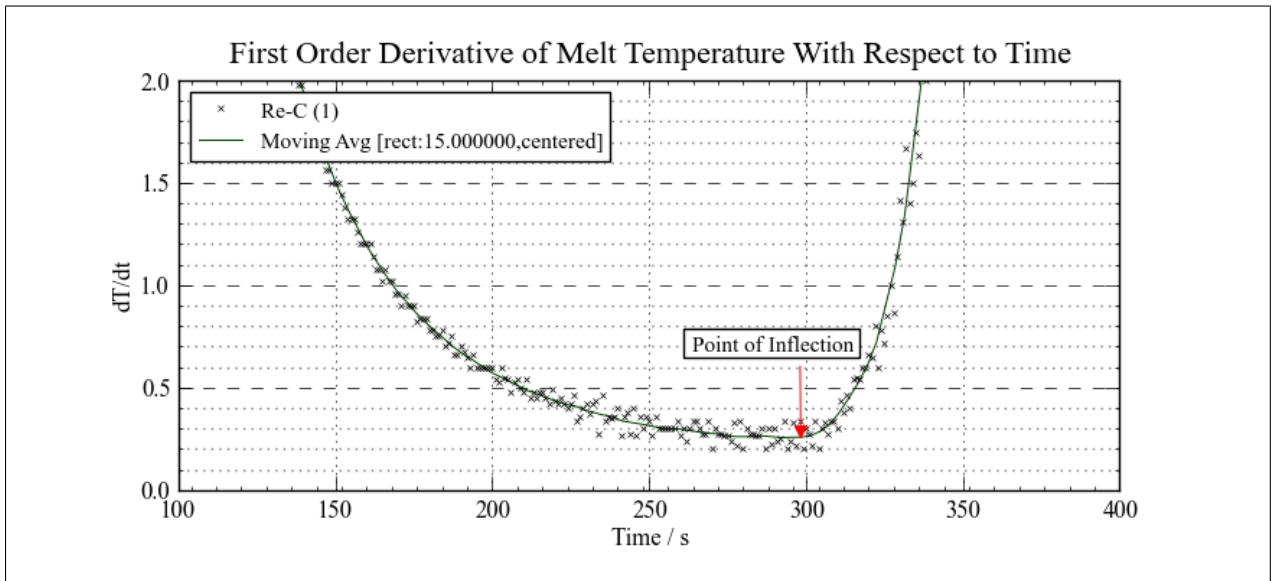


Figure 3.3: Determination of the point of inflection of the melting plateau for a Re-C eutectic cell

A typical freezing plateau for the Re-C eutectic cells is given in Figure 3.4. The freeze temperature is taken as the maximum value on the curve (curve fitting was not required).

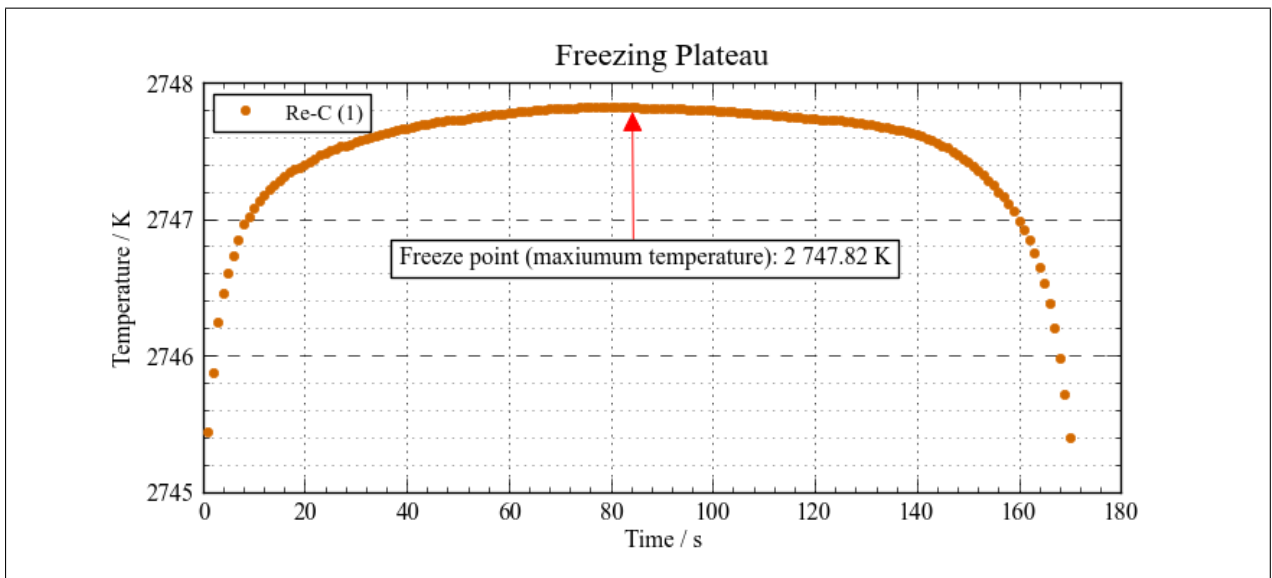


Figure 3.4: A typical freezing plateau observed for Re-C eutectic cells

At first, measurements were performed on the Re-C (2) eutectic cell. In order to utilise the existing measurement configuration, the LP4 was initially (over day 1 and 2) focussed on the

eutectic cell aperture plane at a distance of 1 m, with a cylindrical eutectic holder which did not allow convenient alignment. It was thus decided to adapt the measurement set-up to specifically accommodate the measurement of eutectics. The distance between the LP4 and eutectic cell was changed to 750 mm and the cylindrical crucible holder was replaced with a ring-holder (shown in Figure 2.2). All subsequent measurements were performed in this measurement configuration. The measurement results for all melt-and-freeze cycles per day for each eutectic cell, are presented graphically in Figures 3.5, 3.6, 3.7 and 3.8.

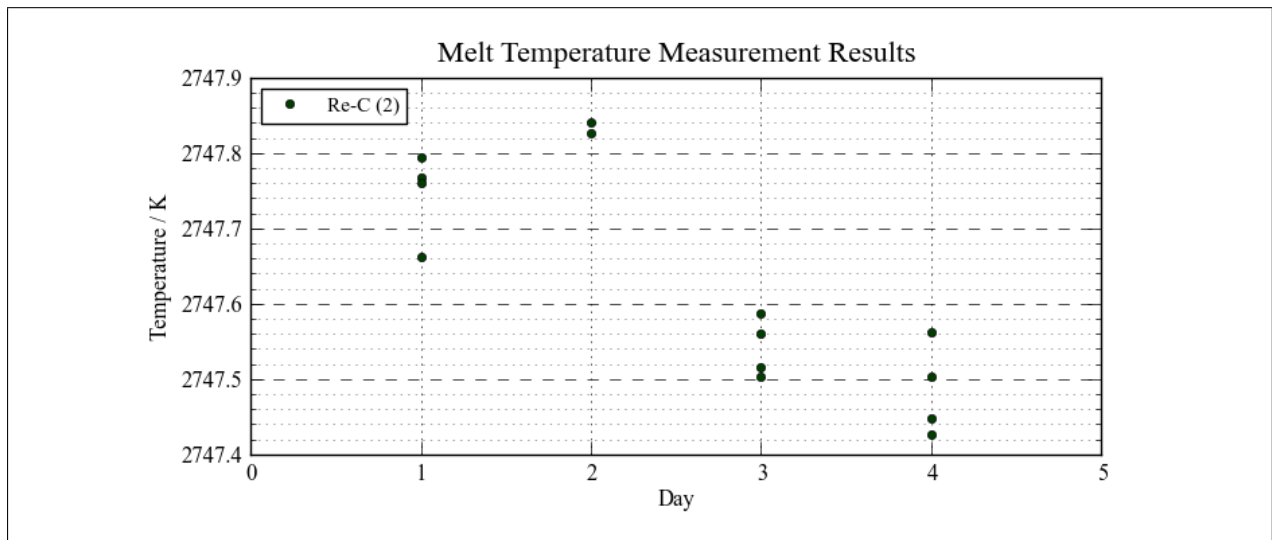


Figure 3.5: Melt temperatures of the Re-C (2) cell measured over four different days

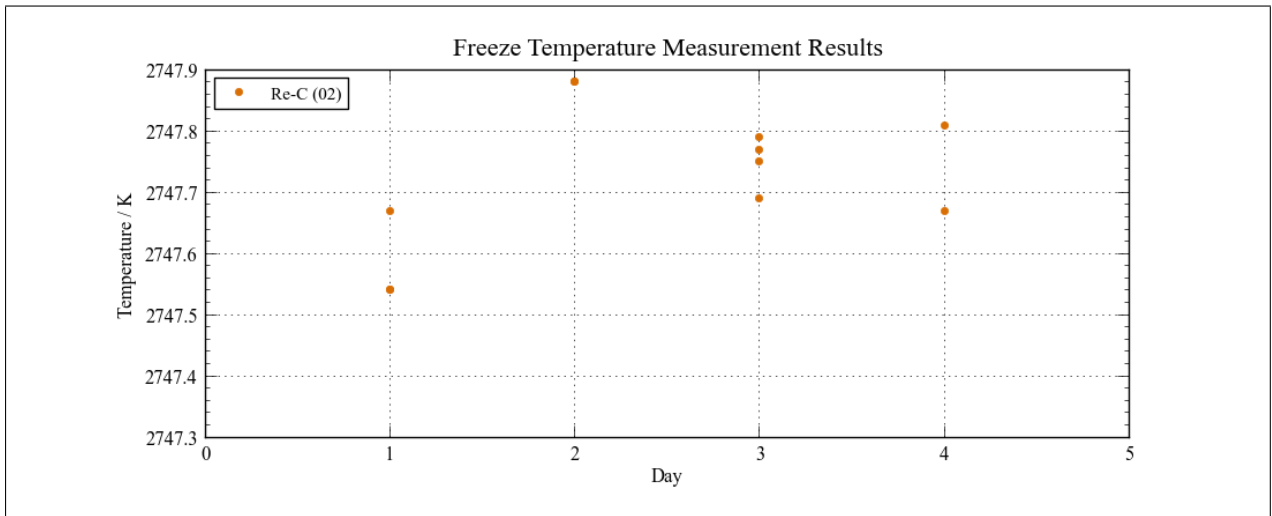


Figure 3.6: Freeze temperatures of the Re-C (2) cell measured over four different days

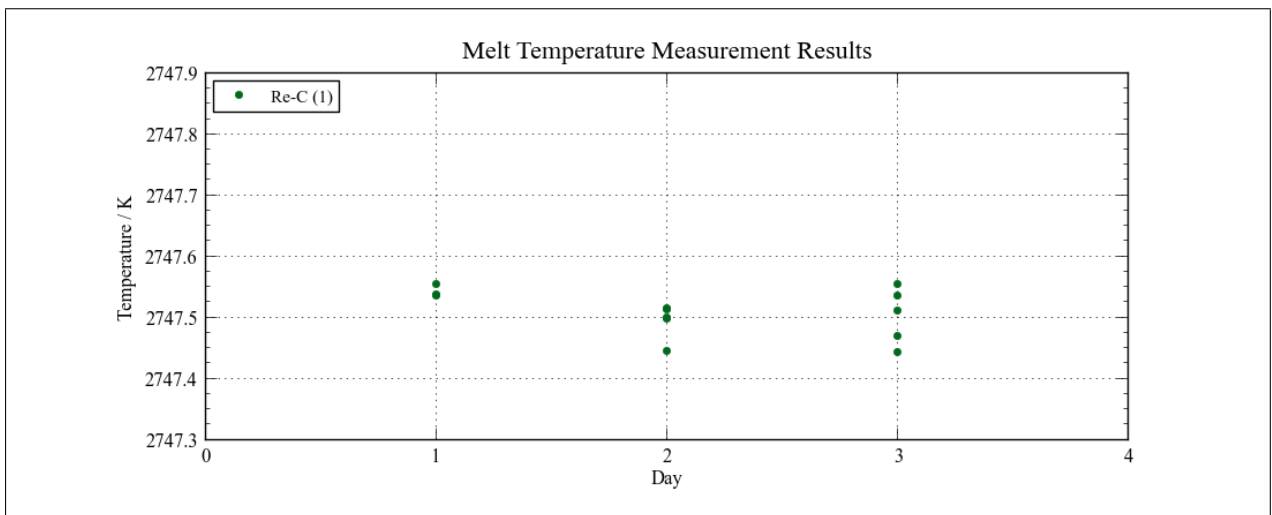


Figure 3.7: Melt temperatures of the Re-C (1) cell measured over three different days

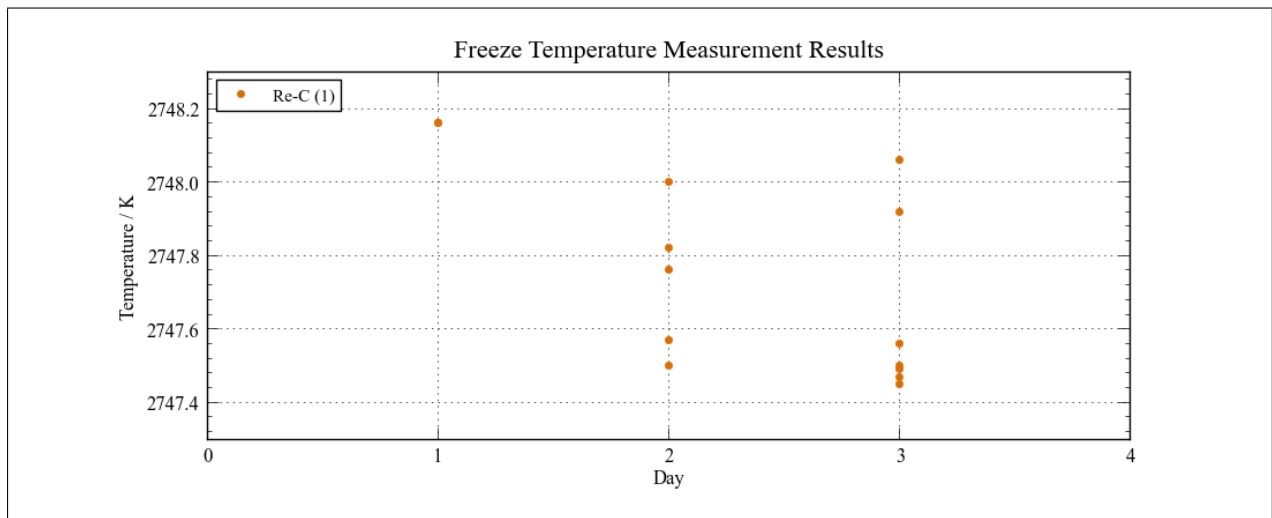


Figure 3.8: Freeze temperatures of the Re-C (1) cell measured over three different days

A difference of approximately 300 mK is observed between the average melt temperatures measured on days 1 and 2, versus days 3 and 4, for the Re-C (2) eutectic cell. Since this difference is significantly larger than the standard deviation for all subsequent measurements (≤ 61 mK), it is attributed to the change in focal distance of the LP4 as well as improvement of the ease of alignment. The average phase transition temperatures (in kelvin) measured on each day for the Re-C (2) and Re-C (1) cells are given in Tables 3.1 and 3.2, respectively.

Table 3.1: Phase transition temperatures of the Re-C (2) eutectic cell measured with the LP4 (in kelvin)

	Re-C (2)	Day 3	Day 4
No. of melt/freeze cycles:		4	4
Melt average:		2 747,54	2 747,48
Standard deviation:		0,04	0,06
Freeze average:		2 747,75	2 747,93
Standard deviation:		0,05	0,19

Table 3.2: Phase transition temperatures of the Re-C (1) eutectic cell measured with the LP4 (in kelvin)

Re-C (1)	Day 1	Day 2	Day 3
No. of melt/freeze cycles:	3	5	5
Melt average:	2 747,54	2 747,49	2 747,50
Standard deviation:	0,01	0,03	0,05
Freeze average:	2 747,58	2 747,73	2 747,64
Standard deviation:	0,82	0,20	0,25

The average melt temperature for both the Re-C (1) and Re-C (2) cells is 2 747,51 K with a measurement uncertainty of 2,43 K ($k = 2$). The reproducibility of the melt temperature was found to be within 100 mK.

3.1.2 $\delta(\text{MoC})\text{-C}$ Eutectic Cells

The NMISA constructed $\delta(\text{MoC})\text{-C}$ cells were taken to VNIIOFI, Russia, to determine their phase transition temperatures. Each cell was placed inside a BB3500mp black body in turn, heated to the expected melt temperature of 2 856 K and taken through several melt-and-freeze cycles. However, both cells cracked during this process and no further measurements were undertaken. The cells were replaced by a $\delta(\text{MoC})\text{-C}$ cell constructed by VNIIOFI and the phase transition temperatures of this cell were measured with a transfer standard pyrometer (TSP-2) calibrated at VNIIOFI. A series of 5 melt-and-freeze cycles was measured. The average melt temperature measured was 2 856,40 K with an expanded uncertainty ($k = 2$) of 2,0 K. The results obtained are shown in Table 3.3 below.

Table 3.3: Phase transition temperatures of the VNIIOFI $\delta(\text{MoC})\text{-C}$ eutectic cell measured with the TSP-2 (in kelvin)

Cycle	Melt	Freeze
1	2 856,47	2 856,31
2	2 856,28	2 856,45
3	2 856,24	2 856,50
4	2 856,57	2 856,47
5	2 856,46	2 856,48
Average:	2 856,40	2 856,44
Standard deviation:	0,14	0,08

The phase transition temperatures of the $\delta(\text{MoC})\text{-C}$ eutectic cell constructed by VNIIOFI (denoted RU $\delta(\text{MoC})\text{-C}$) was measured at the NMISA using the LP4, utilising the BB3200pg black body as a furnace. The distance between the LP4 and the aperture of the eutectic cell was 750 mm. Twenty-one melt-and-freeze cycles were made over 4 days. A typical melt-and-freeze cycle is shown in Figure 3.9.

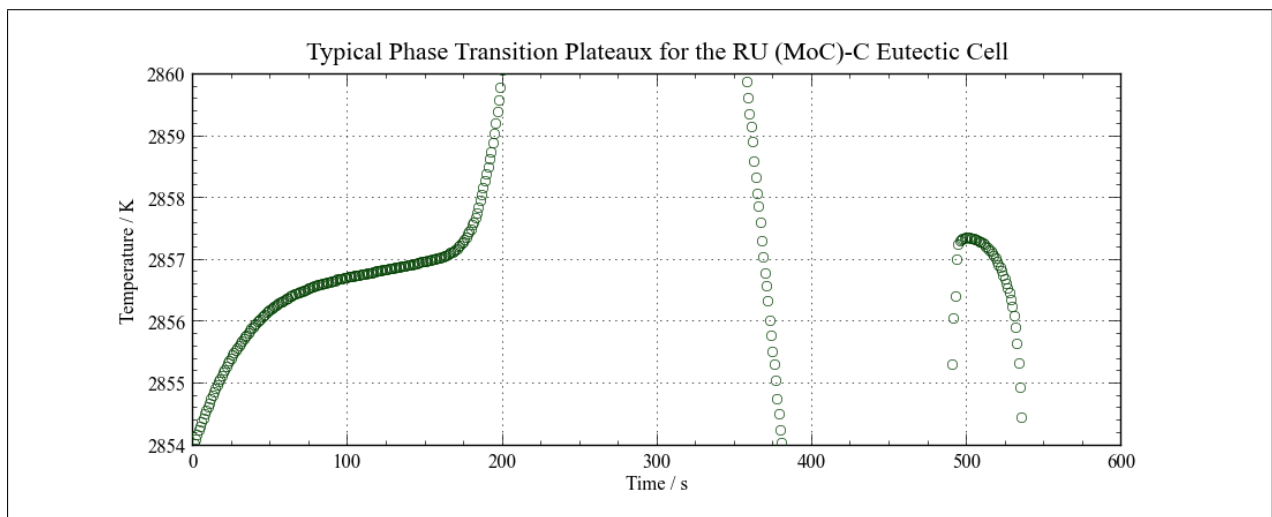


Figure 3.9: Typical phase transition plateaux observed for the RU $\delta(\text{MoC})\text{-C}$ eutectic cell

A melting plateau observed for the RU $\delta(\text{MoC})\text{-C}$ eutectic cell is shown in Figure 3.10. The

first derivative of temperature with respect to time is shown in Figure 3.11. The melt temperature is defined as the minimum of this curve (i.e. the POI) and has been estimated after applying a moving average curve smoothing technique.

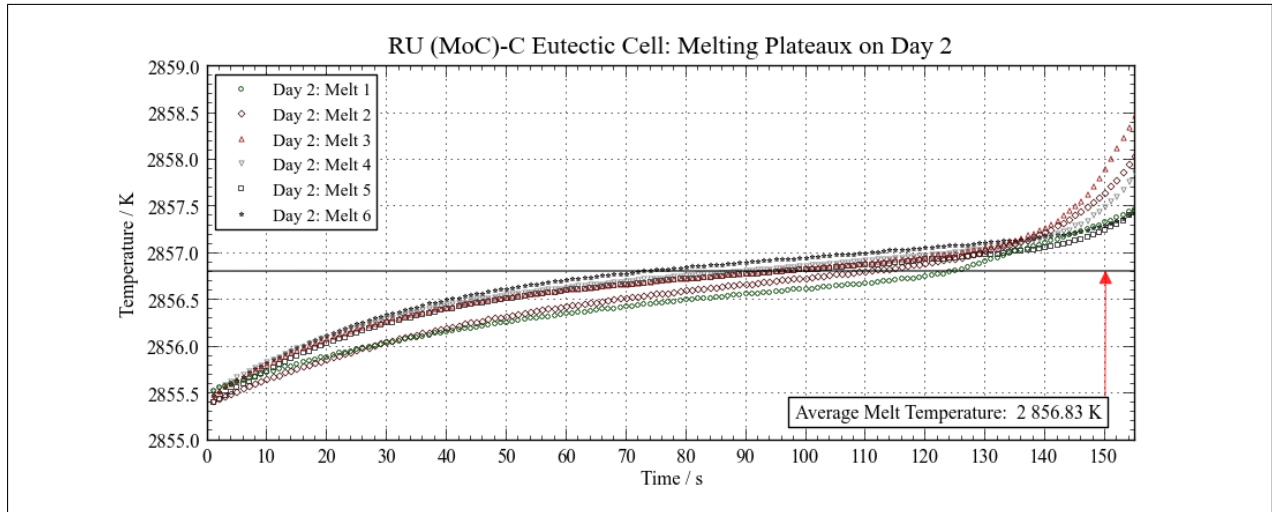


Figure 3.10: Typical melting plateaux observed for the RU δ (MoC)-C eutectic cell

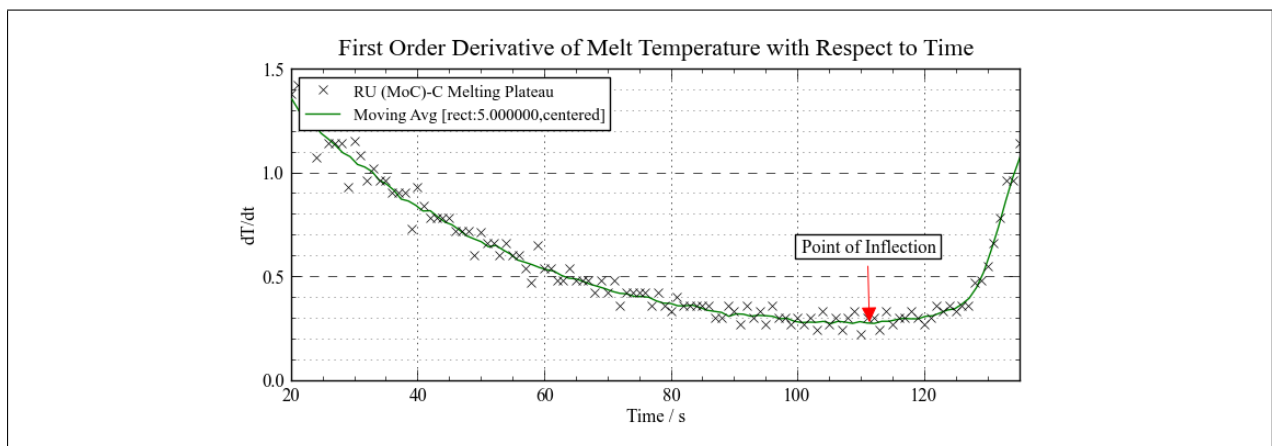


Figure 3.11: Determination of the point of inflection of the melting plateau for the RU δ (MoC)-C eutectic cell

Typical freezing plateaux for the RU δ (MoC)-C eutectic cell is shown in Figure 3.12. The freeze temperature was taken as the maximum value on each curve.

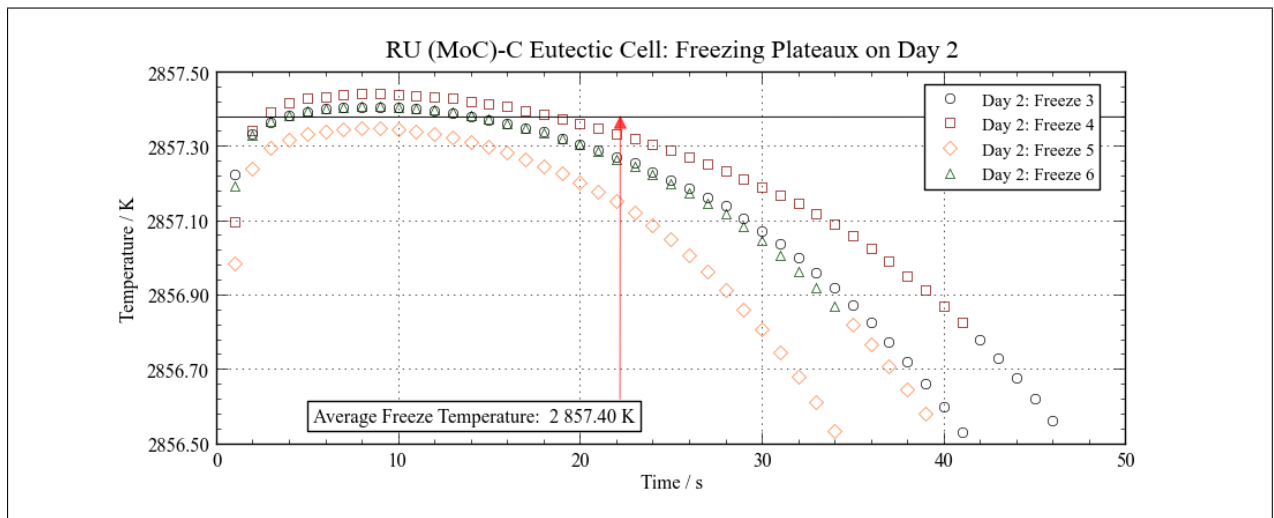


Figure 3.12: Typical freezing plateaux observed for the RU δ (MoC)-C eutectic cell

The results of measurement of melt temperature for the RU δ (MoC)-C eutectic cell are shown in Figure 3.13.

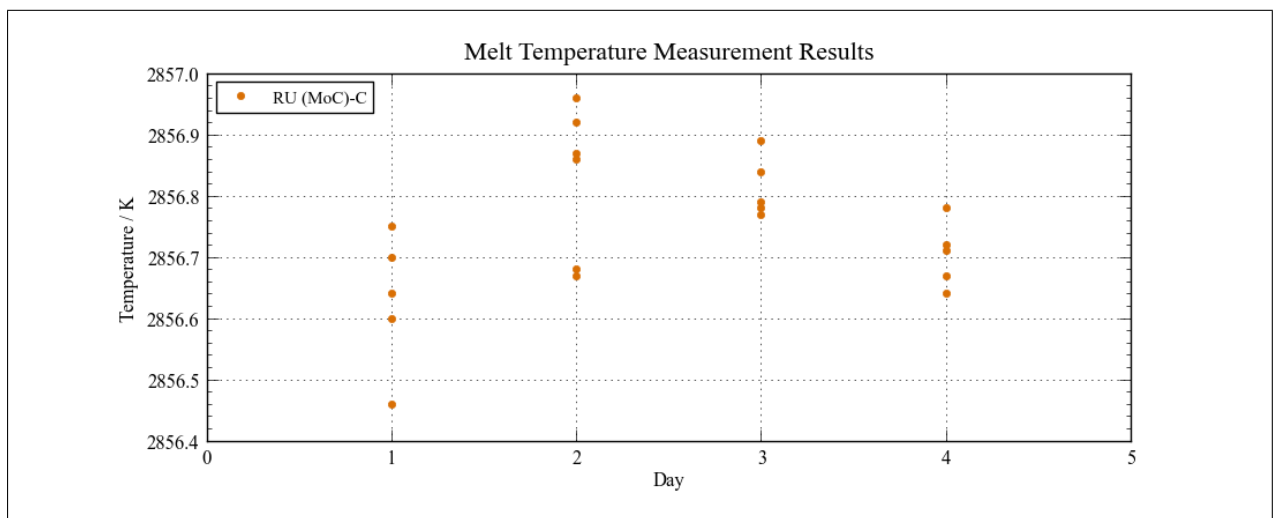


Figure 3.13: Melt temperature measurement results for the RU δ (MoC)-C eutectic cell

The results of measurement of the freeze temperature for the RU δ (MoC)-C eutectic cell are shown in Figure 3.14.

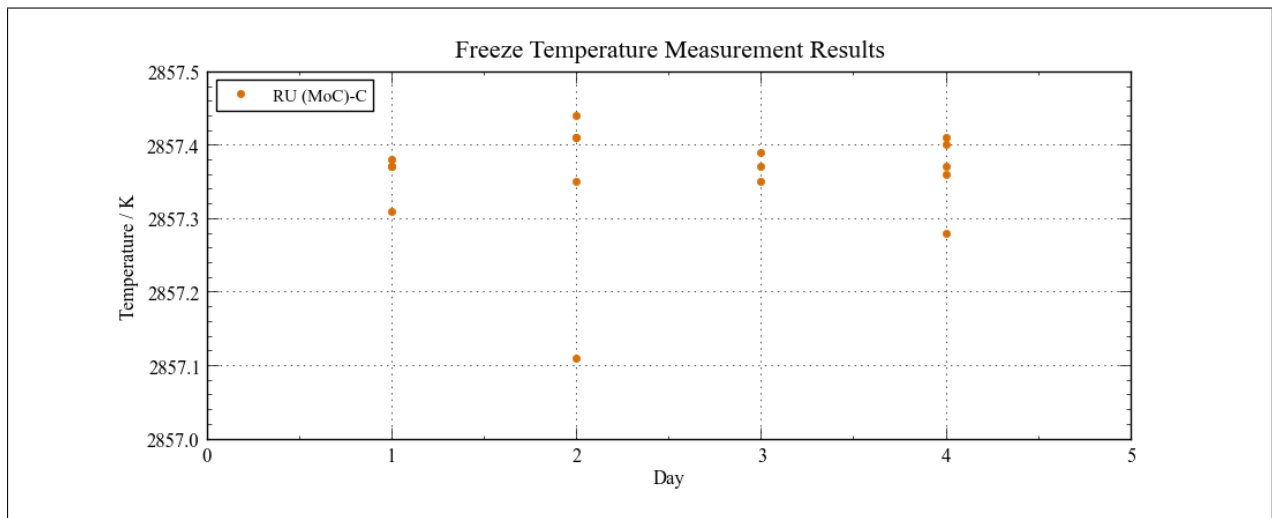


Figure 3.14: Freeze temperature measurement results for the RU $\delta(\text{MoC})\text{-C}$ eutectic cell

The results of measurement of the melt and freeze temperatures are shown in Tables 3.4 and 3.5, respectively.

Table 3.4: Melt temperature results for the RU $\delta(\text{MoC})\text{-C}$ eutectic cell (in kelvin)

RU $\delta(\text{MoC})\text{-C}$	Day 1	Day 2	Day 3	Day 4
No. of melt cycles:	5	6	5	5
Average:	2 856,63	2 856,83	2 856,81	2 856,70
Standard deviation:	0,11	0,12	0,05	0,05

Table 3.5: Freeze temperature results for the RU $\delta(\text{MoC})\text{-C}$ eutectic cell (in kelvin)

RU $\delta(\text{MoC})\text{-C}$	Day 1	Day 2	Day 3	Day 4
No. of freeze cycles:	4	4	3	5
Average:	2 857,35	2 857,40	2 857,37	2 857,36
Standard deviation:	0,03	0,04	0,02	0,05

For comparison purposes, the phase transition characteristics of the NMISA constructed $\delta(\text{MoC})$ -C (2) eutectic cell (denoted SA $\delta(\text{MoC})$ -C), which broke during experiments in Russia) were measured as well. This eutectic cell has a hairline crack in the outer wall of the crucible. It was placed inside an enclosed, cylindrical holder (with the crack facing the upper wall) in order to prevent possible leakage of the eutectic alloy inside the black body. During measurements a small amount of molten eutectic alloy seeped through the crack at a particular location. This made a small dent inside the eutectic cell holder. The leakage appeared after the measurements on day 2 and did not increase noticeably during subsequent measurements (see Figure 3.15).

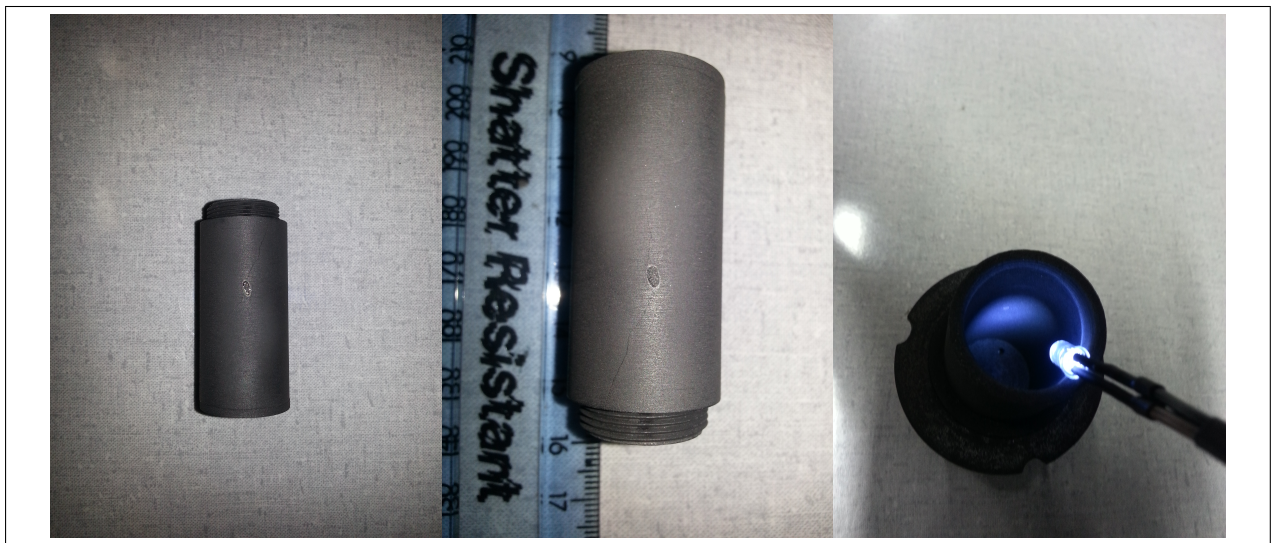


Figure 3.15: The SA $\delta(\text{MoC})$ -C eutectic cell showing the leakage of the eutectic within the hairline crack and the resulting small dent inside the cylindrical cell holder

The same measurement configuration was used and twenty-five melt-and-freeze cycles were made over 5 days. A typical melt-and-freeze cycle is shown in Figure 3.16.

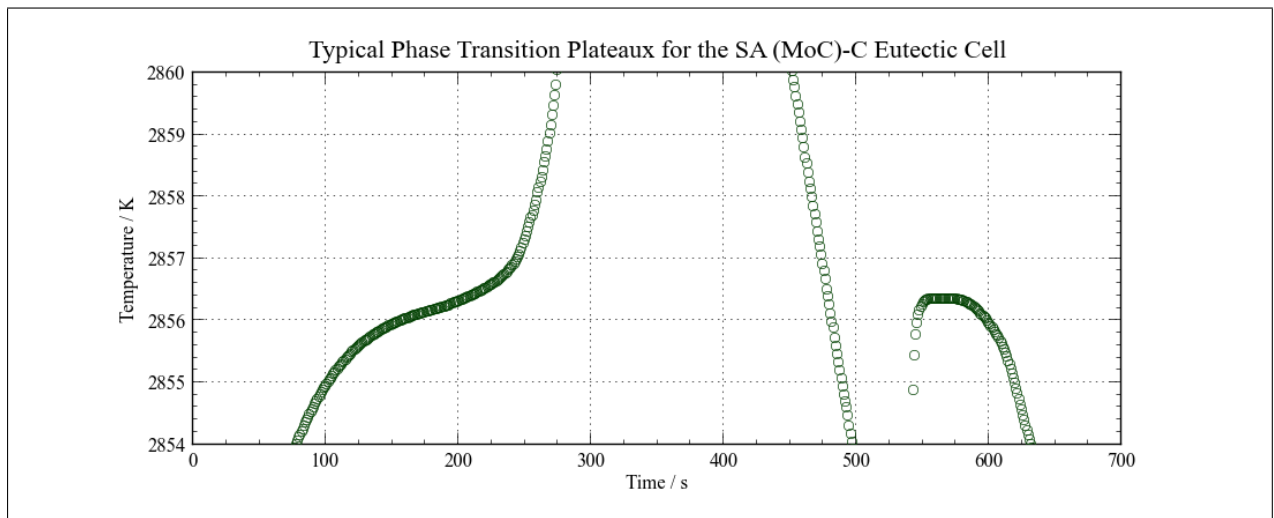


Figure 3.16: Typical phase transition plateaux observed for the SA $\delta(\text{MoC})\text{-C}$ eutectic cell

A melting plateau observed for the SA $\delta(\text{MoC})\text{-C}$ cell is shown in Figure 3.17. The first derivative of temperature with respect to time is shown in Figure 3.18. The melt temperature has been estimated after applying a moving average curve smoothing technique.

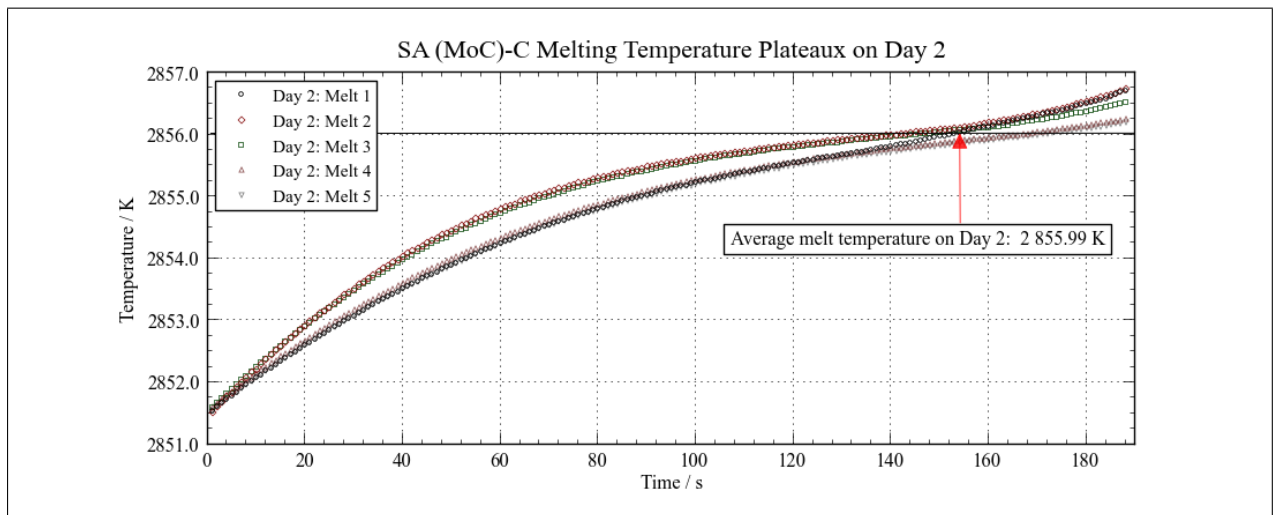


Figure 3.17: Typical melting plateaux observed for the SA $\delta(\text{MoC})\text{-C}$ eutectic cell

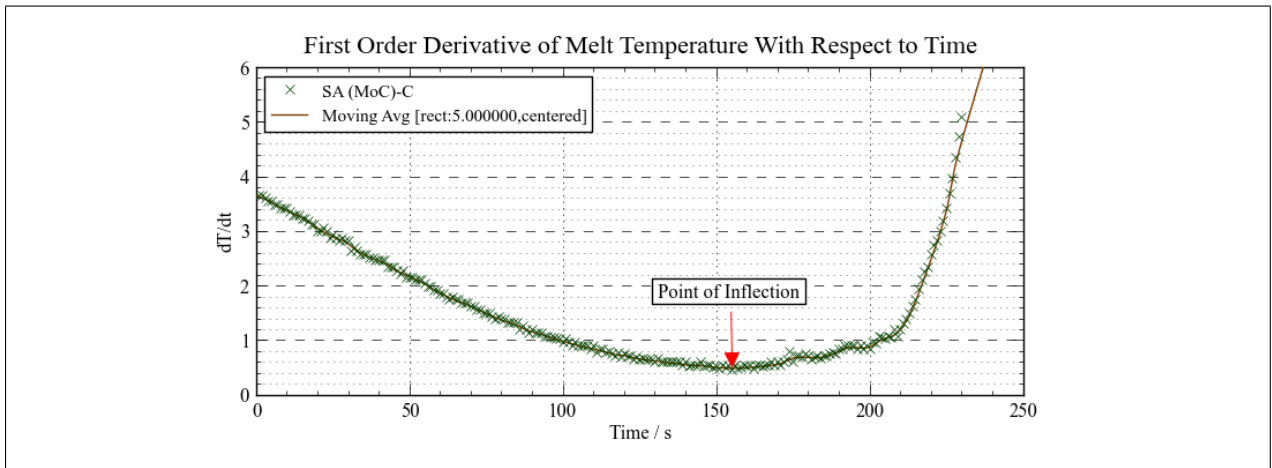


Figure 3.18: Determination of the point of inflection of the melting plateau for the SA $\delta(\text{MoC})\text{-C}$ eutectic cell

Typical freezing plateaux for the SA $\delta(\text{MoC})\text{-C}$ eutectic cell is shown in Figure 3.19. The maximum value of each curve was taken as the freeze point.

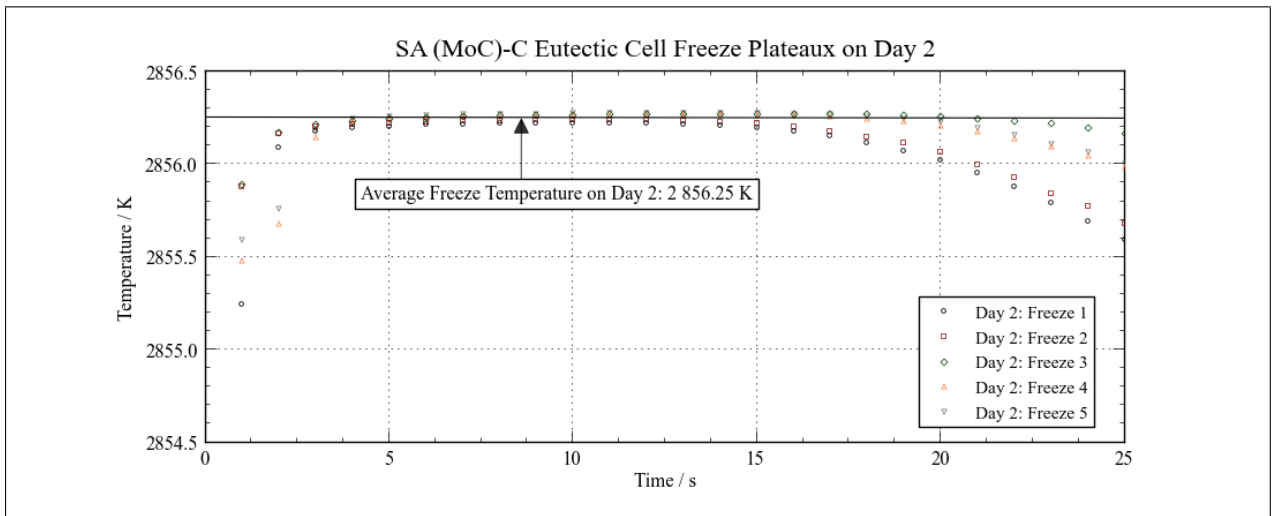


Figure 3.19: Typical freezing plateaux observed for the SA $\delta(\text{MoC})\text{-C}$ eutectic cell

The results of measurement of the melt temperature for the SA $\delta(\text{MoC})\text{-C}$ eutectic cell are shown in Figure 3.20.

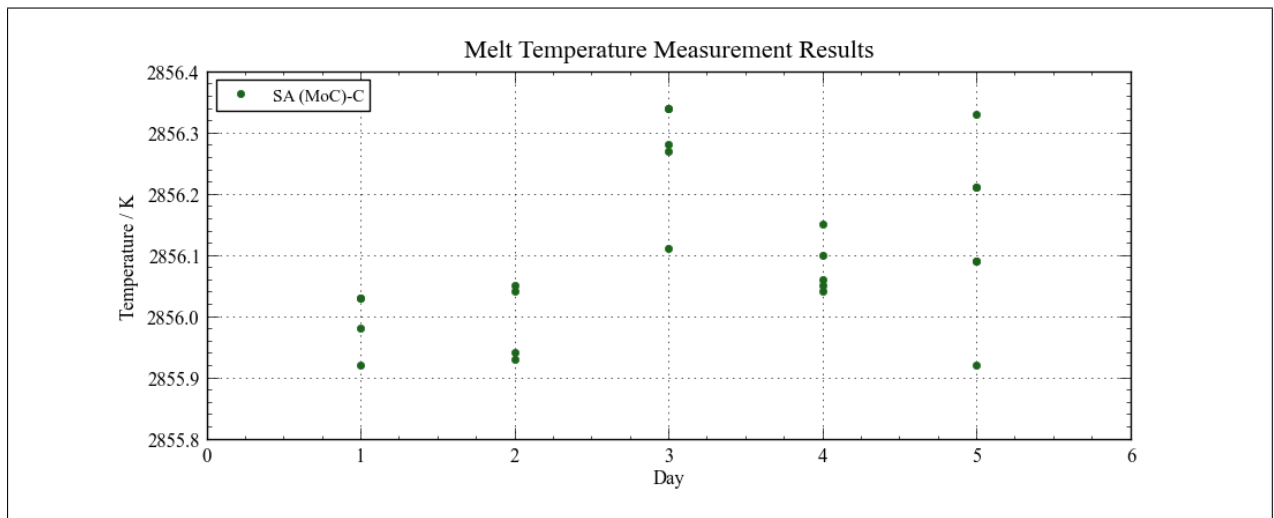


Figure 3.20: Melt temperature measurement results for the SA $\delta(\text{MoC})\text{-C}$ eutectic cell

The results of measurement of the freeze temperature for the SA $\delta(\text{MoC})\text{-C}$ eutectic cell are shown in Figure 3.21.

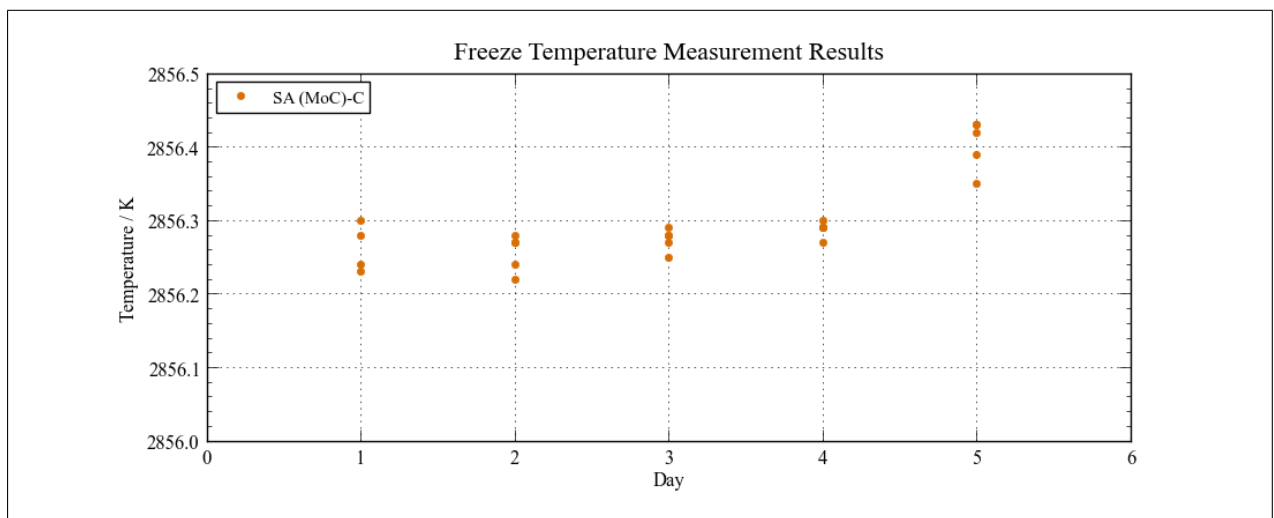


Figure 3.21: Freeze temperature measurement results for the SA $\delta(\text{MoC})\text{-C}$ eutectic cell

The results of measurement of the melt and freeze temperatures are shown in Tables 3.6 and 3.7, respectively.

Table 3.6: Melt temperature results for the SA $\delta(\text{MoC})\text{-C}$ eutectic cell (in kelvin)

SA $\delta(\text{MoC})\text{-C}$	Day 1	Day 2	Day 3	Day 4	Day 5
No. of melt cycles:	4	4	5	5	6
Average:	2 855,99	2 855,99	2 856,26	2 856,08	2 856,14
Standard deviation:	0,05	0,06	0,09	0,05	0,14

Table 3.7: Freeze temperature results for the SA $\delta(\text{MoC})\text{-C}$ eutectic cell (in kelvin)

SA $\delta(\text{MoC})\text{-C}$	Day 1	Day 2	Day 3	Day 4	Day 5
No. of freeze cycles:	4	5	5	5	6
Average:	2 856,24	2 856,25	2 856,27	2 856,29	2 856,46
Standard deviation:	0,03	0,03	0,02	0,01	0,15

3.2 Measurement Uncertainties in Temperature Determination

A number of factors influence the accuracy of the results of the temperature measurements and are attributed to uncertainties introduced by: the measurement standard, (LP4 pyrometer); the specific measurement configuration; and the eutectic crucible. Uncertainties related to the LP4 includes size of source effect, non-linearity, drift and the calibration uncertainty. The measurement configuration contributes to uncertainties due to positioning and alignment. The eutectic material and crucible contribute uncertainties related to the temperature drop at the crucible cavity bottom, emissivity of the cavity, impurities within the eutectic material and to the determination of the POI. All above mentioned components of the system contribute the repeatability of measurement result. The expanded uncertainties ($k = 2$) calculated for the Re-C and $\delta(\text{MoC})\text{-C}$ cells are given in Tables 3.8 and 3.9, respectively.

3.2.1 Typical Sources of Uncertainty

3.2.1.1 Calibration of the standard pyrometer

The LP4 (serial number: 80-54) was calibrated (at the PTB in Germany) using a 5-point interpolation method (calibration reference number: 2193-PTB-07, given in Appendix B). The measurement uncertainty given at a temperature of 2 504,3 °C (2 777,45 K) with interference filter B1 (nominal effective wavelength: 650 nm) is 2 °C ($k = 2$).

3.2.1.2 Size of source effect

According to a report on tests done by the manufacturer on the NMISA's LP4, the signal change at 976 °C for filter B1 when the diameter of an aperture in front of a sodium heat pipe black body was changed from 1,1 mm to 25 mm was < 0,025 %, which is below the instrument's accuracy limit. This corresponds to an upper temperature uncertainty limit of 49 mK at the Re-C point and 53 mK at the $\delta(\text{MoC})$ -C point.

3.2.1.3 Drift

The spectral responsivity of the pyrometer could change during prolonged measurements due to heating of the interference filter fitted to the photo-diode. The manufacturer specified the effect of this temperature drift at ambient conditions (22 °C to 28 °C) as 3×10^{-4} K. The LP4 was shielded from incident radiation by aluminium foil (around the lens) in order to reduce this effect.

3.2.1.4 Non-linearity

Detector non-linearity is not considered to have a significant effect (> 900 mK if the reference temperature is the copper, gold or silver freezing point) on these temperature measurements, since the temperature values of interest (2 747 K and 2 856 K) are close to the calibration point 2 777 K (refer to the Certificate of Calibration of the LP4 given in Appendix B). The non-linearity uncertainty contribution (295 mK) is estimated from literature values (Fischer et al. (2003)).

3.2.1.5 Positioning and alignment

At a distance of 75 mm the LP4 pyrometer's target diameter is approximately 1 mm and is centred on the cavity opening, which is 4 mm in diameter. Alignment was done before the black body

was switched on. The cavity of the eutectic crucible was illuminated by a LED attached to a wire enabling proper alignment. The alignment was confirmed before the black body reached the eutectic melt temperature (the different (radiating) graphite parts become clearly visible once a sufficiently large temperature gradient exists). The position of the crucible within the black body varies during measurements due to thermal expansion and contraction. The effect of alignment was determined by deliberately misaligning the LP4 within the likely positioning limits, while observing the change in temperature reading. It was found to be 15 mK.

3.2.1.6 Emissivity of the crucible cavity

The calculated emissivity of the crucible cavity can differ from its true emissivity due to: inaccurate estimation of the graphite wall emissivity owing to the type of graphite used and machining (which introduces specularity); temperature gradients within the cavity; unknown geometrical factors; and machining imperfections changing the conical shape of the cavity. The contribution of determination of emissivity of the crucible cavity to the uncertainty of the temperature measurement is estimated to be approximately 50 mK for typical crucibles at a temperature of 3 000 K, according to literature values (Fischer et al. (2003)).

3.2.1.7 Temperature drop at the cavity bottom

A drop in temperature occurs at the bottom of the cavity as a result of radiant energy lost through the cavity aperture. The contribution of radiative cooling to the measurement uncertainty has been obtained from literature for crucibles with similar dimensions operating at 3 000 K (Fischer et al. (2003)).

3.2.1.8 Determination of the point of inflection

The melt temperature is defined as the point of inflection, therefore the uncertainty of estimating the POI directly impacts the accuracy of the melt temperature. It is determined by the ease of locating the minimum value of the first order derivative of temperature versus time curve, which depends on the quality of the plateau shape. The POI for Re-C cells could be determined within an uncertainty of 25 mK. In comparison, the plateau shapes for the $\delta(\text{MoC})\text{-C}$ cells were of lesser quality, resulting in a larger uncertainty of 35 mK for determining the POI.

3.2.1.9 Impurities

The eutectic cells were constructed using metals of the highest purity commercially available at the time (five nines (5N), 99,999 %). No conclusive data of the effect of higher purity metals (> 6N) on the melt or freeze temperatures of eutectics are available as it depends on the nature and distribution of the impurities within the eutectic alloy. According to literature, the contribution of impurities to the measurement uncertainty is estimated not to exceed 50 mK at 3 000 K for metals of 5N or 6N purity ((Fischer et al., 2003)).

3.2.1.10 Repeatability

The repeatability of the phase transition temperatures was obtained by calculating the standard deviation of the temperature measurement results for successive melt-and-freeze cycles under identical experimental conditions. It comprised between 4 and 6 cycles per day over 3 to 5 days per cell. The repeatability of the measurement result is mainly affected by the stability of the optical components, detector drift and alignment and is indistinguishable from the non-repeatability of the eutectic material itself. The repeatability of the Re-C eutectic melt was 57 mK and that for the $\delta(\text{MoC})\text{-C}$ melt was 115 mK.

3.2.2 Uncertainty Budgets for the Eutectic Cells

The uncertainty budgets showing the uncertainty contributions to the phase transition temperature measurements of the Re-C and $\delta(\text{MoC})\text{-C}$ eutectic cells are given in Tables 3.8 and 3.9, respectively. The main sources of uncertainty were the calibration of the LP4 pyrometer, detector drift, linearity of the detector and repeatability (for $\delta(\text{MoC})\text{-C}$ cells). The contribution of the uncertainties of about 50 K or less is negligible, but shown for completeness.

Table 3.8: Uncertainty contributions to the temperature determinations of the Re-C eutectic cells

Index	Source of Uncertainty	Standard Uncertainty (mK)	Reference
1	Calibration of LP4 pyrometer	1 155	PTB calibration certificate
2	Size of source effect	49	Manufacturer specification
3	Positioning and alignment	15	Experimental observation
4	Drift	197	Manufacturer specification
5	Non-linearity	295	Literature (Fischer et al. (2003))
6	Repeatability	57	Experimental observation
7	Emissivity of crucible cavity	50	Literature (Fischer et al. (2003))
8	Temperature drop at cavity bottom	49	Literature (Fischer et al. (2003))
9	Determination of POI	25	Experimental observation
10	Impurities	50	Literature ((Fischer et al., 2003)
Standard Uncertainty (k = 1):		1 214	1,21 K
Expanded Uncertainty (k = 2):		2 427	2,43 K

Table 3.9: Uncertainty contributions to the temperature determinations of the $\delta(\text{MoC})\text{-C}$ eutectic cells

Index	Source of Uncertainty	Standard Uncertainty (mK)	Reference
1	Calibration of LP4 pyrometer	1 386	PTB calibration certificate
2	Size of source effect	53	Manufacturer specification
3	Positioning and alignment	17	Experimental observation
4	Drift	213	Manufacturer specification
5	Non-linearity	319	Literature (Fischer et al. (2003))
6	Repeatability	115	Experimental observation
7	Emissivity of crucible cavity	50	Literature (Fischer et al. (2003))
8	Temperature drop at cavity bottom	53	Literature (Fischer et al. (2003))
9	Determination of POI	35	Experimental observation
10	Impurities	50	Literature ((Fischer et al., 2003)
Standard Uncertainty (k = 1):		1 446	1,45 K
Expanded Uncertainty (k = 2):		2 891	2,89 K

3.3 Summary of Results

The measurement results are summarised in Table 3.10 below.

Table 3.10: Summary of results: measured phase transition temperatures of the eutectic cells

(in kelvin)	Re-C (1)	Re-C (2)	RU $\delta(\text{MoC})\text{-C}$	SA $\delta(\text{MoC})\text{-C}$
Melt temperature:	2 747,51	2 747,51	2 856,76	2 856,09
Standard deviation:	0,04	0,06	0,10	0,12
Freeze temperature:	2 747,67	2 747,85	2 857,37	2 856,30
Standard deviation:	0,23	0,17	0,02	0,09
Uncertainty (k = 2):	2,43		2,89	

Chapter 4

Discussion of Results

Given the phase transition characteristics of the constructed Re-C and $\delta(\text{MoC})$ -C eutectic cells, their suitability as reference standards in terms of reproducibility and stability need to be ascertained. The melt temperature of Re-C cells was repeatable within 60 mK, which is equal to a relative spectral radiance value of 0,02 % at 650 nm. The melt temperature of the $\delta(\text{MoC})$ -C cell was repeatable within 100 mK, which is equal to a relative spectral radiance value of 0,03 % at 650 nm. Without implementing eutectics, NMIs typically achieve a best measurement capability of 3 K ($k = 2$) at 2 800 K, which contributes approximately 1 % to the overall spectral radiance measurement uncertainty. By using eutectics, the reproducibility of spectroradiometric scales can thus be improved by a factor of 10.¹

Since the pyrometer was calibrated (by the PTB), it was possible to assign temperature values to the melt and freeze points of the eutectics which could be compared to the those published by other NMIs. A list of results by NMIs is given in Table 4.1. The values were taken from the list published by Sadli et al. (2004), unless otherwise indicated.

¹This outcome improves the precision of measurement but not the accuracy, therefore the uncertainty of measurement remains unchanged.

Table 4.1: Comparison of melt temperatures for high temperature eutectics between NMIs

Institute	Re-C		$\delta(\text{MoC})\text{-C}$	
	Temperature / K	Uncertainty ($k = 2$) / K	Temperature / K	Uncertainty ($k = 2$) / K
BIPM	2 747,15	0,5		
	2 747,65	0,7		
LNE-INM ² , France	2 746,45	1,4		
NIST, United States of America (Machin et al. (2004))	2 747,15	0,5		
	2 747,17	0,51		
NPL, United Kingdom	2 747,95	1,1		
NMIJ, Japan	2 747,15	3,1	2 856,15	4
NRC, Canada (Todd & Woods (2013))	2 748,056	0,95		
PTB, Germany	2 747,55	1,9		
	2 747,40	0,75		
VNIIOFI, Russian Federation	2 748,45	1	2 856,40	2,0
	2 747,50	1,3		
NMISA, South Africa (from this study)	2 747,51	2,43	2 856,76	2,89
Average:	2 747,47	-	2 856,44	-
Standard deviation:	0,50	-	0,31	-
Preliminary Consensus:	2 747,35	1	-	-

Published melt temperatures for the Re-C eutectic were found for the BIPM and 8 NMIs. The NMISA result for Re-C is consistent with international values and agrees with the preliminary consensus value within the stated uncertainties. The uncertainty claimed by NMISA is larger than what is stated by most other institutes. The reason for this is that the NMISA imports traceability, while the other institutes quoted thermodynamic temperatures assumed to be linked to their independently realised radiometric scales.

As far as could be determined, only one institute, NMIJ (NMI of Japan), published a measurement result for the melt temperature of the $\delta(\text{MoC})\text{-C}$ eutectic. It is known that several other NMIs

²previously BNM-INM

attempted construction of this eutectic, but abandoned efforts due to frequent breakages of such cells (Lowe & Machin (2002)). The larger NMIs specialising in the field of high temperature eutectics, such as NMIJ and VNIIOFI, are currently focussing efforts on other metal-carbon-carbide eutectics, in particular TiC-C (3 034 K) and ZrC-C (3 155 K). The TiC-C eutectic is of special interest since its melt temperature is close to the colour temperature of a tungsten filament (approximately 3 050 K), which is the filament used in the standard lamps maintained as national measurement standards for spectral (ir)radiance by NMIs. In order to study these metal-carbon-carbide eutectics, NMIs are utilising ultra-high temperature black bodies as furnaces specifically designed and manufactured for this purpose. Although the NMISA black body is able to reach a maximum temperature sufficiently high to construct and investigate these eutectics, it is not considered feasible as it would significantly reduce the life-time of the black body's graphite rings, requiring more frequent replacement.

The NMISA result for $\delta(\text{MoC})\text{-C}$ compares well with that published by NMIJ and the result of measurements performed at VNIIOFI on this particular cell. As far as can be ascertained, the most comprehensive study of $\delta(\text{MoC})\text{-C}$ was done by the NMISA (besides the initial tests by NMIJ). In the absence of measurement data from various institutes, reproducibility of the melt temperature of this eutectic cannot be determined and it is thus unlikely that it would be incorporated into a future international temperature scale. The significance of this cell is that the measurement of its phase transition temperatures by VNIIOFI provides the NMISA with an independent verification of its temperature scale at 2 856 K. According to measurements at the NMISA, the difference in melt temperature between the SA $\delta(\text{MoC})\text{-C}$ and RU $\delta(\text{MoC})\text{-C}$ eutectics is < 70 mK, however it is not possible to determine to what extent the crack in the crucible affected the result (if at all).

Chapter 5

Conclusion

In this study the process followed to construct two types of high temperature eutectic cells, namely Re-C (metal-carbon) and $\delta(\text{MoC})\text{-C}$ (metal-carbon-carbide), are described. Two of each Re-C and $\delta(\text{MoC})\text{-C}$ cells were made. The $\delta(\text{MoC})\text{-C}$ cells were sent to the Russian NMI (VNIIOFI) to be characterised in terms of its phase transition temperatures for comparison purposes. The crucible wall of both crucibles cracked during the first cycle of measurement and were replaced by a cell made by VNIIOFI (using a crucible with the same dimensions) to allow continuation of the project. The NMISA thus have 3 working high temperature eutectic cells and obtained the expertise and reference materials to build more as the need arises.

In order to determine the suitability of the eutectic cells as temperature reference standards, it was necessary to determine the reproducibility of their phase transition temperatures. If the melt (and/or freeze) temperature of such a cell is sufficiently reproducible (< 200 mK), it can be used to perform intermediate checks to verify the stability of the spectral (ir)radiance scale, extending the re-calibration period of the standard detectors.

The eutectic cell was placed inside a black body (used as a furnace) and heated radiatively to observe its phase transitions. A standard high temperature pyrometer, set at a distance of approximately 750 mm from (and focussed on) the cavity opening, was used to measure the cavity temperature of the eutectic cell. The process was repeated to obtain 3 to 6 melt-and-freeze cycles per day over 3 to 5 days in total, for each cell. The melt temperature of Re-C cells was repeatable within 60 mK, which is equal to a relative spectral radiance value of 0,02 % at 650 nm. The melt temperature of the $\delta(\text{MoC})\text{-C}$ cell was repeatable within 100 mK, which is equal to a relative spectral radiance value of 0,03 % at 650 nm. Without implementing eutectics, NMIs typically achieve

a best measurement capability of 3 K ($k = 2$) at 2 800 K, which contributes approximately 1 % to the overall spectral radiance measurement uncertainty. By using eutectics, the reproducibility of spectroradiometric scales can thus be improved by a factor of 10.

The published melt temperatures and inter-comparison results show that a number of eutectics are sufficiently reproducible to be considered as potential secondary reference points in a future international temperature scale. The next step is then to establish best practice guidelines for the construction and characterisation of such eutectics. A research project for this purpose was undertaken under the auspices of the BIPM CCT Working Group 5, which aims to assign robust thermodynamic temperatures to particular eutectics (high temperature fixed points), namely Co-C, Pt-C and Re-C. For this purpose a number of high quality eutectic cells of each type was constructed between 7 NMIs (20 in total and 6 or 7 of each type). Thermodynamic temperatures (i.e. with pyrometers or filter radiometers traceable to a cryogenic radiometer (which is a primary standard)) were assigned to these cells. A progress report by this working group in 2013 showed that the measurement uncertainty for Re-C ranged from 0,64 K to 1,38 K ($k = 2$), and that the maximum and minimum differences to the average melt temperature were $< 0,75$ K and $< 0,20$ K, respectively (Machin et al. (2013)). This demonstrates that a measurement uncertainty of approximately 1 K for Re-C is realistic. Consequently, high temperature eutectics can reduce the contribution of temperature scale realisation to the spectral radiance measurement uncertainty by a factor of 3 (from 0,9 % to 0,3 %, approximately).

The next phase towards improving the accuracy of NMISA's high temperature scale, is to calibrate its standard high temperature pyrometer (LP4) against trap detectors traceable to the cryogenic radiometer. This would allow for lower uncertainties than what is possible by using traditional ITS-90 methods. Once internationally agreed to melt temperatures for a selected set of high temperature eutectics are approved by the BIPM CCT and incorporated into an updated *mise en pratique* for the definition of the kelvin (Ripple et al. (2010)), which could be as soon as at the next meeting in 2016), the NMISA could assign the international consensus value to its Re-C cells and re-realise its high temperature scale from 961,78 °C (the silver freeze point) up to 2 474 °C (or higher) and immediately, in retrospect, realise the substantially reduced uncertainty outlined above. Furthermore, the development and implementation of eutectics is an important milestone towards linking the high temperature and spectroradiometric source-based (spectral irradiance and radiance) and detector-based scales at NMISA. A cohesive network of interlinked measurement scales provides additional means for verification and is more robust.

Besides providing a means to improve the accuracy of scale realisations, eutectics can be used

as stable, durable and convenient artefacts in international comparisons. Standard lamps, radiation sources, detectors (including pyrometers, filter radiometers and platinum resistance thermometers) are fragile and prone to drift, even when hand-carried between NMIs. It is foreseen that eutectic cells will be come commercially available as certified reference materials, which could be applied by industrial calibration laboratories to verify their standards and to inter-compare through proficiency testing schemes.

The results of this study is intended to contribute to the international effort to gain sufficient data from research results by NMIs in order to implement appropriate high temperature fixed points in a future international temperature scale. The melt temperature results for Re-C obtained by the NMISA was presented at an international conference.¹ It was accepted for publication by the *International Journal of Metrology and Quality Engineering* (Nel-Sakharova, 2015). The NMISA has also reported on the progress of this study at the bi-annual meetings of the BIPM CCPR in Paris, France.

In conclusion, demonstrating international equivalence of South Africa's national measurement standards is necessary to facilitate trade, to support health and safety of citizens, to protect the environment and to contribute accurate data to international research projects. For instance, international solar constant monitoring and remote earth observation data from different space agencies must be linked to nationally recognised spectral irradiance and spectral responsivity scales, in order to be reliable and inter-comparable. The improved measurement capabilities at the NMISA as described above support these initiatives in South Africa.

"Measured once, accepted everywhere".

¹"The Development and Characterisation of High Temperature Fixed Points at NMISA", N. Nel-Sakharova, The 5th International Metrology Conference (CAFMET 2014), April 2014, Pretoria, South Africa

Appendix A

NMISA Spectral Irradiance Scale

The NMISA is developing a primary measurement facility to realise the spectral irradiance scale. A schematic diagram of the planned facility is shown in Figure A.1.

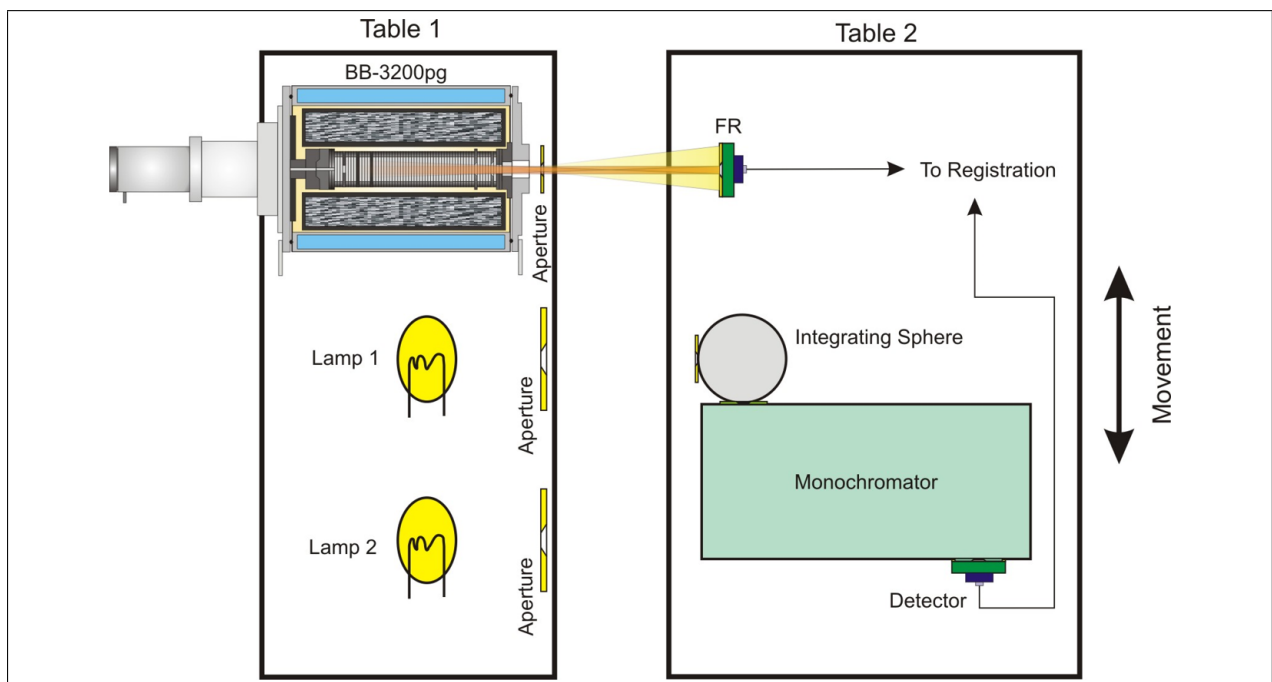


Figure A.1: Schematic diagram of the primary spectral irradiance facility being established at the NMISA

The primary radiation source is the BB3200pg black body, which is stabilised at a specified temperature, usually close to the colour temperature of a standard tungsten lamp (approximately

3 050 K). The temperature of the black body is measured with a filter radiometer, which is traceable to the NMISA primary standard cryogenic radiometer. The spectral radiance (and spectral irradiance, taking the geometrical factors into account) of the black body can be calculated from its temperature at a given wavelength (the effective wavelength of the interference filter fitted to the radiometer) from Planck's equation (1.2).






The monochromator, fitted with an integrating sphere at the entrance port and a reference detector at the exit port, is positioned opposite the black body in the path of the light beam by moving optical table 2. It is aligned with the optical axis of black body radiation by utilising positioning equipment. The spectral irradiance of the black body (still stable at the reference temperature) is measured over the wavelength range of interest (usually 250 nm to 2 500 nm). These values are compared with the calculated values and correction factors are calculated over the spectral range. The monochromator ensemble is positioned opposite a standard spectral irradiance lamp placed on optical table 1, by moving optical table 2. The lamp is stabilised at its operating current (after alignment) and its spectral irradiance is measured over the same wavelength range mentioned above. The correction factors are applied to the measured data at each wavelength to obtain the spectral irradiance values. The process is repeated for additional standard lamps. These lamps are subsequently used as secondary standards to calibrate working standards (for routine calibrations) on a different measurement facility. The reference detector does not need to be calibrated, it must be stable and linear within the required range (deviations are accounted for in the uncertainty budget).


Currently, the NMISA imports traceability for spectral irradiance by sending the primary standard lamps to another NMI for calibration. The uncertainties of calibration are 4 % to 8 % ($k = 2$) over the wavelength range of 400 nm to 1 500 nm. Through developing this facility, the NMISA aims to achieve an uncertainty of < 1 % over the visible wavelengths. Implementation of eutectic cells was necessary in order to reduce the uncertainty of the temperature measurement. The constructed eutectic cells will be used to perform intermediate checks to verify the reproducibility and stability of the temperature measurements, which also determines the re-calibration interval of the filter radiometer.



Appendix B

Certificate of Calibration for Pyrometer

The Certificate of Calibration (reference number: 2193-PTB-07) for the standard pyrometer (LP4, serial number: 80-54) issued by the PTB (Germany) in May 2007, is given below.

Physikalisch-Technische Bundesanstalt Braunschweig und Berlin			
 Kalibrierschein <i>Calibration Certificate</i>			
Gegenstand: Object:	Strahlungsthermometer		
Hersteller: Manufacturer:	KE Technologie GmbH		
Typ: Type:	Linearpyrometer LP4		
Kennnummer: Serial number:	80-54		
Auftraggeber: Applicant:	KE Technologie GmbH Pfaffenwaldring 31 70569 Stuttgart		
Anzahl der Seiten: Number of pages:	4		
Geschäftszeichen: Reference No.:	7.3-1.1-07-05		
Kalibrierzeichen: Calibration mark:	2193-PTB-07		
Datum der Kalibrierung: Date of calibration:	07. Mai 2007 bis 21. Mai 2007		
Im Auftrag By order:	Berlin, 12.06.07		Bearbeiter: Examiner:  Stephan Schiller
 Dr. Jürgen Hartmann	Siegel Seal		
<small>Kalibrierscheine ohne Unterschrift und Siegel haben keine Gültigkeit. Dieser Kalibrierschein darf nur unverändert weiterverbreitet werden. Auszüge bedürfen der Genehmigung der Physikalisch-Technischen Bundesanstalt. Calibration certificates without signature and seal are not valid. This calibration certificate may not be reproduced other than in full. Extracts may be taken only with the permission of the Physikalisch-Technische Bundesanstalt.</small>			

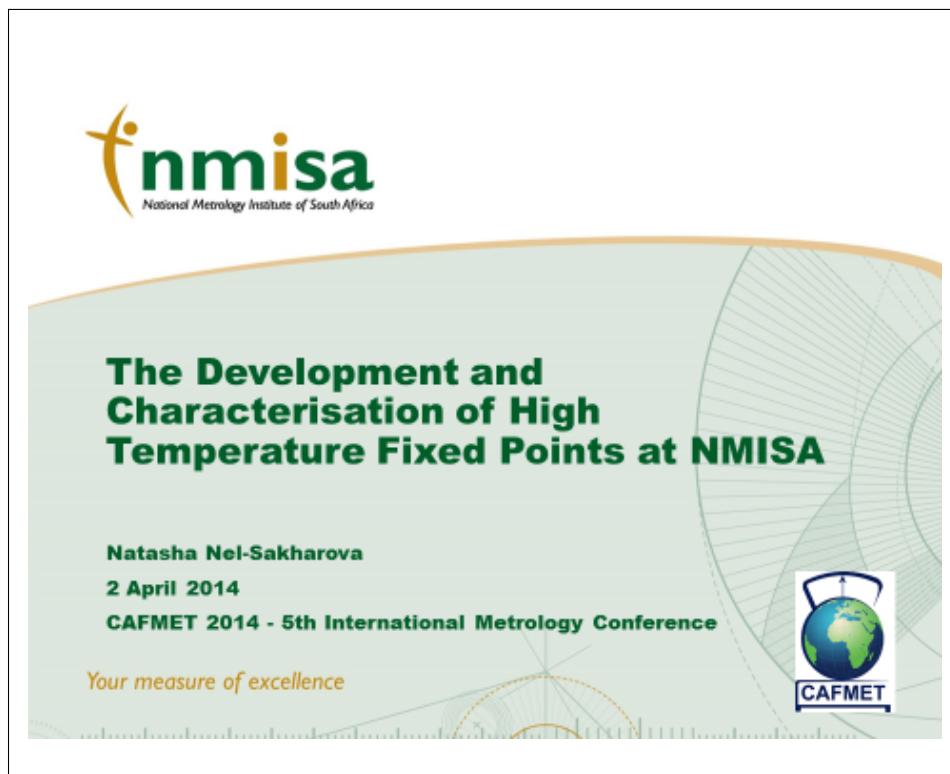
Physikalisch-Technische Bundesanstalt Seite 2 zum Kalibrierschein vom 12.06.07 Kalibrierzeichen: 2193-PTB-07 Page 2 of calibration certificate of 12.06.07 Calibration mark: 2193-PTB-07			
1 Kalibriergegenstand			
Der Kalibriergegenstand ist ein Strahlungsthermometer für den Temperaturbereich 750 °C bis 3000 °C.			
Das Strahlungsthermometer besteht aus dem Messkopf mit integrierter Versorgungs-, Anzeige- und Auswerteeinheit. Das Gerät enthält ein fokussierbares Objektiv, Gesichtsfeldblende, Kollimatorlinse, Aperturblende, ein Justierteleskop, ein einklappbares Spektralfilter, einen photoelektrischen Siliziumdetektor mit zugehörigem Strom-Spannungs-Wandler, Einrichtungen zur Messsignalverarbeitung, eine alphanumerische Anzeige und eine serielle Schnittstelle für den Anschluss an einen Computer. Zur Messwerterfassung dient das vom Hersteller entwickelte Programm LP4DEV43.			
Die Nominalwerte der Wellenlänge, definiert durch die Spektralfilter sind:			
$\lambda_{\text{nom}} = 650 \text{ nm}$ in Filterradposition 1 $\lambda_{\text{nom}} = 900 \text{ nm}$ in Filterradposition 2 $\lambda_{\text{nom}} = 550 \text{ nm}$ in Filterradposition 3			
Der Siliziumdetektor und die wesentlichen Teile des Strom-Spannungswandlers (Operationsverstärker und Hochohmwiderstände) befinden sich in einer thermostatisierten Zelle innerhalb des Messkopfes.			
2 Kalibrierverfahren			
Die Kalibrierung bei 900 °C erfolgte an einem Natrium-Wärmerohr-Hohlraumstrahler. Die Strahlungstemperatur an den Kalibrierwerten wurde mit einem Platin-Widerstandsthermometer unter Berücksichtigung von Korrekturwerten eingestellt. Für alle höheren Temperaturen wurde ein Hochtemperatur-Hohlraumstrahler verwendet, dessen Strahlungstemperatur aus dem Vergleich mit der Strahlungstemperatur der Vakuum-Wolframbandlampe C514 und dem Filterradiometer FR800 bestimmt wurde. Bei der Beobachtung der genannten Hohlraumstrahler der PTB wurden zum Zeitpunkt der Kalibrierung die in der Tabelle in Abschnitt 4 angegebenen Temperaturen an dem Prüfling abgelesen. Die Messungen wurden mit der Filterradposition 1 durchgeführt.			
Die in diesem Kalibrierschein angegebenen Temperaturwerte t_{50} entsprechen der Internationalen Temperaturskala von 1990.			

<p>Physikalisch-Technische Bundesanstalt </p> <p>Seite 3 zum Kalibrierschein vom 12.06.07 Kalibrierzeichen: 2193-PTB-07 Page 3 of calibration certificate of 12.06.07 calibration mark: 2193-PTB-07</p> <p>3 Messbedingung</p> <table border="0"> <tr> <td>Anordnung der Hohlraumstrahler</td> <td>horizontal</td> </tr> <tr> <td>Messabstand des Prüflings von der Hohlraumöffnung</td> <td>700 mm</td> </tr> <tr> <td>Durchmesser der strahlenden Hohlraumöffnung</td> <td></td> </tr> <tr> <td> Natrium-Wärmerohr-Hohlraumstrahler</td> <td>20 mm</td> </tr> <tr> <td> Hochtemperatur-Hohlraumstrahler</td> <td>20 mm</td> </tr> <tr> <td>Emissionsgrad (ε) des Natrium-Wärmerohr-Hohlraumstrahlers</td> <td>0,99960 ± 0,00017</td> </tr> <tr> <td>Emissionsgrad (ε) des Hochtemperatur-Hohlraumstrahlers</td> <td>0,9990 ± 0,0005</td> </tr> <tr> <td>Umgebungstemperatur</td> <td>23 °C ± 1 °C</td> </tr> <tr> <td>Relative Luftfeuchte</td> <td>(44 ± 8) % rH</td> </tr> <tr> <td>Gemessener Dunkelstrom des Prüflings im Messbereich R1</td> <td>(8,7 · 10⁻¹⁹ ± 8,2 · 10⁻¹⁹) A</td> </tr> <tr> <td>Gemessener Dunkelstrom des Prüflings im Messbereich R2</td> <td>(3,3 · 10⁻¹⁹ ± 6,3 · 10⁻¹⁹) A</td> </tr> <tr> <td>Gemessener Dunkelstrom des Prüflings im Messbereich R3</td> <td>(-1,6 · 10⁻¹⁹ ± 2,0 · 10⁻¹⁹) A</td> </tr> </table> <p>4 Messergebnisse</p> <table border="1"> <thead> <tr> <th>Strahlungstemperatur des Hohlraumstrahlers <i>t₉₀</i> / °C bei A=650nm</th> <th>Messunsicherheit (k=2) <i>U</i> / °C</th> <th>Photostrom <i>I_{ph}</i> in A</th> </tr> </thead> <tbody> <tr> <td>900,0</td> <td>0,5</td> <td>1,418142E-11</td> </tr> <tr> <td>1206,0</td> <td>1,0</td> <td>6,869069E-10</td> </tr> <tr> <td>1604,6</td> <td>1,2</td> <td>1,618704E-08</td> </tr> <tr> <td>2006,8</td> <td>1,6</td> <td>1,261674E-07</td> </tr> <tr> <td>2504,3</td> <td>2,0</td> <td>7,230547E-07</td> </tr> </tbody> </table> <p>5 Messunsicherheit</p> <p>Die in der Tabelle im Abschnitt 4 angegebene erweiterte Messunsicherheit ergibt sich aus der Standardmessunsicherheit durch Multiplikation mit dem Erweiterungsfaktor k=2. Sie wurde gemäß dem "Guide to the Expression of Uncertainty in measurement" (ISO, 1995) ermittelt. Die angegebene Messunsicherheit berücksichtigt die Messunsicherheit mit der die Strahlungstemperatur der Hohlraumstrahler gemäß der ITS-90 realisiert wurde und die Kurzzeitstabilität des Prüflings während der Ablesung. Der Wert der Messgröße liegt im Regelfall mit einer Wahrscheinlichkeit von annähernd 95 % im zugeordneten Wertintervall.</p>	Anordnung der Hohlraumstrahler	horizontal	Messabstand des Prüflings von der Hohlraumöffnung	700 mm	Durchmesser der strahlenden Hohlraumöffnung		Natrium-Wärmerohr-Hohlraumstrahler	20 mm	Hochtemperatur-Hohlraumstrahler	20 mm	Emissionsgrad (ε) des Natrium-Wärmerohr-Hohlraumstrahlers	0,99960 ± 0,00017	Emissionsgrad (ε) des Hochtemperatur-Hohlraumstrahlers	0,9990 ± 0,0005	Umgebungstemperatur	23 °C ± 1 °C	Relative Luftfeuchte	(44 ± 8) % rH	Gemessener Dunkelstrom des Prüflings im Messbereich R1	(8,7 · 10 ⁻¹⁹ ± 8,2 · 10 ⁻¹⁹) A	Gemessener Dunkelstrom des Prüflings im Messbereich R2	(3,3 · 10 ⁻¹⁹ ± 6,3 · 10 ⁻¹⁹) A	Gemessener Dunkelstrom des Prüflings im Messbereich R3	(-1,6 · 10 ⁻¹⁹ ± 2,0 · 10 ⁻¹⁹) A	Strahlungstemperatur des Hohlraumstrahlers <i>t₉₀</i> / °C bei A=650nm	Messunsicherheit (k=2) <i>U</i> / °C	Photostrom <i>I_{ph}</i> in A	900,0	0,5	1,418142E-11	1206,0	1,0	6,869069E-10	1604,6	1,2	1,618704E-08	2006,8	1,6	1,261674E-07	2504,3	2,0	7,230547E-07	<p>Physikalisch-Technische Bundesanstalt </p> <p>Seite 4 zum Kalibrierschein vom 12.06.07 Kalibrierzeichen: 2193-PTB-07 Page 4 of calibration certificate of 12.06.07 calibration mark: 2193-PTB-07</p> <p>Die Physikalisch-Technische Bundesanstalt (PTB) in Braunschweig und Berlin ist das natur- und ingenieurwissenschaftliche Staatsinstitut und die technische Oberbehörde der Bundesrepublik Deutschland für das Messwesen und Teile der Sicherheitstechnik. Die PTB gehört zum Dienstbereich des Bundesministeriums für Wirtschaft und Technologie. Sie erfüllt die Anforderungen an Kalibrier- und Prüflaboratorien auf der Grundlage der DIN EN ISO/IEC 17025.</p> <p>Zentrale Aufgabe der PTB ist es, die gesetzlichen Einheiten in Übereinstimmung mit dem internationalen Einheitensystem (SI) darzustellen, zu bewahren und - insbesondere im Rahmen des gesetzlichen und industriellen Messwesens - weiterzugeben. Die PTB steht damit an oberster Stelle der metrologischen Hierarchie in Deutschland. Kalibrierscheine der PTB dokumentieren die Rückführung des Kalibriergegenstandes auf nationale Normale.</p> <p>Zur Sicherstellung der weltweiten Einheitlichkeit der Maße arbeitet die PTB mit anderen nationalen metrologischen Instituten auf regionaler europäischer Ebene in EUROMET und auf internationaler Ebene im Rahmen der Meterkonvention zusammen. Das Ziel wird durch einen intensiven Austausch von Forschungsergebnissen und durch umfangreiche internationale Vergleichsmessungen erreicht.</p> <p><i>The Physikalisch-Technische Bundesanstalt (PTB) in Braunschweig and Berlin is the national institute for science and technology and the highest technical authority of the Federal Republic of Germany for the field of metrology and certain sectors of safety engineering. The PTB comes under the auspices of the Federal Ministry of Economics and Technology. It meets the requirements for calibration and testing laboratories as defined in the EN ISO/IEC 17025.</i></p> <p><i>It is the fundamental task of the PTB to realize and maintain the legal units in compliance with the International System of Units (SI) and to disseminate them, above all within the framework of legal and industrial metrology. The PTB thus is on top of the metrological hierarchy in Germany. Calibration certificates issued by it document that the object calibrated is traceable to national standards.</i></p> <p><i>To ensure worldwide coherence of measures, the PTB cooperates with other national metrology institutes within EUROMET on the regional European level and on the international level within the framework of the Metre Convention. The aim is achieved by an intensive exchange of results of research work carried out and by comprehensive international comparison measurements.</i></p> <p>Physikalisch-Technische Bundesanstalt Bundesallee 100 D-38116 Braunschweig</p> <p>Abteilstelle 2-12 D-10587 Berlin</p>
Anordnung der Hohlraumstrahler	horizontal																																										
Messabstand des Prüflings von der Hohlraumöffnung	700 mm																																										
Durchmesser der strahlenden Hohlraumöffnung																																											
Natrium-Wärmerohr-Hohlraumstrahler	20 mm																																										
Hochtemperatur-Hohlraumstrahler	20 mm																																										
Emissionsgrad (ε) des Natrium-Wärmerohr-Hohlraumstrahlers	0,99960 ± 0,00017																																										
Emissionsgrad (ε) des Hochtemperatur-Hohlraumstrahlers	0,9990 ± 0,0005																																										
Umgebungstemperatur	23 °C ± 1 °C																																										
Relative Luftfeuchte	(44 ± 8) % rH																																										
Gemessener Dunkelstrom des Prüflings im Messbereich R1	(8,7 · 10 ⁻¹⁹ ± 8,2 · 10 ⁻¹⁹) A																																										
Gemessener Dunkelstrom des Prüflings im Messbereich R2	(3,3 · 10 ⁻¹⁹ ± 6,3 · 10 ⁻¹⁹) A																																										
Gemessener Dunkelstrom des Prüflings im Messbereich R3	(-1,6 · 10 ⁻¹⁹ ± 2,0 · 10 ⁻¹⁹) A																																										
Strahlungstemperatur des Hohlraumstrahlers <i>t₉₀</i> / °C bei A=650nm	Messunsicherheit (k=2) <i>U</i> / °C	Photostrom <i>I_{ph}</i> in A																																									
900,0	0,5	1,418142E-11																																									
1206,0	1,0	6,869069E-10																																									
1604,6	1,2	1,618704E-08																																									
2006,8	1,6	1,261674E-07																																									
2504,3	2,0	7,230547E-07																																									

Appendix C

Research Output

The melt temperature measurement results for the two Re-C eutectic cells were represented at The 5th International Metrology Conference (CAFMET 2014) on 2 April 2014 in Pretoria, South Africa. The presentation delivered is given below. These results were also submitted and accepted for publication in the *International Journal of Metrology and Quality Engineering*. The paper to be published is given below.



Applications: Spectral Irradiance

CAFMET 2014 - 5th International Metrology Conference
© 2014 nmisa

Background

Max Planck proposed that light have quantum nature and based on this assumption, he formulated a relationship between the temperature of a black body and the spectrum of radiation emitted by it.

Planck's radiation law:

$$I(\lambda, T) = \frac{c_1}{\pi} \frac{1}{\lambda^5} \left(\exp\left[\frac{c_2}{\lambda T}\right] - 1 \right)^{-1}$$

- where $c_1 = 2\pi^5 k^4 / 15c^3$ and $c_2 = hc$
- where h and k are Planck's and Boltzmann's constants respectively, and c is the speed of light

CAFMET 2014 - 5th International Metrology Conference
© 2014 nmisa

Background

The spectrum depends only on the temperature of the black body. Measuring the temperature, the spectral power distribution can be determined and vice versa.

Spectral Irradiance from Black Body (Ø400 mm, aperture 8 mm):

CAFMET 2014 - 5th International Metrology Conference
© 2014 nmisa

Realisation of Spectral Irradiance Scale

- NMIs realise the spectral irradiance scale through calibrated filter radiometers – traceable to a cryogenic standard radiometer
- Filter radiometers determines the temperature of a high temperature blackbody (reference source)
- Spectral radiance determined from Planck's equation

CAFMET 2014 - 5th International Metrology Conference
© 2014 nmisa

VNIOFI BB3200pg Blackbody Characteristics:

- Clamping spring
- Adjusting unit
- Carby opening
- Rear quartz window
- Inert gas purge inlet
- Water-cooled chamber
- Radiation shields
- Thermal insulation unit
- Carby inner conical bottom

CAFMET 2014 - 5th International Metrology Conference
© 2014 nmisa

NMISA BB3200pg Blackbody:

Specifications	
Temperature Range: 1300 - 1350 K	Effective Emittance at 300 nm > 0.999
Carby Diameter: 8 mm	Maximum Current: 300 A
Carby Opening Diameter: 22 mm	Maximum Voltage (DC): 30 V
Carby Length: 220 mm	Service life: at 1300K: 1.5k hours at 1350K: 500 hours
Optional External Aperture Dia: 13 mm	

CAFMET 2014 - 5th International Metrology Conference
© 2014 nmisa

Realisation of Spectral Irradiance Scale

CAFMET 2014 - 5th International Metrology Conference
© 2014 nmisa

Significance of Metal-Carbon Eutectics

- Towards an improved high temperature scale
- High temperature fixed points (above the copper point) could lead to significant improvements in high temperature metrology
- 1996: a joint working group between CIPM and CCT encouraged NMIs to develop high temperature fixed points above 2300 K with a reproducibility better than 100 mK
- 1999: Yamada et al. (NMI) published 1st melt and freeze temperature results of metal-carbon eutectic points
- co-operative projects and comparisons between NMIs to characterise these points in order to reach consensus on the transition temperatures and implementation procedures
- Eutectic fixed points could be considered as potential fixed points in a future international temperature scale

CAFMET 2014 - 5th International Metrology Conference
© 2014 nmisa

Primary and Eutectic Fixed Points

CAFMET 2014 - 5th International Metrology Conference
© 2014 nmisa

Proposed HTPF Values

Current (26 July 2012) proposed values for a selected set of high-temperature fixed points (HTFPs).

The following HTFP values have been determined through a critical analysis of the literature [1].

HTFP	Thermodynamic temperature/ ^o C	Uncertainty (95%)/ ^o C
Re-C	1537.8	0.6
Re-C	1493.3	0.3
Re-C	1727.6	0.8
Re-C	2473.2	1.0

This table will be reviewed and updated periodically.

Reference
[1] Saito, M., Kishio, J., Tomoda, Y., Saotome, Y., Looze, D., Marfilin, G., "Review of metal-carbon eutectic temperatures proposal for new ITS-90 secondary points", in: Benjumeil, M., The 5th International Symposium on Temperature and Thermal Measurements in Industry and Science, Zagreb, Croatia, Editor in Chief Davor Zivotic, Published: IAPM/PTB, 343-348, 2009.

CAFMET 2014 - 5th International Metrology Conference
© nmsa 2014

High Temperature Fixed Points at NMISA

- NMISA constructed and characterised two Re-C eutectic cells
- Objective: investigate its suitability as high temperature reference standards
- Re-C is the metal-carbon fixed point with the highest melt temperature (nominal melting temperature: 2 768 K)
- allows interpolation from copper point over full temperature range required for NMISA applications
- Re-C extensively studied internationally
- reliable reference to compare results with
- This paper: presents the results of development work and measurements at NMISA and compares the results obtained with those of other NMISA

CAFMET 2014 - 5th International Metrology Conference
© nmsa 2014

Preparation of Metal-Carbon Eutectic Containing Cells: Crucibles

- Graphite crucibles
- Purity: > 99.9995 %
- Supplied by the All-Russian Research Institute of Optical and Physical Measurements (VNIIO) and Carbotec
- Construction similar to the eutectic-containing crucibles commonly used by NMISA
- The emissivity of the blackbody cavity in the centre of the cylindrical crucible was taken to be $\epsilon < 0.9995$
- Filled with a plug at the opposite end of the cavity opening to enable filling with eutectic

CAFMET 2014 - 5th International Metrology Conference
© nmsa 2014

Preparation of Metal-Carbon Eutectic Containing Cells: Eutectic Mixture

- Pure carbon and metal powders used to prepare the eutectic mixture
- Supplier: Alfa Aesar
- Prepared in an "inert" glove-box in an argon atmosphere

Material	Purity	Proportion of Graphite in Mixture (see weight)
Rhenium (Re)	99.999 % (3N)	1:2 - 1:5 %
Graphite powder (crucible material)	99.9999 % (5N)	n/a
Solid graphite (crucible material)	99.9999 % (5N)	n/a

CAFMET 2014 - 5th International Metrology Conference
© nmsa 2014

Preparation of Metal-Carbon Eutectic Containing Cells:

CAFMET 2014 - 5th International Metrology Conference
© nmsa 2014

Preparation of Metal-Carbon Eutectic Containing Cells: Filling Procedure

- Empty crucibles annealed at approximately 2 800 K for 1 hour
- Filled with eutectic mixture in inert atmosphere
- Filled into an eutectic holder designed to fit into the BB3200g blackbody
- Eutectic holder placed inside the blackbody
- in centre of black cavity with the plug being the opening blackbody operated in a vertical position
- Blackbody cavity purged with argon while heated (to about 20 K above melting point)
- About 20 mixture-adding and melting cycles were necessary to fill each crucible completely

CAFMET 2014 - 5th International Metrology Conference
© nmsa 2014

Preparation of Metal-Carbon Eutectic Containing Cells: Filling Procedure

A schematic view of the filling procedure:

CAFMET 2014 - 5th International Metrology Conference
© nmsa 2014

Preparation of Metal-Carbon Eutectic Containing Cells: Equipment

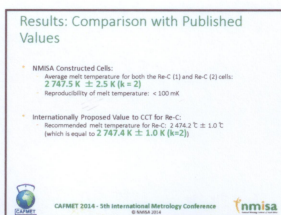
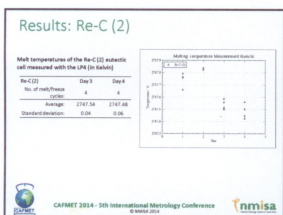
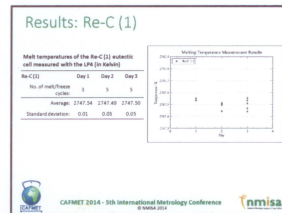
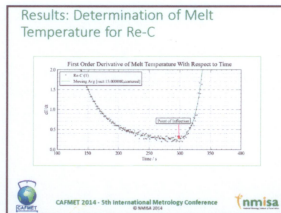
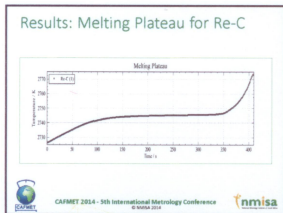
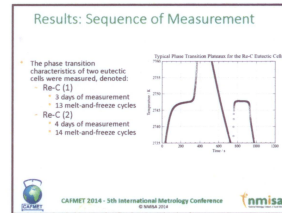
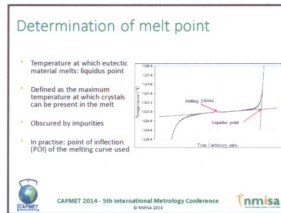
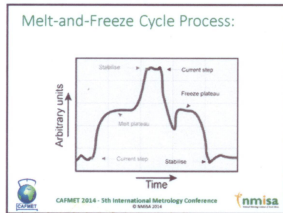
Instrumentation: the high temperature black body (BB3200g):

CAFMET 2014 - 5th International Metrology Conference
© nmsa 2014

Measurement of Melting Temperature

- Phase-transition characteristics of eutectics measured with blackbody opened in horizontal position
- A linear pyrometer (LP4) was used to measure the phase transition temperature
- Calibrated in terms of ITS-90 by the Physikalisch-Technische Bundesanstalt (PTB) in Germany
- Operated with an interference filter with nominal wavelength 650 nm and bandwidth of 20 nm
- Target distance: approximately 750 mm

CAFMET 2014 - 5th International Metrology Conference
© nmsa 2014



Conclusion

- Melt temperature of the Re-C eutectic cells constructed and characterised by the NMISA is in agreement with the internationally published values within the stated uncertainties
- Important outcome: the repeatability of these Re-C cells is sufficient to be utilised as stable reference standards for temperatures above the copper point
- This provides the NMISA with a practical means to verify the stability of its radiometric (spectral radiance and spectral irradiance) and temperature scales.

CAFMET 2014 - 5th International Metrology Conference © 2014 nmisa

The Development and Characterisation of High Temperature Fixed Points at NMISA

N. Nel-Sakharova

National Metrology Institute of South Africa (NMISA), Pretoria, South Africa

Received:

Abstract. Many National Metrology Institutes (NMIs) realise the spectral irradiance scale by obtaining traceability from a cryogenic radiometer through the use of calibrated filter radiometers. The filter radiometers are used to determine the temperature of a high temperature black body which is then used as a reference source, which spectral radiance can be determined from Planck's equation. The uncertainty of the temperature measurement makes the most significant contribution to the uncertainty of realising the spectral irradiance scale. High temperature fixed points (HTFPs), above the copper point, can be used to improve these uncertainties. After more than ten years of research, results obtained on metal-carbon eutectic fixed points by several NMIs, showed that these novel high temperature fixed points could lead to significant improvements in high temperature metrology and could be considered as potential fixed points in a future International Temperature Scale. This paper describes the development and characterisation of selected high temperature metal-carbon fixed points at NMISA. It is demonstrated that these fixed points can be utilised as reproducible, stable reference standards for temperatures above the copper point.

Keywords: eutectic cell; high temperature fixed point; phase transition; melt temperature; radiometry

1 Introduction

A wide range of industrial and medical applications require high precision spectral power distribution measurement of light sources, including solid state lighting, compact fluorescent lamps, conventional lamps, flat panel displays and solar radiation. The accuracy of these measurements is demonstrated by calibrating industrial reference standards against the national measurement standards for spectral irradiance, which are maintained by the National Metrology Institute of South Africa (NMISA).

Many National Metrology Institutes (NMIs) realise the spectral irradiance scale by obtaining traceability from a cryogenic radiometer through the use of calibrated filter radiometers. The filter radiometers are used to determine the temperature of a high temperature black body which is then used as a reference source, which spectral radiance can be determined from Planck's equation.

The uncertainty of the temperature measurement makes the most significant contribution to the uncertainty of realising the spectral irradiance scale. High temperature fixed points (HTFPs), above the copper point, can be used to improve these uncertainties. After more than ten years of research, results obtained on metal-carbon eutectic fixed points by several NMIs,

showed that these novel high temperature fixed points could lead to significant improvements in high temperature metrology and could be considered as potential fixed points in a future International Temperature Scale.

In 1996, the joint working group of the Comité Consultatif de Photométrie et Radiométrie CCPR) and the Comité Consultatif de Thermométrie (CCT) encouraged NMIs to develop high temperature fixed points above 2 300 K with a reproducibility better than 100 mK [1]. Three years later, in 1999, Yamada et al. published the first results of melt and freeze of metal-carbon eutectic points [2]. Since then, many NMIs have initiated cooperative projects and comparisons to characterise these points in order to reach a consensus on the transition temperatures and implementation procedures [3,4].

Some metal-carbon eutectic points (such as Co-C, Pd-C, Pt-C and Re-C) are reaching such a level of confidence and are proving to be sufficiently reproducible, through comparisons and long-term studies [5]. Other fixed points, such as the metal carbide-carbon (MC-C) fixed points for radiometry applications, still require further study before temperatures can be assigned to them with acceptable uncertainties.

* Correspondence: nnelsakharova@nmisa.org

The NMISA constructed and characterised two Re-C eutectic cells to investigate its suitability as high temperature reference standards. Re-C was selected as it is the metal-carbon eutectics with the highest melt temperature, allowing interpolation from the copper point over the full temperature range required for NMISA applications. This eutectic has also been extensively studied internationally and therefore provides a suitable reference to compare results with.

Provisional melt temperature values for a limited sub-set of eutectics have been published and the recommended melt temperature for Re-C is $2\,474.2\text{ °C} \pm 1.0\text{ °C}$ (which is equal to $2\,747.4\text{ K} \pm 1.0\text{ K}$ ($k=2$)) [5].

This paper presents the results of development work and measurements at the NMISA and compares the results obtained here with those of other NMIs.

2 Experimental setup

Eutectic Cell Preparation

Graphite crucibles supplied by the All-Russian Research Institute of Optical and Physical Measurements (VNIIOFI) and designed to fit into the high-temperature black body BB3200pg (used as a furnace), were used. The cells were made from fine-grained pure ($> 99.9995\%$) graphite. The construction was similar to the eutectic-containing crucibles commonly used by national metrology institutes (NMIs) and was cylindrical, with a length of 54 mm and a diameter of 24 mm. The black body cavity in the centre of the cylindrical crucible had a depth of 35 mm, a diameter of 4 mm and was conical at the bottom. The emissivity of the cavity was considered to be $\epsilon = 0.9995$. The crucible was fitted with a plug at the opposite end of the cavity opening to enable filling with the metal-carbon mixture. A diagram showing the crucible dimensions is given in Figure 1. Pictures of the crucibles used are shown in Figure 2.

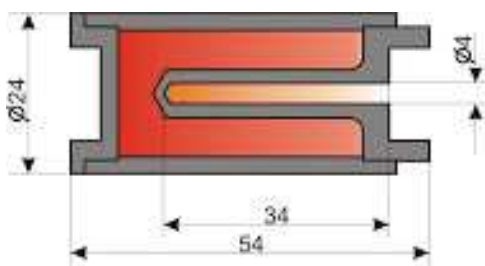


Fig. 1. Crucible dimensions (in mm)

Pure carbon (99.9999 %) and metal powders (99.999 %) were used to prepare the eutectic mixture. Table 1 shows the material purities and mixture proportions for each type of eutectic. The metal and graphite powders were supplied by the company Alfa Aesar. The purities shown in the table were provided by the supplier. The powders were mixed in an air-tight “glove-box” in an argon atmosphere.

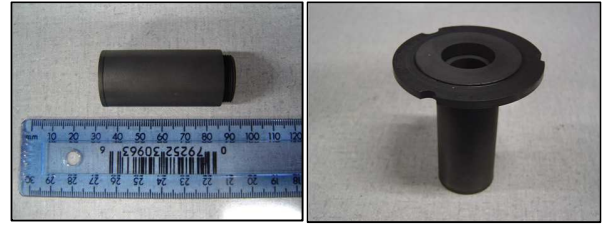


Fig. 2. Graphite crucible (left) fitted with a ring-holder (right)

Table 1. Material specifications and powder mixing proportions

Material	Purity	Proportion of Graphite in Mixture (per weight)
Rhenium (Re)	99.999 % (5N)	1.0 - 1.5 %
Graphite powder	99.9999 % (6N)	n/a
Solid graphite (crucible material)	99.9995 % (5N5)	n/a

The empty crucible and black body were purified by annealing above the eutectic material melting temperature (at approximately 2 800 K) for 1 hour. It was then filled with a metal-carbon powder mixture in an argon atmosphere and placed inside the black body (in the centre of the main cavity with the plug facing the opening) operated in a vertical position. The black body cavity was purged with argon to prevent electrical arcing while heated to melt the powder mixture to form the eutectic alloy. The filling process involved heating the crucible with the powder mixture to approximately 20 K above the eutectic melt point, cooling to room-temperature, re-filling with the powder mixture and re-heating to approximately 20 K above the melt point. This process was repeated until the crucible was completely filled with the eutectic alloy. About twenty (typical for Re-C) mixture-adding and melting cycles were necessary to fill each crucible completely.

Measurement of Melt Temperature

A linear pyrometer (LP4), calibrated in terms of ITS-90 by the Physikalisch-Technische Bundesanstalt (PTB) in Germany, was used to measure the phase transition temperatures of the Re-C cells. It was operated with an interference filter with a nominal centre wavelength of 650 nm and a bandwidth of approximately 20 nm. The LP4 was focussed on the eutectic cell aperture plane (with the black body at room temperature) at a target distance of 750 mm. The target size at this distance is $< 1\text{ mm}$, which is significantly smaller than the cavity aperture, therefore the size-of-source effect should be negligible [6].

In order to measure the phase transition characteristics of the eutectic cells, the black body was operated in a horizontal position. The crucible was placed inside the black body cavity, at the centre, with the crucible cavity facing the LP4. This configuration is shown in Figure 3.

The black body was heated to approximately 20 K below the melt temperature of the eutectic material. Once the system had stabilised at this temperature, the current to the black body was increased and the eutectic melt was observed as a plateau in the

pyrometer's signal versus time diagram. The melt finishes with a break-off point followed by a sharp temperature rise from the plateau to the set temperature of the black body. The system was again stabilised at approximately 20 K above the melt temperature. Thereafter, the current to the black body was decreased to reach a temperature below the freezing point of the eutectic material. The freeze plateau was observed, usually after undergoing super cool. The temperature of the system was stabilised at approximately 20 K below the freeze temperature before the next cycle was started.

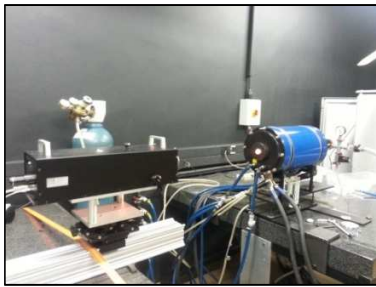


Fig. 3. Measurement configuration

The unique temperature at which the eutectic material melts is the liquidus point. It is defined as the maximum temperature at which crystals can be present in the melt at thermal equilibrium (i.e. it is the temperature at which the last solid melts) [7]. In practice, the presence of impurities in the eutectic material obscures the liquidus point. The point of inflection (POI) of the melting curve has been found to be a reproducible indicator of the melt temperature [8] and is being used in most studies.

3 Results and discussions

The phase transition temperatures of two different Re-C eutectic cells were measured (denoted Re-C (1) and Re-C (2), respectively). Over 3 days altogether, 13 melt-and-freeze cycles of the Re-C (1) cell were measured, while 14 cycles of the Re-C (2) cell was measured over 4 different days. A typical melt-and-freeze cycle for Re-C eutectic cells is shown in Figure 4. A temperature plateau indicates a phase transition.

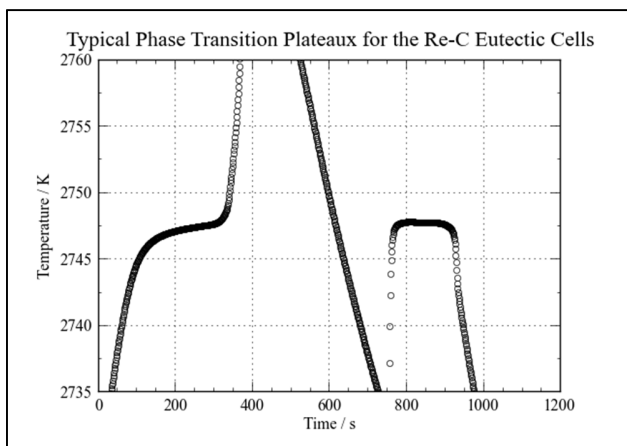


Fig. 4. Typical melt and freeze plateaux for the Re-C eutectic cells

A melting plateau observed for the Re-C (1) cell is shown in Figure 5. The first derivative of melting temperature with respect to time is shown in Figure 6. The melt temperature is defined as the minimum of this curve (i.e. the POI) and has been estimated after applying a moving average curve smoothing technique.

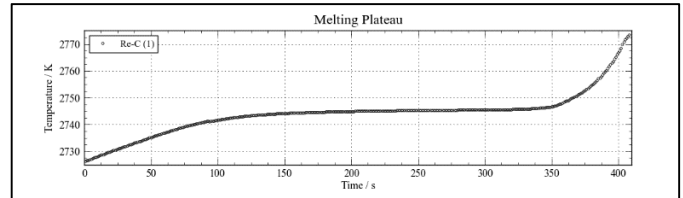


Fig. 5. A typical melting plateau observed for Re-C eutectic cells

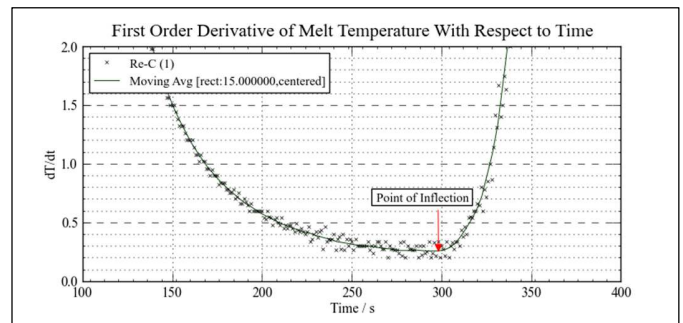


Fig. 6. Determination of the point of inflection of the melting plateau for a Re-C eutectic cell

At first, measurements were performed on the Re-C (2) eutectic cell. In order to utilise the existing measurement configuration, the LP4 was initially (over day 1 and 2) focussed on the eutectic cell aperture plane at a distance of 1 m, with a cylindrical eutectic holder which did not allow convenient alignment. It was thus decided to adapt the measurement setup to specifically accommodate the measurement of eutectics. The distance between the LP4 and eutectic cell was changed to 750 mm and the cylindrical crucible holder was replaced with a ring-holder (shown in Figure 2). All subsequent measurements were performed in this measurement configuration.

The measurement results for all melt-and-freeze cycles per day for each eutectic cell, are presented graphically in Figures 6 and 7.

A difference of 277 mK is observed between the average melt temperatures measured on days 1 and 2, versus days 3 and 4, for the Re-C (2) eutectic cell. Since this difference is significantly larger than the standard deviation for all subsequent measurements (≤ 61 mK), it is attributed to the change in focal distance of the LP4 as well as improvement of the ease of alignment.

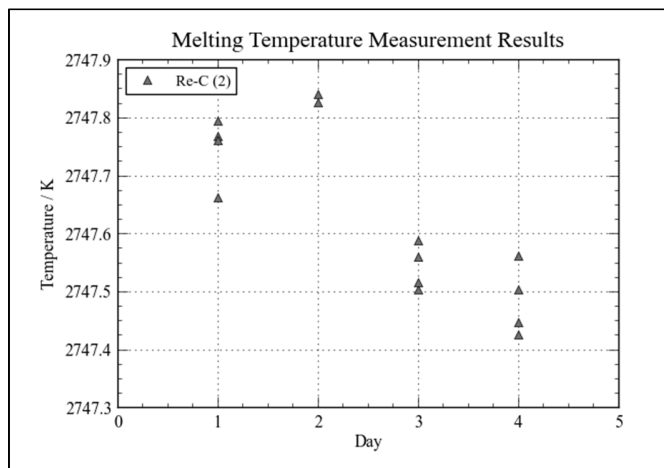


Fig. 7. Melt temperatures of the Re-C (2) cell measured over four different days

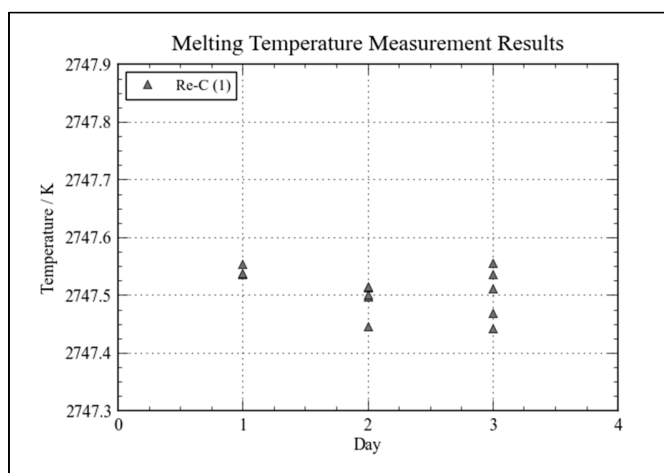


Fig. 8. Melt temperatures of the Re-C (1) cell measured over three different days

The average melt temperatures (in kelvin) measured on each day for the Re-C (1) and Re-C (2) cells are given in Tables 2 and 3, respectively.

Table 2. Melt temperatures of the Re-C (1) eutectic cell measured with the LP4 (in kelvin)

Re-C (1)	Day 1	Day 2	Day 3
No. of melt/freeze cycles:	3	5	5
Average:	2747.54	2747.49	2747.50
Standard deviation:	0.01	0.03	0.05

Table 3. Melt temperatures of the Re-C (2) eutectic cell measured with the LP4 (in kelvin)

Re-C (2)	Day 3	Day 4
No. of melt/freeze cycles:	4	4
Average:	2747.54	2747.48
Standard deviation:	0.04	0.06

The average melt temperature for both the Re-C (1) and Re-C (2)

cells is 2747.5 K with a measurement uncertainty of 2.5 K ($k = 2$). The reproducibility of the melt temperature was found to be within 100 mK.

4 Conclusion

The results presented in this paper show that the melt temperature of the Re-C eutectic cells constructed and characterised by the NMISA is in agreement with the internationally published values within the stated uncertainties. The important outcome is that the repeatability of these Re-C cells is sufficient to be utilised as stable reference standards for temperatures above the copper point. This provides the NMISA with a practical means to verify the stability of its radiometric (spectral radiance and spectral irradiance) and temperature scales.

References

1. Comité Consultatif de Thermométrie Rapport de la 19e Session, Bureau International des Poids et Mesures, Paris (1998)
2. Y. Yamada, H. Sakate, F. Sakuma and A. Ono, Radiometric Observation of Melting and Freezing Plateaus for a Series of Metal-Carbon Eutectic Points in the Range 1330 °C to 1950 °C, *Metrologia* **36**, 207-209 (1999)
3. G. Machin, Y. Yamada, D. Lowe, N. Sasajima, K. Anhalt, J. Hartmann, R. Goebel, H.C. McEvoy and P. Bloembergen, A comparison of high temperature fixed-points of Pt-C and Re-C constructed by BIPM, NMIJ and NPL, Proc. 9th Int. Symp. on Temperature and Thermal Measurements in Industry and Science (Tempmeko), Zagreb, Croatia, Editor in Chief Davor Zvizdic, Published: LPM/FSB, 1049-56 (2005)
4. K. Anhalt, J. Hartmann, D. Lowe, G. Machin, M. Sadli and Y. Yamada, Thermodynamic temperature determinations of Co-C, Pd-C, Pt-C and Ru-C eutectic fixed-point cells, *Metrologia* **43**, S78-S83 (2006)
5. M. Sadli, J. Fischer, Y. Yamada, V. Sapritsky, D. Lowe and G. Machin, Review of metal-carbon eutectic temperatures proposal for new ITS-90 secondary points, Proc. 9th Int. Symp. on Temperature and Thermal Measurements in Industry and Science (Tempmeko), Zagreb, Croatia, Editor in Chief Davor Zvizdic, Published: LPM/FSB, 341-348 (2005)
6. H.W. Yoon, D.W. Allen and R.D. Saunders, Methods to reduce the size-of-source effect in radiometers, *Metrologia* **42**, 89-96 (2005)
7. D. Lowe and G. Machin, Evaluation of Methods for Characterising the Melting Curves of a High Temperature Cobalt-Carbon Fixed Point to Define and Determine its Melting Temperature, *Metrologia* **49**, 189-199 (2012)
8. E.R. Woolliams, G. Machin, D.H. Lowe, and R. Winkler, Metal (carbide)-carbon eutectics for thermometry and radiometry: a review of the first seven years, *Metrologia* **43**, R11-R25 (2006)

Bibliography

- BIPM (1998). *Comité Consultatif de Thermométrie Rapport de la 19e Session*. Bureau International des Poids et Mesures, Paris.
- BIPM (2012). *International Vocabulary of Metrology - Basic and General Concepts and Associated Terms*. Bureau International des Poids et Mesures, Paris, third edn.
- BIPM-JCGM (2008). *Evaluation of measurement data - Guide to the expression of uncertainty in measurement*. Bureau International des Poids et Mesures, Paris, first edn.
- P. Bloembergen, et al. (2002). ‘On the Effect of Impurities on the Melting Curve of the Eutectic System Fe-C’. In Ripple (2002), pp. 261–266.
- P. Bloembergen, et al. (2007). ‘The Effect of the Eutectic Structure and the Residual Effect of Impurities on the Uncertainty in the Eutectic Temperatures of Fe-C and Co-C’. *Metrologia* **44**:279–293.
- P. Bloembergen, et al. (2011). ‘On the Impurity Parameters for Impurities Detected in the Eutectics Co-C and Pt-C and Their Role in the Estimate of the Uncertainty in the Eutectic Temperatures’. *International Journal of Thermophysics* **32**:2633–2656.
- W. Callister (2007). *Material Science and Engineering: An Introduction*. John Wiley and Sons, New York.
- CIE (2007). ‘CIE Standard Illuminants for Colorimetry’. Tech. Rep. CIE S 014-2/E:2006/ISO 11664-2:2007(E), Commission Internationale de L’Eclairage, Vienna, Austria.
- J. Fischer, et al. (2003). ‘Uncertainty Budgets for Realization of ITS-90 by Radiation Thermometry’. In *8th Proceedings of Temperature: Its Measurement and Control in Science and Industry*, vol. 684, pp. 631–638, Chicago. American Institute of Physics.

Bibliography

- H. Fukuyama & Y. Waseda (2009). *High-Temperature Measurement of Materials - Advances in materials research*. Springer Science and Business Media, Berlin.
- S. Galal Yousef, et al. (2000). ‘Measurement and Calculation of the Emissivity of a High Temperature Blackbody’. *Metrologia* **37**:365–368.
- T. W. Hänsch, et al. (2007). *Metrology and Fundamental Constants*. IOS Press, Amsterdam.
- L. Hanssen, et al. (2005). ‘Study of the Infrared Emissivity of Fixed-Point Blackbody Cavities’. In J. Gröbner (ed.), *Proceedings of NEWRAD 2005, 9th International Conference on Developments and Applications in Optical Radiometry*, pp. 133–134, Davos. Physikalisch-Meteorologisches Observatorium Davos, Weltstrahlungszentrum.
- D. G. Kingwill (1990). *The CSIR - The First 40 Years*. CSIR, Pretoria.
- S. Leschiutta & T. J. Quinn (2001). *Recent Advances in Metrology and Fundamental Constants*. IOS Press, Amsterdam.
- D. Lowe (2013). ‘A Pyrometer for Calibration Traceable to a Future Thermodynamic Temperature Scale’. *Measurement Science and Technology* **24**(1):015901.
- D. Lowe & G. Machin (2002). ‘Development of Metal-carbon Eutectic Blackbody Cavities to 2500 °C at NPL’. In *Proceedings of TEMPMEKO 2001, 8th International Symposium on Temperature and Thermal Measurements in Industry and Science*, vol. 1, pp. 519–524, Berlin. VDE Verlag.
- D. Lowe & G. Machin (2012). ‘Evaluation of Methods for Characterising the Melting Curves of a High Temperature Cobalt-Carbon Fixed Point to Define and Determine its Melting Temperature’. *Metrologia* **49**:189 – 199.
- D. H. Lowe & Y. Yamada (2006). ‘Reproducible Metal-Carbon Eutectic Fixed Points’. *Metrologia* **43**:S135–S139.
- G. Machin, et al. (2004). ‘A Comparison of ITS-90 and Detector-based Scales Between NPL and NIST Using Metal Carbon Eutectics’. In *Proceedings: 9th International Symposium on Temperature and Thermal Measurements in Industry and Science (Tempmeko)*, vol. 2, pp. 1057–1062.

Bibliography

- G. Machin, et al. (2013). 'Progress Report for the CCT-WG5 High Temperature Fixed Point Research Plan'. *AIP Conference Proceedings* **1552**:317–322.
- Z. Malik, et al. (2011). 'A Solidification Approach to Correcting for the Effect of Impurities in Fixed Points'. *International Journal of Thermophysics* **32**:1589 – 1601.
- M. McDowell (1997). *The National Metrology Laboratory of South Africa - The First 50 Years (1947 - 1997)*. CSIR, Pretoria.
- N. Nel-Sakharova (2015). 'The Development and Characterisation of High Temperature Fixed Points at NMISA'. *International Journal of Metrology and Quality Engineering* (in press).
- S. A. Ogarev, et al. (2004). 'New High-Temperature Pyrolytic Graphite Blackbody Sources for Precision Measurements in Radiation Thermometry'. In *9th Proceedings of Temperature: Its Measurement and Control in Science and Industry*, vol. 1, pp. 569–574.
- T. J. Quinn (1991). 'History of the Pavillon de Breteuil - A brief outline from 1672 to the present day'. <http://www.bipm.org/en/about-us/pavillon-de-breteuil/> (viewed on 8 April 2015).
- D. Ripple, et al. (2010). 'The Roles of the Mise en Pratique for the Definition of the Kelvin'. *International Journal of Thermophysics* **31**(8-9):1795–1808.
- D. C. Ripple (ed.) (2002). *8th Proceedings of Temperature: Its Measurement and Control in Science and Industry*, vol. 684. American Institute of Physics.
- M. Sadli, et al. (2004). 'Review of Metal-Carbon Eutectic Temperatures: Proposal for New ITS-90 Secondary Points'. In *Proceedings: 9th International Symposium on Temperature and Thermal Measurements in Industry and Science (Tempmeko)*, vol. 1, pp. 341–348.
- N. Sasajima, et al. (2004). 'A Comparison of Re-C and TiC-C Eutectic Fixed-Point Cells Among VNIIOFI, NMIJ and BIPM'. In *9th Proceedings of Temperature: Its Measurement and Control in Science and Industry (Tempmeko)*, pp. 1107–1115.
- A. Todd & D. Woods (2013). 'Thermodynamic Temperature Measurements of the Melting Temperatures of Co-C, Pt-C and Re-C Fixed Points at NRC'. *Metrologia* **50**(1):20–26.

Bibliography

- E. R. Woolliams, et al. (2006). 'Metal (Carbide)-Carbon Eutectics for Thermometry and Radiometry: a Review of the First Seven Years'. *Metrologia* **43**:R11–R25.
- Y. Yamada (2005). 'Advances in High-Temperature Standards above 1000 °C'. *MAPAN - Journal of Metrology Society of India* **20**(2):183–191.
- Y. Yamada, et al. (1999). 'Radiometric Observation of Melting and Freezing Plateaus for a Series of Metal-Carbon Eutectic Points in the Range 1330 °C to 1950 °C'. *Metrologia* **36**:207 – 209.
- Y. Yamada, et al. (2002). 'High Temperature Furnace Systems for Realizing Metal-Carbon Eutectic Fixed Points'. In Ripple (2002), pp. 985–990.
- H. W. Yoon, et al. (2005). 'Methods to Reduce the Size-of-Source Effect in Radiometers'. *Metrologia* **42**:89–96.
- R. E. Zupko (1990). *Revolution in Measurement: Western European Weights and Measures Since the Age of Science*, vol. 186. American Philosophical Society, Philadelphia.